Order Number 9108081

Pulse propagation in nonlocal and nonlinear media

Branis, Spiros V., Ph.D.

City University of New York, 1990

U·M·I
300 N. Zeeb Rd.
Ann Arbor, MI 48106

A

PULSE PROPAGATION IN NON-LOCAL AND NON-LINEAR MEDIA

by

SPIROS V. BRANIS

A dissertation submitted to the Graduate Faculty in Physics in partial fulfillment of the requirements for the degree of Doctor of Philosophy, The City University of New York.

1990

This manuscript has been read and accepted for the Graduate Faculty in Physics in satisfaction of the dissertation requirement for the degree of Doctor of Philosophy.

8 May 1990
Date

Joseph L. Birman
Chairman of the Examining Committee

23 Aug 1990
Date

Joseph B. Krieger
Executive Officer, Physics Program

Prof. Robert R. Alfano, City College, CUNY
Prof. Herman Z. Cummins, City College, CUNY
Prof. Azriel Z. Genack, Queens College, CUNY
Prof. Olivier Martin, City College, CUNY
Prof. George Papanicolaou, Courant Institute, NYU

Supervisory Committee

The City University of New York

ABSTRACT

PULSE PROPAGATION IN NON-LOCAL AND NON-LINEAR MEDIA

by

SPIROS V. BRANIS

Advisor: Professor Joseph L. Birman

The linear reflection of a finite optical pulse from a semi-infinite non-local medium for various models of spatial dispersion (Additional Boundary Conditions: ABCs) is investigated theoretically. The effects of spatial dispersion for the reflected transients are important when the laser frequency is in the vicinity of an exciton-polariton resonance. For various ABC models, quantitative differences are found in the transient regime after the pulse dies out, and this can be used to analyze different ABCs experimentally.

The propagation of steady-state (solitary) pulses in local dielectric media is examined theoretically. Previous studies in the slowly varying envelope approximation (SVEA) in gases indicated that short pulses could propagate as solitons, giving rise to Self-Induced Transparency (SIT). By going beyond the SVEA to solve the Maxwell-Bloch equations, it is shown that polariton-soliton and SIT solutions do not exist except for solitary waves of special pulse widths, especially inside the polariton gap.

DEDICATION
ΑΦΙΕΡΩΣΗ

DEDICATED TO MY PARENTS

VASILIOS BRANIS and SPIRIDOULA BRANI

ΑΦΙΕΡΩΝΕΤΑΙ ΣΤΟΥΣ ΓΟΝΕΙΣ ΜΟΥ

ΒΑΣΙΛΕΙΟΣ ΜΠΡΑΝΗΣ και ΣΠΥΡΙΔΟΥΛΑ ΜΠΡΑΝΗ

Μαυρη μεγαλη μοναξια με τοσα βοτσαλα τριγυρω
στο λαιμο τοσα
χρωματιστα πετραδια στα μαλλια σου.

Νικος Γκατσος, **ΑΜΟΡΓΟΣ**

ACKNOWLEDGEMENTS

I am deeply indebted to Professor Joseph L. Birman, for introducing me to the fields of non-local and non-linear optics and supervising the work done in this thesis. I am grateful to him for his encouragement, confidence, advice and collaboration.

I am grateful to Prof. K. Arya for collaborating with me in the first part of this thesis. I would like to thank him for his continuous advice in the analytical and numerical study of optical pulse reflection from spatially dispersive media.

I am grateful to Prof. O. Martin for collaborating with me in the second part of this thesis. I would like to thank him for his systematic support and guidance through the mathematical and numerical study of the intense optical pulse propagation in local dielectric media.

Many thanks to those who have been associated with our group; their questions and fruitful suggestions clarified a lot of problems in understanding the physical concepts of this thesis. They include: Prof. R. Berenson, Prof. Bing Shen Wang, Prof. J. Jaric, Prof. D. Schmeltzer, Dr. J. Malinsky, Dr. J.P. Lu, Dr. A. Tolpin, and Mr. M. Artoni.

I thank Profs. H.Z. Cummins, R. Alfano, A.Z. Genack, G. Papanicolaou and J. Koplik for their education, advice and discussion.

Special thanks to Profs. A. Puri and G.P. Agrawal for discussions during the preliminary parts of the first part of this work. Also, to Prof. P. Lavallard, Drs. C. Gourdon, C. Hillerman, J.P. Morhange, and N. Piccioli for discussions during a short visit at Université de Paris VI in November 1987.

Special thanks, also, to Dr. S. McCall for discussions on the SIT problem during a visit to Bell Labs, Murray Hill, NJ in December 1989.

Last, but not the least, I thank my girl friend Sonja Zeidler for her patience, support, encouragement, love, and for the wonderful time we have spent together.

TABLE OF CONTENTS

LIST OF FIGURES

CHAPTER 1

INTRODUCTION

Light is common by nature to all bodies, celestial and terrestrial.... Light is the substantial form of bodies; by their greater or lesser participation in light, bodies acquire the truth and dignity of their being.

St. Bonaventure, **In II Sent.**, 13, 2, 2

1.1 OUTLINE

In this thesis we shall examine problems relating to optical pulse reflection from bounded, spatially, dispersive media and to intense optical pulse propagation in local dielectric media.

In spatially dispersive media, the dielectric function describes the linear non-local relationship between the response of the dipoles of the medium and the applied E-M field. The dielectric function is not only frequency dependent but also wave vector dependent: $\varepsilon(\mathbf{k}, \omega)$. One of the important consequences of the **k**-dependence of the dielectric function is that additional modes arise for transverse E-M propagation as solutions of Maxwell's wave equation. In the usual local optics where the dielectric function is only frequency dependent (frequency dispersive medium), the transverse solutions are given as solutions of $k^2=(\omega^2/c^2)\varepsilon(\omega)$. For spatial dispersion, the equation $k^2=(\omega^2/c^2)\varepsilon(\mathbf{k}, \omega)$ becomes a higher order algebraic equation in k. One of the many new consequences resulting from the additional solutions is that the solution of the elementary reflection and transmission problem (Fresnel equations) is not possible, since the Maxwell Boundary Conditions (MBCs) are not enough to solve the problem at the interface of a semi-infinite spatially dispersive medium and the vacuum. The MBCs and Additional Boundary Conditions (ABCs) are required to solve reflection and transmission problems. Many different ABCs have been proposed in the literature since the the proposal of wave vector effects in crystal optics by Pekar in 1957 [1]. The existence of two propagating modes has been demonstrated in various ways with innovative techniques made possible by the development of tunable lasers, but the problem of which is the correct ABC still remains unsolved.

In the first part of this thesis, we study manifestations of the wave vector dependent dielectric function $\varepsilon(\mathbf{k}, \omega)$. We consider a new method in the ultrafast picosecond time domain in which spatial dispersion becomes a distinct feature, especially near the exciton

resonance ω_t of a semiconductor. In Chapter 2, the electrodynamics of spatially dispersive media is reviewed showing the difference between local and non-local (spatially dispersive) optics. The problem of ABCs arises naturally from the greater number of necessary boundary conditions needed to solve the reflection and transmission problem completely. A review of the historical development of the different ABCs, with the various microscopic and macroscopic ways of solving it, is given. In addition, a short review of the experimental status on ABC demonstrates the crucial experiments that have proved the existence of two propagating modes inside the spatially dispersive dielectrics plus the latest techniques of time-of-flight measurements for the group velocity of exciton polaritons. All these measurements are necessary, to determine the correct ABC, but they are not sufficient as will be reviewed in that Chapter.

In Chapter 3, we study the effects of spatial dispersion (non-locality) on transient reflectivity in the picosecond regime, for different ABCs. Specifically, for an E-M pulse of finite duration T incident normally on a non-local interface, we present the analytical form of the reflected field that consists of the steady-state signal part (of duration T) and the transient part arising from the front and the back of the pulse. Since it is more convenient to look at the trailing edge transient reflectivity for a finite width pulse, we consider an incident square pulse and obtain expressions for steady-state and transient reflectivity after the main body of the pulse has died out, for different ABCs. The results show that the transient reflectivity consists of a "local" part (E-M dephasing process) and a "non-local" (spatial dispersion enhanced process) part. Both expressions for the local and non-local parts show the differences between the ABCs, especially close to the exciton-polariton resonance frequency ω_t. The study of the total transient reflectivity opens a new channel of information regarding the "true" ABC for the material.

Intense optical pulses have become available in the last 20-25 years, contributing to the understanding of the dynamics of interaction of light with matter in condensed matter physics. The development of high intensity, narrow band-width lasers has led to the

investigation of optical resonances at very close spectral range for any dilute gas or dielectric. Very near resonance, dilute gases and crystals can display new phenomena entirely alien to classical Lorentzian media. One of these is the propagation of intense short optical pulses. McCall and Hahn in 1967 [55] showed that for dilute gases short pulses can propagate with anomalously low energy loss and their velocities can be many orders of magnitude slower than the velocity of light, c. This effect is called self-induced transparency (SIT) since the medium in which the short intense pulse propagates behaves like a transparent medium for the pulse. In addition, SIT phenomena were proposed for semiconductors, while experimental results showed the same kind of lossless propagation with long delays, results that have been related to SIT for the exciton in semiconductors.

In the second part of this thesis, we study the possibility of solitary solutions for intense optical pulse propagation in dielectrics, especially near a sharp resonance ω_t. In Chapter 4, we review the phenomenon of SIT for dilute gases (absorbers) and for local and non-local dielectric media (semiconductors). We present the assumptions of McCall and Hahn's work which lead to the derivation of soliton solutions for SIT in the slowly varying envelope approximation (SVEA). In addition, a historical review is presented of the work beyond the SVEA for dilute gases and semiconductors. The difference between soliton and solitary solutions is defined; soliton solutions are derived from integrable systems, whereas solitary waves do not require any conservation laws.

In Chapter 5, we present a perturbative expansion method for the solution of Maxwell-Bloch equations beyond the SVEA, based on a series expansion in powers of a small parameter which is related to the electric field amplitude. We study the generalized perturbation expansion by using a uniform approximation approach to prove that solitary pulse solutions do not exist for arbitrary pulse width τ, but only for selected pulse widths, especially inside the gap of a semiconductor. General expressions for the solitary waves and their phase modulations are derived that lead to results for short and long pulses inside and outside the polariton gap. We show, that this uniform expansion is only locally valid.

It is not uniformly valid on the whole domain of the local time variable $\xi \in (-\infty, +\infty)$, and we cannot determine whether there exist soliton solutions, globally. Therefore external boundary conditions like the fine tuning of of the pulse width τ (non-linearity) and frequency detuning (dispersion) need to be imposed for solitary pulses to exist. Numerical results resulting from the integration of Maxwell-Bloch equations confirm this statement. Selected solitary branch solutions are generated especially inside the polariton gap. A general conclusion is that solitons do not exist under the stated conditions.

CHAPTER 2

ELECTRODYNAMICS OF SPATIALLY DISPERSIVE MEDIA

Zugemessen ward dem Lichte seine Zeit; aber zeitlos und raumlos ist der Nacht Herrschaft.

Its time was measured out to Light; but Night's reign is timeless and spaceless.

Μετρημενος διοριστηκε για το Φως ο καιρος του; ομως εξω καιρου και τοπου ειναι της Νυχτας η βασιλεια.

Novalis, **Hymnen an die Nacht**, II

2.1 INTRODUCTION

In 1957 Pekar [1] proposed that finite wavevector effects in the dispersion equation for the total energy of an exciton could play an important role in crystal optics. These finite wavevector effects had been known in optics since the time of Lorentz [2] who studied optical rotatory power in solids, as well as in other areas of modern physics e.g. plasma physics, ionospheric physics, but in crystal or solid-state matter physics it seems to have been Pekar who first showed the importance of these spatial dispersion effects in the resonance regime of optical region of excitonic resonances. Soon after, Ginzburg, Agranovich and Rukhadze [3, 4] and others made significant contributions to this subject. A full update of these scientific contributions theoretical and experimental can been found in two excellent monographs by Pekar [5], Agranovich and Ginzburg [6].

In the same period Hopfield [7] studied the polariton effects on optical absorption, due to the mixing of a photon and a finite mass exciton. In 1963, Hopfield and Thomas [8] called attention to the possible existence of spatial dispersion effects in crystal optics. In their paper, they introduced the resonant oscillator model (now known as the "dielectric approximation"), and suggested an exciton-free "dead layer" due to surface repulsion of excitons, and explained many optical effects observed by spectroscopical methods in CdS.

As remarked by Pekar [9] and Agranovich and Ginzburg [4] the earliest known recognition of the importance of wavevector dependence in optics goes back to H.A. Lorentz [2] who, studied the molecular optics theory of gyrotropy by taking into account wavelength dependent terms in the molecular polarizability.

2.2 THE SPATIALLY DISPERSIVE MEDIUM

In crystal optics spatial dispersion refers to effects due to the "motion" of the electronic excitations for example excitons in the medium. This motion is characterized by transport of kinetic energy: $\hbar^2k^2/2m^*$ where $\mathbf{p}=\hbar\mathbf{k}$ is the exciton quasi-momentum and m^* the total exciton mass (the sum of electron and hole effective band masses: $m^*=m_c^*+m_h^*$). The motion of the finite excitonic mass is taken into account in spatial dispersion. When $m^* \rightarrow \infty$ the excitation is localized and non-spatially dispersive. This leads to classical optical phenomena when only frequency dispersion of the dielectric function is considered.

Spatial dispersion refers to the linear non-local relationship between the response and the applied field. This can be represented in the integral constitutive relationship for the polarization $\mathbf{P}(\mathbf{r},\omega)$:

$$\mathbf{P}(\mathbf{r},\omega) = \hat{\chi}\mathbf{E} \equiv \int \chi(\mathbf{r},\mathbf{r}',\omega)\mathbf{E}(\mathbf{r}',\omega)\mathrm{d}\,\mathbf{r}' \qquad (2.2.1)$$

The essential physical point here is that the polarization $\mathbf{P}(\mathbf{r}, \omega)$ at a point $\mathbf{r}$ in the medium is determined by the incident applied field $\mathbf{E}(\mathbf{r}',\omega)$ in the range of $\chi(\mathbf{r}, \mathbf{r}', \omega)$. Here anisotropy has been neglected.

A simple mechanical model to describe the effect of spatial dispersion was given by Hopfield and Thomas [8] in terms of coupled localized simple harmonic oscillations. The localized oscillations represent excitons whose coupling give rise to the motion (delocalization) by means of which the kinetic energy and the mass of the excitons enter the theory. Considering the simple case of a single electric dipole active exciton resonance with isotropic effective mass, the differential equation of motion of $\mathbf{P}(\mathbf{r}, t)$ is

$$(\frac{\partial^2}{\partial t^2}+\omega_t^2-\frac{\hbar\omega_t}{m^*}\nabla^2+\Gamma\frac{\partial}{\partial t})\mathbf{P}(\mathbf{r},t)=\omega_t^2\alpha_0\mathbf{E}(\mathbf{r},t) \tag{2.2.2}$$

where ω_t is the resonance frequency, m^* is the exciton effective mass, Γ is the exciton damping, $\alpha_0=2Nd^2/\hbar\omega_t$ where d is the dipole matrix element for optical excitation of the exciton. In this case the dielectric response function is

$$\varepsilon(\mathbf{k},\omega)=\varepsilon_0+4\pi\chi(\mathbf{k},\omega)=\varepsilon_0+\frac{4\pi\alpha_0\ \omega_t^2}{\omega_t^2-\omega^2-i\omega\Gamma+(\frac{\hbar\omega_t}{m^*})k^2} \tag{2.2.3}$$

where ε_0 is the background dielectric constant. i.e., the contribution to the dielectric constant from other high frequency excitonic resonances and other crystal excitations.

This "dielectric approximation" to the susceptibility has the advantage of being a simple, analytic expression which contains the physics of spatially dispersive media when the exciting laser frequency is close to an exciton resonance. It applies well inside a crystal away from the surface where evanescent waves have decayed and surface effects are not important. The terminology "non-local" (spatially dispersive) which was first used by Hopfield [10] in the context of exciton-polariton optics is justified if one observes near resonance $\omega \rightarrow \omega_t$ the range of dipole-dipole interaction can be very large. Consequently the departure of $\chi(\mathbf{r}, \mathbf{r}', \omega)$ in Eq. (2.2.1) from proportionality to $\delta(\mathbf{r}-\mathbf{r}')$ signals the non-locality (spatial dispersion). If the effective exciton mass is infinite $m^* \rightarrow \infty$, the dielectric function in Eq. (2.2.3) takes the form familiar in local optics: i.e. the conventional model for a frequency dispersive dielectric medium (Jackson [11], Landau and Lifshitz [12]).

Equation (2.2.3) plus the Maxwell equations constitute the complete set of equations one needs to find the normal modes of the crystal in the resonance frequency region. For

the isotropic case, there exist two types of modes: transverse (with $\mathbf{P}, \mathbf{E} \perp \mathbf{k}$) and longitudinal (with $\mathbf{P}, \mathbf{E} \parallel \mathbf{k}$). The modes satisfy the dispersion equations

$$\varepsilon(\mathbf{k},\omega) = \left(\frac{ck}{\omega}\right)^2 \text{ (transverse mode)}, \quad \omega = \omega_t ;$$

$$\varepsilon(\mathbf{k},\omega) = 0 \qquad \text{(longitudinal mode)}, \ \omega = \omega_\ell \tag{2.2.4}$$

Figures 2.2.1(a) and 2.2.1(b) (pages 21 and 22) show the dispersion curves of the normal modes in the vicinity of the exciton resonance. The exciton-photon interaction renormalizes the energy spectra of photons and excitons leading to coupled exciton-photon modes, the exciton-polaritons. Figure 2.2.1(a) (page 21) presents the polariton dispersion relation (without damping, Γ=0) in the absence of spatial dispersion (local medium), i.e., for the case where the dielectric function depends on frequency [$\varepsilon(\omega)$], but not on the wavevector. The characteristic feature of a local medium is the presence of 2 branches of polariton transverse modes (upper and lower) separated by a gap for which the propagation of the transverse modes is forbidden either for Γ=0, or for heavily damped polaritons (effectively "forbidden"). The upper polariton mode propagates for $\omega > \omega_\ell$ while the lower polariton does for $\omega < \omega_t$. The longitudinal transverse splitting for the gap region is given by

$$\omega_{LT} = \frac{2\pi\alpha_0\omega_t}{\varepsilon_0} = \frac{4\pi N d^2}{\hbar\varepsilon_0} \tag{2.2.5}$$

Figure 2.2.1(b) (page 22) shows the polariton dispersion relation (without damping) in the presence of spatial dispersion (m^* is finite). The new situation here is the lower polariton mode can propagate inside the gap region and continues for $\omega > \omega_\ell$ where two transverse modes can propagate in the non-local medium.

Using Eqs. (2.2.3) and (2.2.4), one can find the refractive indices $n_j=ck_j/\omega$ (j=1, 2, 3) corresponding to exciton polaritons (upper=1 and lower =2) and longitudinal excitons (j=3) for $\Gamma=0$:

$$n_{2,1}^2 = \frac{\varepsilon_0}{2}[(1+\frac{\omega^2-\omega_t^2}{\varepsilon_0\omega^2\delta^2}) \pm [(1-\frac{\omega^2-\omega_t^2}{\varepsilon_0\omega^2\delta^2})^2 + 4(\frac{\beta\omega_t}{\varepsilon_0\omega\delta})^2]^{1/2}] \tag{2.2.6}$$

$$n_3^2 = \frac{\varepsilon_0}{(\omega\delta)^2}[\omega^2 - \omega_t^2(1+\frac{\beta^2}{\varepsilon_0})] \tag{2.2.7}$$

It should be noted that the refractive indices n_1, n_2, n_3 are connected by the relation: $n_3^2 = n_1^2 n_2^2/\varepsilon_0$. The origin of the longitudinal mode is the long-range Coulomb interaction of exciton. When $\Gamma\neq0$, even if $m^* \rightarrow \infty$, coupled inhomogeneous modes propagate in the "gap".

2.3 THE PROBLEM OF ADDITIONAL BOUNDARY CONDITIONS (ABCs)

Let us assume that the dielectric consists of a semi-infinite medium in the region z > 0 terminated by a plane surface Σ at z=0 with vacuum located in the region z < 0. The medium is homogeneous right up to the boundary. The dielectric function for z < 0 is ε=1 (vacuum) while for z > 0, the dielectric function is $\varepsilon(\mathbf{r}, \mathbf{r}', \omega)$. At z=0, a surface discontinuity Σ is produced by the sharp change of the dielectric function ε.

The Maxwell equations for the dielectric in the absence of free and surface charges, true currents, and magnetization are in G.C.S. units [11]:

$$\nabla \times \mathbf{E} = -\frac{1}{c}\frac{\partial \mathbf{B}}{\partial t} \qquad \nabla \times \mathbf{H} = \frac{1}{c}\frac{\partial \mathbf{D}}{\partial t}$$

$$\nabla \cdot \mathbf{B} = 0 \qquad \nabla \cdot \mathbf{D} = 0 \tag{2.3.1}$$

which the Maxwell Boundary Conditions (MBCs) on the surface Σ at z=0 can be derived by the usual Maxwell constructions (Stratton [13], Born and Wolf [14]):

$$\hat{\mathbf{n}} \times (\mathbf{E}_2 - \mathbf{E}_1) = 0 \quad \text{or} \quad \mathbf{E}_{t_1} = \mathbf{E}_{t_2} \;\; \& \;\; \hat{\mathbf{n}} \times (\mathbf{H}_2 - \mathbf{H}_1) = 0 \quad \text{or} \quad \mathbf{H}_{t_1} = \mathbf{H}_{t_2}$$

$$\hat{\mathbf{n}} \cdot (\mathbf{B}_2 - \mathbf{B}_1) = 0 \quad \text{or} \quad \mathbf{B}_{n_1} = \mathbf{B}_{n_2} \;\; \& \;\; \hat{\mathbf{n}} \cdot (\mathbf{D}_2 - \mathbf{D}_1) = 0 \quad \text{or} \quad \mathbf{D}_{n_1} = \mathbf{D}_{n_2} \tag{2.3.2}$$

For local optics consider a crystal having dielectric coefficient $\epsilon(\omega)$ and $\mu=1$ (non-magnetic medium). The crystal surface Σ is the plane z=0. Assume a plane polarized E-M wave travelling in vacuum in the +z direction is incident normally on this surface and take the electric field with unit intensity as $E_{INC} \exp[+ik_0 z]$. The reflected wave is $E_R \exp[-ik_0 z]$, while the transmitted $E_T \exp[+ik_0 z]$. Here $k_0=\omega/c$. In order to calculate all fields (reflected and transmitted), we need to use the MBCs and assume that the incident field is independently controllable. The continuity of E_t and H_t across the boundary z=0 gives two boundary conditions:

$$E_{INC} + E_R = E_T \quad , \quad E_{INC} - E_R = nE_T \quad \text{where } n=k/k_0=[\epsilon(\omega)]^{1/2} \tag{2.3.3}$$

from which one can obtain the Fresnel equations for normal incidence:

$$\frac{E_T}{E_{INC}} = \frac{2}{1+n}; \qquad \frac{E_R}{E_{INC}} = \frac{1-n}{1+n} \tag{2.3.4}$$

Thus the conventional MBCs exactly determine the two unknown field amplitudes.

For non-local optics one obtains a completely different physical situation. The dispersion equation for transverse wave propagation is now $(k/k_0)^2=\varepsilon(\omega,k)$ where $\varepsilon(\omega,k)$ is given by Eq. (2.2.3). The algebraic equation for solutions k_j is quadratic in k^2 (each with $\pm$ sign). Consequently two propagating transverse fields $E_j \exp[+ik_jz]$ (j=1, 2) in the +z direction exist in the medium at the frequency ω plus incident and reflected waves. Hence there are three amplitudes in question: R, E_1, and E_2, but only two MBCs. The problem of determining the additional unknown can be solved if one is presented with one more boundary condition. This need for supplementary boundary conditions in order to fully determine the structure of the transmitted field inside the non-local medium has given rise to the problem of "Additional Boundary Conditions" or the ABC problem.

2.4 REVIEW OF DIFFERENT ABCs

Simultaneously with the prediction of the existence of additional waves in spatially dispersive media the need for more than the usual MBCs was realized [15] (Pekar [1], Ginzburg [16]).

In his first paper, S.I. Pekar [1] discussed a quantum mechanical approach to obtaining an ABC. He proposed that in the non local medium the macroscopic polarization $\mathbf{P}_{exc}(\mathbf{r},t)$ originating from excitons satisfies the equation of motion:

$$(-\omega_0^2+\frac{\partial^2}{\partial t^2}+b\nabla^2+\Gamma\frac{\partial}{\partial t})\mathbf{P}_{exc}(\mathbf{r},t)=\alpha\mathbf{E}(\mathbf{r},t) \qquad (2.4.1)$$

with $-\omega_0^2$, $b=1/m^*$, Γ, α being coefficients and the macroscopic field $\mathbf{E}(\mathbf{r}, t)$ acting as a driving force on the exciton polarization. For harmonic plane-wave propagation in the medium in +z direction (normal incidence), Eq. (2.4.1) leads to a macroscopic constitutive relation for $\mathbf{P}_{exc}(\mathbf{r}, t)$:

$$\mathbf{P}_{exc}(\mathbf{k},\omega) = \chi_{exc}(\mathbf{k},\omega)\mathbf{E}(\mathbf{k},\omega) \tag{2.4.2}$$

with

$$\chi_{exc}(\mathbf{k},\omega) = \frac{\alpha}{(\omega_0^2 + bk^2 - \omega^2 - i\Gamma\omega)} \tag{2.4.3}$$

or by adding a background term connected with the high frequency resonances of the medium far from ω_0 the total susceptibility is:

$$\chi(\mathbf{k},\omega) = \chi_0 + \chi_{exc}(\mathbf{k},\omega) \tag{2.4.4}$$

Eq. (2.4.1) is an equation of motion which is obtained as a long wavelength approximation to an exciton Schrödinger equation with polarization defined defined via the exciton eigenfunction in a bounded medium. The total macroscopic polarization $\mathbf{P}$ is the sum of this excitonic polarization plus a background χ_0. The equation (2.4.1) was solved subject to an assumed boundary condition :

$$\mathbf{P}_{exc}(\mathbf{r},t)|_{\Sigma} = 0 \qquad \text{or} \qquad (n_1^2 - \varepsilon_0)E_1 + (n_2^2 - \varepsilon_0)E_2 = 0 \tag{2.4.5}$$

Since the polarization vanishes outside the medium, where Σ is the boundary of the medium, this ansatz seems reasonable. In Eq. (2.4.5), n_1, n_2 are the complex indices of refraction for the two propagating modes while ε_0 is the dielectric constant of the background. The boundary condition in Eq. (2.4.5) is not a mathematical consequence of

the assumed susceptibility, but an assertion imposed by Pekar to complete the solution of Maxwell equations in the presence of spatial dispersion. In other words, Pekar's boundary condition is not a mathematical consequence of the assumed susceptibility.

In a review article Agranovich and Ginzburg [4] further analyzed boundary conditions starting from a constitutive relation for the exciton polarization,

$$-\omega^2 \mathbf{P}_{exc} + \beta \mathbf{P}_{exc} + \gamma \nabla \mathbf{P}_{exc} + \alpha \nabla^2 \mathbf{P}_{exc} = \lambda \mathbf{E} \tag{2.4.6}$$

and they observe that the general form of boundary condition at Σ is

$$(-\omega^2 + \beta)\mathbf{P}_{exc} + \gamma(\nabla \mathbf{P}_{exc}) = \lambda \mathbf{E} \text{ on } \Sigma, \tag{2.4.7}$$

all fields evaluated on Σ. A somewhat more general phenomenological boundary condition was given by Agranovich and Ginzburg [17] in which

$$(-\omega^2 + \beta)\mathbf{P}_{exc} + \gamma(\nabla \mathbf{P}_{exc}) = \Lambda \mathbf{E} + \Lambda^{(1)} \nabla \mathbf{E} \text{ on } \Sigma, \tag{2.4.8}$$

They remark on the frequency-independence of the coefficients β, γ, Λ, $\Lambda^{(1)}$ and propose for their susceptibility a limiting (long wavelength) ABC:

$$\mathbf{P}_{exc} + \Gamma \mathbf{E} = 0 \text{ at } \Sigma, \tag{2.4.9}$$

with Γ frequency independent.

At about this time Hopfield and Thomas [8], took up the ABC problem. Following somewhat along the lines of Pekar's paper they introduced the equation of motion as in Eq. (2.4.1) and analyzed a quantum-mechanical model which would give a Schrödinger

eigenfunction for the exciton. From this eigenfunction they deduced the needed ABC, using a classical correspondance. They postulated the following ABC:

$$\mathbf{P}_{exc}(\mathbf{r},t)+ A \frac{\partial \mathbf{P}_{exc}(\mathbf{r},t)}{\partial z}|_{\Sigma} = 0 \qquad (2.4.10)$$

where Pekar's ABC is a particular case (A=0). To allow for the fact that a Wannier exciton has a finite radius, and hence must be affected by the presence of the surface even if its center of mass is some distant away, a "dead layer" or exciton-free local region was postulated, and this three layer geometry was introduced in their analysis of experimental data. Note that Eq. (2.4.10) is the most general linear ABC which could apply.

Kiselev [18], gave a more explicit expression for $A=\gamma c/\omega$ where γ is some phenomenological constant or function of frequency. In terms of electric fields, Eq. (2.4.7) is written as follows:

$$(1+i\gamma n_1)(n_1^2-\varepsilon_0)E_1+(1+i\gamma n_2)(n_2^2-\varepsilon_0)E_2 = 0 \qquad (2.4.11)$$

From these published papers the impression was created that there was an "ABC" problem to be solved by following either of two lines:

(i) The first is to set up a quantum mechanical exciton model, solve for the Schrödinger eigenfunction then use this eigenfunction to obtain the boundary condition on the macroscopic polarization to be used in conjunction with a non-local dielectric function. Even if this procedure is in principle correct (one should solve the coupled Schrödinger Maxwell problem self-consistently), in practice no such self-consistent solution was given for the bounded non-local medium. The actual ABC obtained by the authors following this line was not obtained by mathematically clear procedure directly from the assumed macroscopic susceptibility.

(ii) The second is to assume that the macroscopic Maxwell equations hold and a non-local dielectric function describes the response of the medium to E-M waves. In other words, there is a a priori macroscopic constitutive relation between $\mathbf{P}(\mathbf{r},\omega)$ and $\mathbf{E}(\mathbf{r},\omega)$ in the bounded medium, and then obtain the ABC from macroscopic theory only.

Under the second approach, Birman and Sein [19], derived for the first time a mathematically exact procedure using the integral equation method giving an exact ABC. Their contribution was based on the fact that by choosing a non-local susceptibility model, an ABC can be derived through an integral equation formalism of electrodynamics for non-local media, without any additional assumption. Later, Maradudin and Mills [20], Agrawal et al. [21] independently, derived the same ABC by using higher order (4th or 6th degree) generalized Maxwell differential equations. By using Eq. (2.4.4) (dielectric approximation) the result for Birman-Sein ABC is:

$$\frac{\partial \mathbf{P}_{exc}(\mathbf{r},t)}{\partial z} + i k_+ \mathbf{P}_{exc}(\mathbf{r},t)|_{\Sigma} = 0 \qquad \text{or} \qquad \frac{E_1}{n_1 - n_+} + \frac{E_2}{n_2 - n_+} = 0 \tag{2.4.12}$$

with

$$k_+^2 = n_+^2 \frac{\omega^2}{c^2} = \frac{m^*}{\hbar \omega_t}(\omega^2 - \omega_t^2 + i\omega\Gamma)$$

where: m^* is the effective exciton-polariton mass, ω_t is the transverse exciton angular frequency, Γ a phenomenological damping constant and n_+ the refractive index for the lower polariton mode for $\omega >> \omega_t$. This approach is totally macroscopic.

Zeyher et al., [22] gave a microscopic determination of ABCs. The fundamental assumption about the physics of exciton-polariton reflection at the crystal surface decides about the different ABCs. The wave function for the exciton-polariton center-of-mass-motion is approximated as follows:

$$\Psi_{\mathbf{k}}(\mathbf{r},\omega) = \Theta(z)[\exp(ik_z z) + R_{exc}\exp(-ik_z z)]\exp(i\mathbf{k}_{\parallel}\cdot\mathbf{r}) \qquad (2.4.13)$$

where R_{exc} is the exciton reflection coefficient at the surface Σ. For R_{exc}=0, one obtains exactly Hopfield and Thomas ABC Eq. (2.4.10). The physical meaning of the zero exciton reflection coefficient corresponds to the translationally invariant susceptibility or dielectric approximation. This case according to Bishop and Maradudin [23] does not conserve probability since $|R_{exc}|_{\Sigma} \neq 1$. One can obtain Pekar's ABC Eq. (2.4.5) for χ_0=0. For R_{exc}=-1, this corresponds to Frenkel or tight binding excitons, which are totally reflected by the crystal surface. In this case the relative motion of electron-hole is not affected by the process. The last case: R_{exc}=+1, corresponds to Wannier excitons case. This case was treated first by Ting et al. [24] and one obtains a new ABC (Ting's ABC):

$$\frac{\partial \mathbf{P}_{exc}(\mathbf{r},t)}{\partial z}|_{\Sigma} = 0 \quad \text{or} \quad n_1(n_1^2 - \varepsilon_0)E_1 + n_2(n_2^2 - \varepsilon_0)E_2 = 0 \qquad (2.4.14)$$

All the above discussion was based on the assumption that the medium has a single oscillator resonance. Sein [25] also studied a "multi-oscillator" model consisting of N discrete excitonic levels each one with a possibly distinct kinetic energy or mass term. Each additional excitonic resonance gives rise to one additional boundary condition in the case of normal incidence, transverse propagation: or a total of N ABCs. Therefore, it is worth noting that the case of normal incidence reflectivity comprises: one incident field of unit amplitude, one reflected field amplitude $E_R(\omega)$ and (N+1) propagating amplitudes. Consequently one has to determine (N+2) unknowns: R(w), $E_j(\mathbf{k}, \omega)$. The total number of boundary conditions needed is 2 Maxwell B.C. plus N ABCs. All boundary conditions can be derived from the theory.

As a final word, in this review a selective partial account of the historical development of the ABC problem is presented. The emphasis is on the two different approaches: the first

one (Agranovich and Ginzburg, Hopfield and Thomas, Kiselev), has followed Pekar's scenario of setting up a microscopic oscillator model equation of motion like in Eq. (2.4.1) and solving it subject to certain boundary conditions on the oscillator. This yields the susceptibility. The susceptibility and the same boundary conditions are incorporated into Maxwell macroscopic equations. This procedure is not self-consistent at the macroscopic level since every susceptibility $\chi(\mathbf{r}, \mathbf{r}', \omega)$ comes with all the information to extract the needed boundary conditions for an arbitrary surface S of the crystal. The second procedure is a well posed problem in which one tries to solve Maxwell's macroscopic equations in a given non-local medium bounded by surface Σ subject to a prescribed non-local constitutive relation. A general review of this method (Birman and Sein, Maradudin and Mills, Agrawal et al., Zeyher et al., and Ting et al.) was presented here. More details in Birman [15].

2.5 REVIEW OF SOME EXPERIMENTS ON ABC PROBLEM

Shortly after the theoretical prediction of additional electromagnetic waves in solids, several attempts to verify Pekar's theory were made experimentally [26-27]. The first theoretical analysis of steady-state reflectivity was carried out by Pekar [1], while the first analysis of the experimental steady-state reflectivity measurements was done by Hopfield and Thomas [8] for the exciton resonances A(n=1) in CdS crystals. They observed a low reflectivity maximum in their studies in addition to the anomalous "spike" observed near the longitudinal frequency ω_ℓ, which could not be explained by the local optics dielectric function $\varepsilon(\omega)$. The structure of optical spectra near excitonic resonances could be understood using a spatial dispersion approach. Reflectivity spectra also depend strongly on the surface conditions such as surface impurities, surface fields, additional light, electron and ion bombardment,heating, etc. and on the past history of the crystal. Since, reflectivity spectra are extremely sensitive to ABCs, meaningful and reproducible results can be obtained from experiments performed on well-characterized samples.

Direct verification of the existence and dispersion $\omega(\mathbf{k})$ of additional light waves has been achieved by reflectivity and transmissivity measurements in thin CdS and CdSe crystals (Kiselev et al. [28, 29]) and by observation of resonant Brillouin scattering of exciton polaritons in GaAs (Ulbrich and Weisbuch [30]) and CdS (Winterling and Koteles [31]). The interference structure of optical spectra is very sensitive to the form of ABC (Kiselev et al. [32]).

In picosecond spectroscopy measurements of polariton propagation times have been made for various crystals.The polariton propagates in the crystal at the group velocity determined from the dispersion curve. Time-of-flight measurements have been carried out for CuCl by Segawa et al. [33] for GaAs by Ulbrich and Fehrenbach [34], for CdS by Aoyagi et al. [35] and for CdSe by Itoh et al. [36].

Even if the existence of two propagating modes has been demonstrated in various ways with innovative techniques made possible by the development of tunable lasers, the problem of the correct macroscopic dielectric function $\varepsilon(\mathbf{k}, \omega)$ for each system, and then the correct ABC remains unsolved. From a microscopic viewpoint the solution of Schrödinger equation requires specifying some boundary conditions for the exciton-polariton wave function $\Psi(\mathbf{r}, \omega)$ and its normal derivative $\partial\Psi(\mathbf{r}, \omega)/\partial n$ on the surface of the crystal. But it is a delicate and in general unsolved problem, to pass properly from the microscopic theory to the macroscopic, suitably averaging microscopic dipole moments to obtain the macroscopic polarization, and related quantities. From an experimental viewpoint, optical experiments yield strong evidence of spatial dispersion near the vicinity of resonance ω_t, and accurate measurement of exciton-polariton parameter values is needed to check the macroscopic dielectric function $\varepsilon(\mathbf{k}, \omega)$ for the correct ABC.

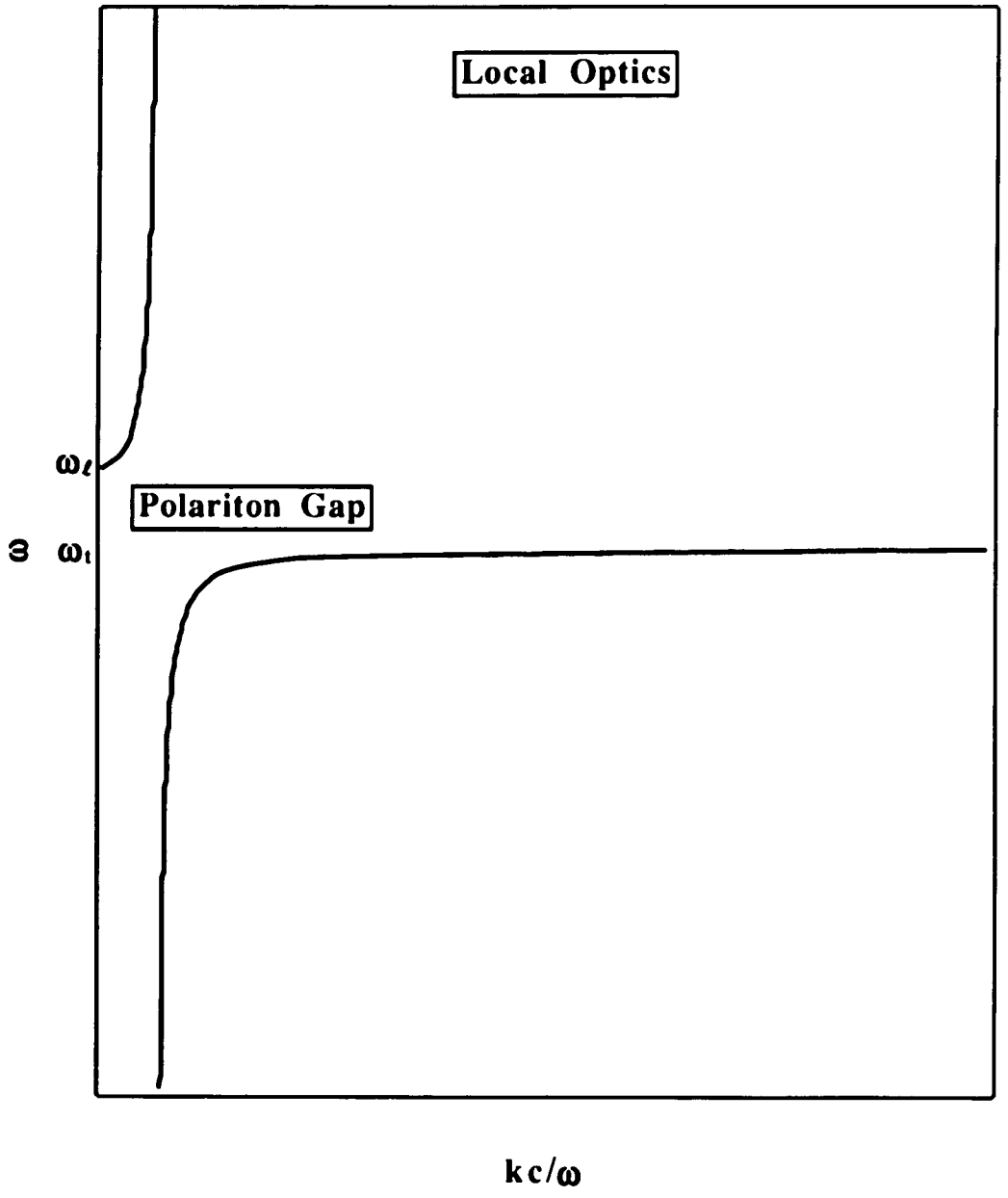

Figure 2.2.1(a) Schematic diagram of transverse polariton dispersion curves in a Local medium.

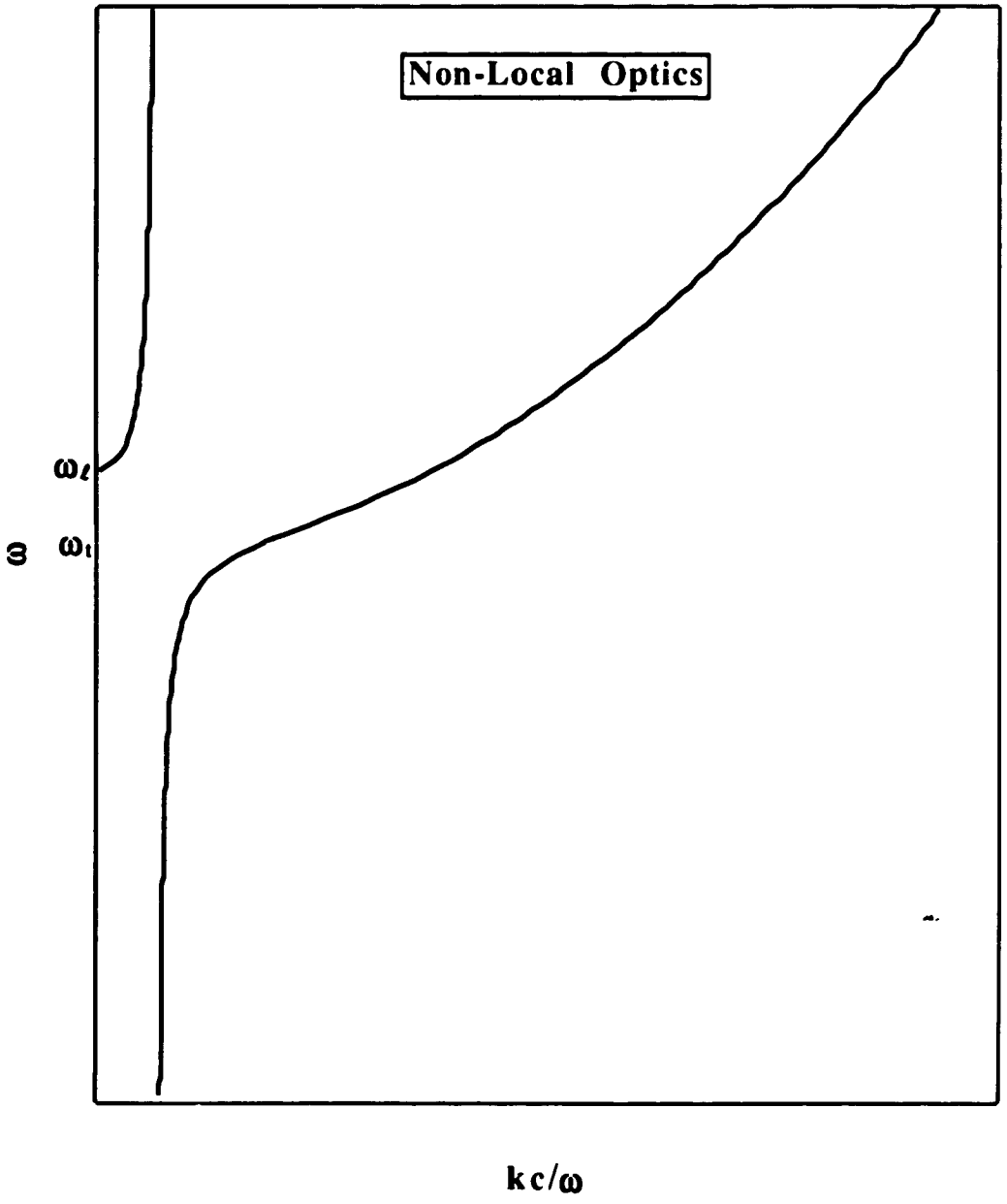

Figure 2.2.1(b) Schematic diagram of transverse exciton-polariton dispersion curves in a Non-Local (spatially dispersive) medium.

CHAPTER 3

TRANSIENT OPTICAL REFLECTIVITY FROM BOUNDED NON-LOCAL MEDIA: NORMAL INCIDENCE

Το δε χρωμα οτε μεν λαμπρον φαινεται των λαμπρων, οτε δε, η τω μειγνυσθαι τω του ενοπτρου η δια την ασθενειαν της οψεως, αλλου χρωματος εμποιει φαντασιαν.

The colour of bright objects sometimes appears bright in the reflection, but sometimes, either owing to contamination by the colour of the mirror or owing to the feebleness of our sight, produces an appearance of another colour.

Αριστοτελης, **Περι Μετεωρων**, III, 372, 7

3.1 INTRODUCTION

A type of experiment which can reveal novel transient effects due to non-locality is transient reflectivity. In this case, one considers the transient reflectivity from a semi-infinite non-local medium with a normally incident pulse of known shape and intensity. The merit of this type of experiment is that no attenuation occurs since both the incident and reflected electromagnetic fields are in vacuum. Transient optical reflectivity from a bounded local medium was first analyzed in detail by Elert [37] more than 50 years ago. A brief summary of his results follows:

Consider a semi-infinite frequency dispersive (local) medium occupying half space z>L and vacuum occupying z < L. At $t=0^+$ and z=L a laser pulse is incident on the local medium. The amplitude of the incident semi-infinite electromagnetic pulse is represented as: $E_I(0, t)=\sin(\omega_0 t)\,\Theta(t)$ where $\Theta(t)$ is the Heaviside function. The amplitude of the reflected field at z=0, can be written in an integral representation as,

$$E_R(0, t, \omega_0) = \operatorname*{Lim}_{\eta \to 0} \frac{\mathrm{Re}}{2\pi} \int_{-\infty}^{+\infty} d\omega \frac{\rho(\omega)}{\omega_0 - \omega - i\eta} \exp[-i\omega\{t - \frac{2L}{c}\}] \qquad (3.1.1)$$

where $\rho(\omega)$ is the frequency dependent reflectivity. For convenience, we placed the boundary surface at z=L. For times t < 2L/c no amplitude is received. Elert discussed the entire regime, starting immediately from the first detection of the front, followed by the oscillatory onset of transient reflectivity due to the response of the dipoles in the medium, which interferes with steady-state reflectivity of the main laser signal. Elert estimated the amplitude of the reflected transients to be 10^{-2} of the incident signal. In the case of a finite square pulse of duration T represented by the form $E_I(0, t)=\sin(\omega_0 t)\,[\Theta(t)-\Theta(t-T)]$, Elert showed that even though the main signal intensity drops drastically after pulse duration *T*,

transient reflectivity in the form of decaying oscillations still emerges from the dielectric medium.

Years later, Eilbeck [38] in the course of studying the propagation of intense, ultrashort optical pulses in a local resonant medium, tested the assumptions of slow varying envelope approximation (SVEA) in nonlinear theory, by calculating the reflected wave generated by short optical pulses incident on a linear dielectric. He argued that, linear theory is applicable at least to the leading and to the trailing edges of a nonlinear pulse; since one finds a large amount of energy reflected in linear theory, it is unjustifiable to ignore reflection and backscattering in any nonlinear theory, especially for dielectric media with densities about 10^{21} atoms per cm^{-3}. As examples, Eilbeck examined the cases of an input sech pulse modulating a resonant carrier wave, and modulating an input δ-function. Eilbeck showed that in both cases the trailing edges of the reflected pulses are larger and lasted longer than of incident ones.

Transient reflectivity from a non-local interface was reported for the first time for normal incidence in the case of Pekar's ABC, [39, 40] for a finite rectangular pulse; in addition to Elert's transient reflection after the incident pulse has died out, spatial dispersion contributes to transients, due to the finiteness of the exciton mass m^*.

Recently, Aaviksoo et al. [41] studied the reflection of a picosecond Gaussian pulse from a semi-infinite local Lorentz medium for normal and in p-polarized oblique incidence. They neglected spatial dispersion and surface phenomena; the reflected pulse is determined by the convolution of the excitation with the exponentially decaying response of the resonance. In this manner, the reflected short pulse acquires an exponential tail with a decay time determined by the width of the resonance (damping factor). Their numerical results for dielectric material like GaAs showed for normal incidence an exponential tail, whereas at Brewster angle incidence the tail is strongly oscillating. Similar results for normal incidence for CdS and CuCl materials were reported by Branis et al. [42].

A detailed numerical investigation of the transient reflection for ultrashort laser pulses close to Brewster angle was reported lately by Campell et al. [43]. Ignoring the non-locality of the dielectric medium, and taking a $sech^2$ input-pulse profile which is characteristic of well-mode-locked femtosecond lasers generating transform-limited pulses, they showed that femtosecond and even picosecond pulses undergo dramatic reshaping at their reflection very close to Brewster's angle for the optical carrier frequency.

Recently, Aaviksoo, et al. [44] presented for the first time, experimental analysis of the temporal structure of picosecond pulses reflected from GaAs, InP, and CdSe crystals near the lowest excitonic resonance at normal and Brewster angle incidence for incident short Gaussian pulses. The reflected pulses exhibit non-exponentially long decaying tails, which is in agreement with the theory of Gaussian pulse reflection [42].

The purpose of this chapter is to provide a detailed analysis of the effects of spatial dispersion on transient reflectivity, for various ABCs. When an electromagnetic pulse of finite duration T is incident on a non-local interface, the reflected field consists of the steady-state signal (of duration T) and transients arising from both the leading and the trailing pulse edges. Experimentally, it may be more convenient to look for trailing-edge transient reflectivity, since steady-state reflectivity will then not interfere with measurements. For long pulses (T > few psecs), transients from the two edges will be essentially decoupled and can be measured independently. In our case, we consider an incident square pulse and obtain expressions for steady-state and transient reflectivity for various ABCs. The results show that the transient reflectivity consists of a "local" part (Elert's part) and a "non-local" part. We obtain expressions for local and non-local parts respectively to show the differences among the ABCs, especially close to the exciton-polariton resonance frequency ω_t, where spatial dispersion effects are enhanced. We propose that by measuring the total transient reflectivity, it is possible to decide about the "true" ABC for the material by discriminating among the results for different ABCs. The local part is on the average larger than the non-local part at fixed time, especially close to

longitudinal frequency ω_ℓ , while the non-local part is enhanced at ω_t . The time oscillatory decay of both parts is also obtained, at fixed frequency. We show different oscillatory decay rates for both parts and for different ABCs. The magnitude of transient intensities should permit an experimental measurement.

The plan of the Chapter 3 is as follows: In Sect. 3.2, an integral representation for the reflected field is obtained, by using Fourier analysis in the time domain, for semi-infinite non-local medium. Using a contour-integration method, expressions for the steady-state and transient parts of the reflectivity are obtained in Sect. 3.3. Sect. 3.4 and 3.5 deal with the "non-local" and "local" parts of transient reflectivity, respectively. Detailed numerical results are presented for parameters appropriate to CdS and CuCl crystals. The results for total transient reflectivity are discussed in Sect. 3.6, while in Sect. 3.7, a brief discussion on "dead-layer" is given. We summarize our results and give some physical interpretation in Section 3.8. Necessary mathematical details are presented in the Appendices A, B, and C.

3.2 INTEGRAL REPRESENTATION FOR THE REFLECTED FIELD

Let us consider a semi-infinite non-local medium occupying the half space z > L with z < L being vacuum (see Fig. 3.2.1, page 47). A detector is placed at z=0. We assume that a normally incident laser pulse corresponds to a linearly, polarized, monochromatic plane wave-field. For a square pulse of unit intensity and duration T at frequency ω_0, the electric field at the plane z=0 is given by:

$$E_I(0,t) = \sin(\omega_0 t)[\Theta(t) - \Theta(t-T)] \qquad (3.2.1)$$

where Θ(t) is the Heaviside step function.

For laser frequency near the exciton resonance the coupling of an exciton state to a photon produces an exciton-polariton. Spatial dispersion or the non-locality of the medium corresponds to the center-of-mass motion of the exciton polariton. A generalized classical Lorenz oscillator model for the dielectric function is often taken as:

$$\varepsilon(\mathbf{k},\omega) = \varepsilon_0 + 4\pi\chi(\mathbf{k},\omega) = \varepsilon_0 + \frac{4\pi\alpha_0\ \omega_t^2}{\omega_t^2 - \omega^2 - i\omega\Gamma + (\frac{\hbar\omega_t}{m^*})k^2} \tag{3.2.2}$$

where ε_0 is the background dielectric constant, α_0 the oscillator strength, m^* the effective exciton-polariton mass, ω_t the transverse exciton-polariton frequency, while Γ is a phenomenological damping constant which has been taken constant in the vicinity of ω_t. In reality, for CdS [45, 46] and CuCl crystals [47], Γ depends on the frequency. Expression (3.2.2) produces a translationally invariant real space dielectric function $\varepsilon(\mathbf{r}, \mathbf{r}', \omega)$ after Fourier transformation. The expression (3.2.2) is called the "dielectric approximation".
For normal incidence, the amplitude reflection coefficient is given by [48, 49]:

$$\rho(\omega) = \frac{1-\bar{n}(\omega)}{1+\bar{n}(\omega)} \tag{3.2.3}$$

where $\bar{n}(\omega)$ is the effective refractive index of the non-local medium and for different ABCs has the following forms:

Pekar: $$\bar{n}(\omega) = \frac{n_1 n_2 + \varepsilon_0}{n_1 + n_2} \tag{3.2.4a}$$

Birman-Sein:

$$\bar{n}(\omega) = n_1 + n_2 - n_+ \tag{3.2.4b}$$

Ting:
$$\bar{n}(\omega) = \frac{n_1 n_2 (n_1 + n_2)}{(n_1^2 + n_2^2 + n_1 n_2) - \varepsilon_0} \tag{3.2.4c}$$

Kiselev:
$$\bar{n}(\omega) = \frac{\varepsilon_0 + n_1 n_2 + i\gamma n_1 n_2 (n_1 + n_2)}{n_1 + n_2 + i\gamma (n_1^2 + n_2^2 + n_1 n_2 - \varepsilon_0)} \tag{3.2.4d}$$

and n_1, n_2 are the solutions of the implicit relation:

$$n_j = +[\varepsilon(k_j, \omega)]^{1/2}, \quad k_j = n_j \frac{\omega}{c}, \quad j = 1,2 \tag{3.2.5}$$

Because of the linearity of the problem, we may time-Fourier analyze Eq. (3.2.1) and treat each frequency component independently by dispersion theory. The reflected field is obtained as a superposition of the reflected components and can be written as the frequency integral:

$$E_R(0,t,\omega_0) = Lim\ \mathrm{Re}\frac{1}{2\pi}\int_{-\infty}^{+\infty} \frac{d\omega\, \rho(\omega)}{\omega_0 - \omega - i\eta}\{1 - \exp(i(\omega - \omega_0)T)\}\exp(-i\omega(t - \frac{2L}{c})) \tag{3.2.6}$$
$$\eta \to 0$$

where the time delay 2L/c corresponds to a round trip between z=0 and z=L.

3.3 STEADY-STATE AND TRANSIENT REFLECTIVITY

The reflected field, in Eq. (3.2.6), can be separated into steady-state and transient parts, after removing the harmonic time dependance: $\exp(-i\omega t)$. The steady-state part gives rise to a reflected pulse (of duration T) whose leading and trailing edges contain the rapidly time-varying transient contributions. The integral in Eq. (3.2.6) is evaluated in the complex ω-plane using the method of contour integration. Using Eq. (3.2.3) in Eq. (3.2.6), the integrand is found to have the following singularities which are the same for all four ABCs:

(i) a simple pole at ω_0-$i\eta$,

(ii) four branch points ω_j (j=1, 4) in the lower half-plane,

(iii) two branch points ω_5 and ω_6 in the upper-half plane.

All six branch points correspond to branch point singularities of the complex functions $n_1(\omega)$, $n_2(\omega)$.

(iv) For Birman-Sein's ABC, there are two additional branch points ω_7 and ω_8 in the lower half-plane, corresponding to the branch point singularities of the complex function $n_+(\omega)=k_+c/\omega$.

The explicit expressions for the location of these branch points are obtained using Eqs. (3.2.2) and (3.2.5) and are obtained in simple form by noting the fact that for most materials like CdS, CuCl, GaSe, GaS, the parameters $\delta=(\hbar\omega_t/m^*c^2)^{1/2}$, $p=\beta^2/2\varepsilon_0$, Γ/ω_t are small ($\leq 10^{-3}$); so that it is sufficient to retain only lowest order terms in δ, p, Γ/ω_t. Thus one obtains:

$$\omega_{1,2} = -i\frac{\Gamma}{2} \pm \omega_t(1+p) \tag{3.3.1}$$

$$\omega_{3,4} = -i\left(\frac{\Gamma}{2} + \beta\delta\omega_t\right) \pm \omega_t \tag{3.3.2}$$

$$\omega_{5,6} = i(\beta\delta\omega_t - \frac{\Gamma}{2}) \pm \omega_t \tag{3.3.3}$$

$$\omega_{7,8} = -i\frac{\Gamma}{2} \pm \omega_t \tag{3.3.4}$$

where:

$$\beta = (4\pi\alpha_0)^{1/2} \qquad \delta = (\frac{\hbar\omega_t}{m^* c^2})^{1/2} \tag{3.3.5}$$

Note that the dimensionless parameter δ is a measure of the extent of non-locality of the medium (spatial dispersion coefficient). We also assume $\Gamma < 2\beta\delta\omega_t$ i.e we exclude very heavily damped exciton polaritons.

For $t < 2L/c$ we chose the contour in the upper-half plane which is chosen so as to exclude the branch-cut line joining ω_5 and ω_6. An evaluation of the integral in Eq. (3.2.6) shows that the branch points ω_5 and ω_6 contribute in such a manner that $E_R(t < 2L/c) = 0$ as required by causality.

For $t \geq 2L/c$, we close the contour in the lower-half plane. The four branch points $\omega_{1,2}$, $\omega_{3,4}$ for the case of Pekar, Ting, Kiselev's ABC and the six branch points $\omega_{1,2}$, $\omega_{3,4}$, $\omega_{7,8}$ for Birman-Sein's ABC are joined by branch-cut lines and the resulting contour for both cases is shown in Figs. 3.3.1(a) and 3.3.1(b) (pages 48 and 49). Evaluation of the integral in Eq. (3.2.6) is lengthy, although straightforward. Algebraic details are presented in the Appendix A. Here we note that the reflected field is found to consist of three parts (see Eq. (A20)):

$$E_R(0,t,\omega_0)=\mathrm{Re}[\tilde{E}_S(t)+\tilde{E}_L(t)+\tilde{E}_{NL}(t)] \tag{3.3.6}$$

The simple pole at ω_0-iη contributes to the steady-state reflected field $\tilde{E}_S(t)$. The four branch points (or the six for Birman-Sein's ABC) contribute to the transient reflected field which consists of a local part $\tilde{E}_L(t)$ and a non-local part $\tilde{E}_{NL}(t)$ Although $\tilde{E}_S(t)$ and $\tilde{E}_L(t)$ both are affected by spatial dispersion, $\tilde{E}_{NL}(t)$ arises solely from it and vanishes as $\delta \rightarrow 0$ ($m^* \rightarrow \infty$). Further in the limit of $\delta \rightarrow 0$, $\tilde{E}_S(t)$ and $\tilde{E}_L(t)$ reduce to the previously obtained results . We now consider the steady-state and transient parts of the reflected field separately.

A. STEADY-STATE REFLECTIVITY

Using Eq. (A21) from the Appendix, $\tilde{E}_S(t)$ is given by

$$\tilde{E}_S(t)=-i\rho(\omega_0)\exp[-i\omega_0(t-\frac{2L}{c})] \tag{3.3.7}$$

for all ABCs for $2L/c < t < 2L/c+T$ and zero otherwise. After an initial delay, a reflected square pulse of duration T arrives at the plane z=0. In Figs. 3.3.2 and 3.3.3 (pages 50 and 51), we have shown the reflectivity: $|R_0|^2=|\rho(\omega_0)|^2$ as a function of ω_0/ω_t in the vicinity of the exciton-polariton resonance for parameters appropriate to CdS and CuCl crystals, for all ABCs, respectively. Reflectivity for a local medium (δ=0) is shown by a solid line for comparison. We notice that the main effect of spatial dispersion is to reduce the peak height of reflectivity for all ABCs but more drastically for Pekar's and Birman-Sein's ABC. The reason is that for Pekar's and Birman-Sein's ABC, the correction to the local medium reflectivity by the spatial dispersion is in order of $O(\delta)$, while for Ting's and Kiselev's ABC is of order of $O(\delta^2)$.

B. TRANSIENT REFLECTIVITY

Transient reflectivity consists of a "local" part and a "non-local part":

$$\tilde{E}_T(t) = \tilde{E}_L(t) + \tilde{E}_{NL}(t) \tag{3.3.8}$$

where "local" part is defined as the part remaining in $E_L(t)$ when $\delta \rightarrow 0$ and from Eq. (A22):

$$\tilde{E}_T(t) = [E_j(t - \frac{2L}{c})\,\Theta(t - \frac{2L}{c}) - \\ -\exp(-i\omega_0 T) E_j(t - \frac{2L}{c} - T)\,\Theta(t - \frac{2L}{c} - T)] \tag{3.3.9}$$

for j=L and NL and $E_L(t)$ and $E_{NL}(t)$ are given by Eqs. (A16) through (A19). The two terms in Eq. (3.3.9) correspond to transients arising from the leading and trailing pulse edges, respectively. If the pulse duration T is longer than the effective time during which transients significantly contribute, leading-and-trailing edge transients will not interfere and can be consider independently. Up to a constant phase factor, transients from both edges are identical in form and magnitude and are governed by $E_j(t)$. Experimentally, it may be more convenient to look for trailing-edge transients which appear just after the reflected pulse is cut off at $t = 2L/c+T$. Using Eqs. (A3) and (A12) in Eq. (A23) the local part of the trailing edge transient reflectivity is found to be given by:

$$E_L(\tau) = \exp(-i\omega_t \tau)\exp(-\frac{\Gamma\tau}{2})(\frac{p\omega_t}{2\pi})\times$$

$$\times\int_0^1 \frac{[\rho(n_1,n_2)-\rho(-n_1,n_2)]}{(\omega_t-\omega_0+p|\omega_t|u-i\frac{\Gamma}{2})}\exp(-ip\omega_t\tau u)\,du+(\omega_t\rightarrow-\omega_t) \qquad (3.3.10)$$

for Pekar, Ting, and Kiselev's ABC. By using Eqs. (A3) and (A14) in Eq. (A25):

$$E_L(\tau)=\exp(-i\omega_t\tau)\exp(-\frac{\Gamma\tau}{2})(\frac{p\omega_t}{2\pi})\times$$

$$\times\int_0^1 \frac{[\rho(n_1,n_2,n_+)-\rho(-n_1,n_2,n_+)]}{(\omega_t-\omega_0+p|\omega_t|u-i\frac{\Gamma}{2})}\exp(-ip\omega_t\tau u)\,du+(\omega_t\rightarrow-\omega_t) \qquad (3.3.11)$$

for Birman-Sein's ABC. Here, the dependence of $\rho(\omega)$ on the refractive indices n_1 and n_2 plus its dependence on n_+ for Birman-Sein's ABC is explicitly shown and n_1, n_2 and n_+ are to be evaluated at frequency: $\omega=\omega_t+p\omega_t u-i\Gamma/2$. As a reminder: $p=2\pi\alpha_0/\epsilon_0=(\omega_\ell-\omega_t)/\omega_t$.
It is easy to verify that $E_L(\tau)$ reduces to Elert's result for all ABCs in the limit of infinite exciton mass. This follows by noting that when $\delta\rightarrow 0$, $\bar{n}=n_1$ for all ABCs and the term in square brackets in Eqs. (3.3.10) and (3.3.11) reduces to $-4n_1/(1-n_1^2)$.
The non-local part is given by Eq. (A24) which together with (A3) and (A12) becomes:

$$E_{NL}(\tau)=\exp(-i\omega_t\tau)\exp(-\frac{\Gamma\tau}{2})(\frac{i\beta\delta\omega_t}{2\pi})\times$$

$$\times\{\int_0^1 \frac{[\rho(n_1,n_2)-\rho(-n_1,n_2)]}{(\omega_t-\omega_0-i\beta\delta|\omega_t|u-i\frac{\Gamma}{2})}\exp(-\beta\delta|\omega_t|\tau u)\,du+(\omega_t\rightarrow-\omega_t)$$

$$+\int_1^{\infty}\frac{[\rho(n_1,n_2)-\rho(-n_2,n_1)]}{(\omega_t-\omega_0-i\beta\delta|\omega_t|u-i\frac{\Gamma}{2})}\exp(-\beta\delta|\omega_t|\tau u)\,du+(\omega_t\rightarrow-\omega_t)\}\qquad(3.3.12)$$

for Pekar, Ting, Kiselev's ABC; and from Eq. (A24) with (A14) and (A3):

$$E_{NL}(\tau)=\exp(-i\omega_t\tau)\exp(-\frac{\Gamma\tau}{2})(\frac{i\beta\delta\omega_t}{2\pi})\times$$

$$\times\{\int_0^1\frac{[\rho(n_1,n_2,n_+)-\rho(-n_1,n_2,-n_+)]}{(\omega_t-\omega_0-i\beta\delta|\omega_t|u-i\frac{\Gamma}{2})}\exp(-\beta\delta|\omega_t|\tau u)\,du+(\omega_t\rightarrow-\omega_t)$$

$$+\int_1^{\infty}\frac{[\rho(n_1,n_2,n_+)-\rho(-n_2,n_1,-n_+)]}{(\omega_t-\omega_0-i\beta\delta|\omega_t|u-i\frac{\Gamma}{2})}\exp(-\beta\delta|\omega_t|\tau u)\,du+(\omega_t\rightarrow-\omega_t)\}\qquad(3.3.13)$$

for Birman-Sein's ABC where the ellipses represent a similar expression obtained by $\omega_t\rightarrow -\omega_t$. Here, the dependence of $\rho(\omega)$ on the refractive indices n_1 and n_2 plus its dependence on n_+ for Birman-Sein's ABC is explicitly shown and n_1, n_2 and n_+ are to evaluated at frequency: $\omega=\omega_t+i\beta\delta\omega_t u-i\Gamma/2$. Note that $\tilde{E}_{NL}(t)$ is proportional to the spatial dispersion parameter δ and vanishes for the case of local medium in the limit of infinite exciton mass ($\delta=0$).

Eqs. (3.3.9) through (3.3.13) give the total transient reflected field associated with a square pulse of duration T. In the following, we focus our attention on transients arising from the trailing pulse edge and set: τ = t-2L/c-T. For T > few picoseconds, leading-edge transients would die out before the trailing edge of the pulse arrives and therefore:

$$\tilde{E}_j(\tau)\cong-\exp(-i\omega_0 T)\,E_j(\tau)\qquad(3.3.14)$$

where $\tau > 0$ and j=L and NL.

Since the transient effects are expected to be important only in the immediate vicinity of an exciton-polariton resonance, we shall assume that the laser frequency $\omega_0=\omega_t$. Under near-resonance conditions, the second term in Eqs. (3.3.10), (3.3.11) and the last two terms in Eqs. (3.3.12), (3.3.13) will not contribute significantly and henceforth will be neglected. It may be noted that these terms arise from the branch points lying in the third quadrant of the complex ω-plane (see Figs. 3.3.1(a) and 3.3.1(b), pages 48 and 49). In the next two sections we consider the non-local and local parts of transient reflectivity separately.

3.4 NONLOCAL TRANSIENT REFLECTIVITY

In this section we simplify the non-local parts of transient reflectivity, [Eqs. (3.3.12) and (3.3.13)] and discuss various features numerically and qualitatively. For this purpose we need to evaluate n_1, n_2 and n_+ at frequency: $\omega=\omega_t+i\beta\delta\omega_t u-i\Gamma/2$. Details of the mathematical evaluation for $\beta/\delta>>1$ are given in Appendix B. The non-local transient reflectivity $E_{NL}(\tau)$ has the form:

$$\mathrm{Re}[E_{NL}(\tau)]=\left|R_1(\tau)\right|\sin(\omega_t\tau-\phi_1) \qquad (3.4.1)$$

where $R_1(\tau)=|R_1(\tau)|\exp[i\phi_1(\tau)]$ is given by:

$$R_1(\tau)=i\exp(-i\omega_t\tau)\exp(-\frac{\Gamma\tau}{2})(\frac{2\beta\delta^3}{\pi^2})^{\frac{1}{2}}\exp(\frac{i\pi}{4})\times$$

$$\times\{\int_0^1 \frac{du\exp(-\beta\delta\,\omega_t\,\tau u)}{(\omega_t-\omega_0-i\beta\delta\,\omega_t u-i\frac{\Gamma}{2})}F_1+\int_1^{\infty}\frac{du\exp(-\beta\delta\,\omega_t\,\tau u)}{(\omega_t-\omega_0-i\beta\delta\,\omega_t u-i\frac{\Gamma}{2})}F_2\} \qquad (3.4.2)$$

where F_1 and F_2 are complicated functions of the integration variable u and $\delta/2\beta$, and are different for different ABC's. Their form is given below:

$$F_1=\frac{\sqrt{1+u}+i\sqrt{1-u}}{1+(\frac{2\delta}{\beta})^{\frac{1}{2}}\exp(\frac{i\pi}{4})[\sqrt{1+u}-i\sqrt{1-u}]} \text{ and } F_2=\frac{\sqrt{u+1}-\sqrt{u-1}}{1+(\frac{2\delta}{\beta})^{\frac{1}{2}}\exp(\frac{i\pi}{4})[\sqrt{u+1}+\sqrt{u-1}]}$$

for Pekar's ABC;

$$F_1=\frac{1}{2}\frac{\sqrt{1+u}+i\sqrt{1-u}}{1+(\frac{2\delta}{\beta})^{\frac{1}{2}}\exp(\frac{i\pi}{4})[\sqrt{1+u}-i\sqrt{1-u}+2\sqrt{u}]}$$

$$F_2=\frac{1}{2}\frac{\sqrt{u+1}-\sqrt{u-1}}{1+(\frac{2\delta}{\beta})^{\frac{1}{2}}\exp(\frac{i\pi}{4})[\sqrt{u+1}+\sqrt{u-1}+2\sqrt{u}]}$$

for Birman-Sein's ABC;

$$F_1=\frac{[(1+2u)\sqrt{1-u}+i\sqrt{1+u}\,(1-2u)]/2}{\sqrt{1-u^2}+(\frac{\delta}{2\beta})^{\frac{1}{2}}\exp(\frac{i\pi}{4})[(1+2u)\sqrt{1-u}-i\sqrt{1+u}\,(1-2u)]}$$

$$F_2=\frac{[(2u+1)\sqrt{u-1}-\sqrt{u+1}\,(2u-1)]/2}{\sqrt{u^2-1}+(\frac{\delta}{2\beta})^{\frac{1}{2}}\exp(\frac{i\pi}{4})[(1+2u)\sqrt{u-1}+\sqrt{u+1}\,(2u-1)]}$$

for Ting's ABC; while for Kiselev's ABC the expressions become quite complicated.

We evaluate $|R_1(\tau)|$ numerically for parameters appropriate to CdS and CuCl crystals. The results are displayed in Figs. 3.4.1 and 3.4.2 (pages 52 and 53 for various ABCs, for the case of exact resonance: $\omega_0=\omega_t$. At a time $\tau=0$, when the trailing edge of the reflected pulse has just passed and steady-state reflectivity has dropped to zero, $|R_1(0)|^2$ is about 0.01-0.1% of the incident intensity, depending on the choice of ABC. As τ increases, $|R_1(\tau)|^2$ begins to decrease exponentially, but about $\tau \approx 1$ psec a crossover from an exponential to a slow power-law decay takes place. The resulting tail shows that, the on-resonance non-local transient reflectivity persists for a few psecs, after the reflected pulse is cut off. The results are qualitatively the same for all ABCs, but they differ quantitatively, depending on the choice of ABC and the material.

Resonant enhancement of the non-local transient reflectivity is another remarkable feature and is illustrated in Figs. 3.4.3 and 3.4.4 (pages 54 and 55) for CdS and CuCl crystals. At fixed time $\tau=0.1$ psec, $|R_1(\omega_0)|$ is shown as a function of the laser frequency ω_0 in the vicinity of the exciton-resonance frequency ω_t. Enhancement of $|R_1(\omega_0)|^2$ by a factor 2-10 for various ABCs is observed in a narrow frequency range.

The non-local part of the transient reflectivity decreases when the effective exciton-polariton mass m^* is increasing (or when the spatial dispersion coefficient δ decreases). In this case, CuCl curves are quantitatively smaller in magnitude than the curves for CdS crystals, because of the higher effective mass for CuCl crystals. Especially, in the limit of infinite mass (local optics: $\delta=0$), non-local transient reflectivity vanishes. Nonlocal transients constitute an additional channel in reflection of optical pulses from crystals. The finiteness of the exciton-polariton mass m^* is the source of non-local transient contribution. The energy of the dipoles is "backscattered" not in electromagnetic reradiation way, but through the mechanical oscillations of the dipoles plus the damping of exciton-polaritons. This can been seen in the exponential form of the non-local transients for all ABC's. In our

case, for both materials [CdS and CuCl] $\Gamma < 2\beta\delta\omega_t$ we have excluded heavily damped excitons.We now consider the local part $E_L(t)$ modified by spatial dispersion.

3.5 LOCAL PART OF TRANSIENT REFLECTIVITY

In this section we simplify the local part of transient reflectivity $E_L(t)$, [Eqs. (3.3.10) and (3.3.11)], following the procedure of Section 3.4 and discuss various features numerically and qualitatively for CdS and CuCl crystals. For this purpose we need to evaluate n_1, n_2 and n_+ at frequency: $\omega=\omega_t+p\omega_t u-i\Gamma/2$. Details of the mathematical evaluation to the leading order in δ are given in Appendix C. The local transient reflectivity $E_L(\tau)$ has the form:

$$\mathrm{Re}[E_L(\tau)]=|R_2(\tau)|\sin(\omega_t\tau-\phi_2) \tag{3.5.1}$$

where $R_2(\tau)=|R_2(\tau)|\exp[i\phi_2(\tau)]$ is given by:

$$R_2(\tau)=i\exp(-i\omega_t\tau)\exp(-\frac{\Gamma\tau}{2})(\frac{2p\omega_t}{\pi\sqrt{\varepsilon_0}})\times$$

$$\times\{\int_0^1 \frac{du\exp(-ip\omega_t\tau u)}{(\omega_t-\omega_0+p\omega_t u-i\frac{\Gamma}{2})}\frac{(u-u^2)^{\frac{1}{2}}}{[1-\frac{(\varepsilon_0-1)}{\varepsilon_0}u]}F(u)\} \tag{3.5.2}$$

where

$$F(u)=1-\frac{2\delta}{\beta}(\frac{\varepsilon_0}{u})^{1/2}\frac{1}{[1-\frac{\varepsilon_0-1}{\varepsilon_0}u]} \tag{3.5.3a}$$

for Pekar's ABC;

$$F(u) = 1 - \frac{\delta}{\beta}\left(\frac{\varepsilon_0}{u}\right)^{1/2} \frac{1}{\left[1 - \frac{\varepsilon_0 - 1}{\varepsilon_0} u\right]} \tag{3.5.3b}$$

for Birman-Sein's ABC;

$$F(u) = 1 - \left(\frac{\varepsilon_0 \delta}{\beta}\right)^2 \frac{1}{\left[u^2 + \left(\frac{\varepsilon_0 \delta}{\beta}\right)^2\right]} \frac{\left[1 - \frac{(\varepsilon_0 + 1)}{\varepsilon_0} u\right]}{\left[1 - \frac{(\varepsilon_0 - 1)}{\varepsilon_0} u\right]} \tag{3.5.3c}$$

for Ting's ABC; and

$$F(u) = 1 - \left(\frac{\varepsilon_0 \delta}{\beta}\right)^2 \frac{1}{\left[u^2 + \left(\frac{\varepsilon_0 \delta}{\beta}\right)^2\right]} \frac{\left[1 - \frac{(\varepsilon_0 + 1)}{\varepsilon_0} u\right] - \frac{2iu}{\gamma \varepsilon_0}}{\left[1 - \frac{(\varepsilon_0 - 1)}{\varepsilon_0} u\right]} \tag{3.5.3d}$$

for Kiselev's ABC.

Eqs. (3.5.3) show how the local part $|R_2(\tau)|$ of transient reflectivity is affected by spatial dispersion. We first consider the case of exact resonance, at $\omega_0=\omega_t$. Figs. 3.5.1 and 3.5.2 (pages 56 and 57) show the time decay of $|R_2(\tau)|$ for parameters appropriate to CdS and CuCl crystals, respectively. By a solid line, we also show the corresponding curves obtained for a local medium ($\delta=0$). A close look shows that the effect of spatial dispersion reduces $|R_2(\tau)|$ and damps out its variation with time faster than the local case (Elert's result). The rate of oscillations depends on the ω_{LT} splitting of the material; CuCl shows faster oscillatory behavior than CdS for the same Γ/ω_t, since for CuCl ω_{LT}=5.7 meV, while for CdS ω_{LT}=2 meV. When we compare Figs. 3.5.1 and 3.5.2 with Figs. 3.4.1 and 3.4.2, respectively, we note that $|R_2(\tau)|^2$ is larger than $|R_1(\tau)|^2$ by about 4-10 times. Spatial dispersion reduces $|R_2(\tau)|$ for Pekar's and Birman-Sein's ABC (first order in δ); while $|R_2(\tau)|$ is almost close to local case ($\delta=0$) for Ting's and Kiselev's ABC (second order in δ). The local transient reflectivity $E_L(\tau)$, is a combination of three different channels of

energy propagation: E-M backscattering due to the oscillatory dephasing process of the dipoles, damping of the dipoles and mechanical oscillations of the dipoles Especially, the E-M contribution corresponds to Elert's result and a closed analytical expression can be obtained for $|R_2(\tau)|$ in Eq. 3.5.2 near resonance $\omega_0 \approx \omega_t$, small damping $\Gamma << \omega_{LT}$ and $\varepsilon_0 >> 1$:

$$|R_2(\tau)| \approx \frac{2}{\sqrt{\varepsilon_0}} \exp(-\frac{\Gamma\tau}{2}) |J_0(\frac{p\omega_t\tau}{2})| \qquad (3.5.4)$$

where $J_0(p\omega_t\tau/2)$ is the Bessel function of zero order. The oscillatory behavior of the local part can be understood due to the fact that for small Γ and for fast cut-off of the pulse. the electric dipole radiation arises when the system of dipoles reemits the light through radiative dephasing of individual processes.

Resonant enhancement of local transient reflectivity is shown in Figs. 3.5.3 and 3.5.4 (pages 58 and 59) for CdS and CuCl crystals. At fixed time t=0.1 psec, $|R_2(\omega_0)|$ is shown as a function of the laser frequency ω_0 in the vicinity of the exciton-resonance frequency ω_t. For comparison, we also show the corresponding curves obtained for a local medium (δ=0). The peak of $|R_2(\omega_0)|$ is now, at ω_ℓ instead of ω_t as it was in the case of $|R_1(\omega_0)|$. A remarkable difference between CdS and CuCl crystals, is that the later shows a richer structure for $|R_2(\omega_0)|$; we observe in Fig. 3.5.4, that for CuCl an additional local maximum at ω_t exists for all ABCs and local case, which cannot be detected for CdS crystals. The difference lies in the different values of the material parameters like: p, ω_t, and ε_0; their combination is larger for CuCl crystals. A possible explanation for this is based on the observation the the gap for CuCl (ω_{LT}=5.7 meV) is broader than the CdS case (ω_{LT}=2 meV) which permits one to see the richer structure of transient reflectivity in the vicinity of ω_t. The structure could be assigned to the decrease of exciton-polariton group velocity in

the gap; exciton-polaritons are heavily damped in this region, which slows down their motion.

3.6 TOTAL TRANSIENT REFLECTIVITY

In Figs. 3.6.1 and 3.6.2, (pages 60 and 61) we now give the time behavior of total transient reflectivity $|R_1(\tau)+R_2(\tau)|$ at resonance $\omega_0=\omega_t$, for CdS and CuCl crystals, respectively, which shows the combined effect of local and non-local parts. The total reflectivity decays in a few psecs, but the local part is stronger and dominates. The oscillatory behavior is faster for CuCl material than CdS because CuCl has larger β^2 (oscillator strength) than CdS. Both materials show damped oscillatory behavior, but CdS has slower decay for the same Γ/ω_t and significant quantitative differences between different ABCs compared to CuCl. So CdS can be a good candidate to observe the time evolution of transient reflectivity. The oscillatory behavior in the local part can be understood to be due to the fact that for small Γ/ω_t and fast cut-off time of the pulse, the response time of the electric dipoles arise in a distinct way [50-52]. However, in case of the non-local part, we do not see the oscillations due to the finite effective exciton-polariton mass. With increase of damping Γ/ω_t (for shorter relaxation times), the reflected pulse energy dissipates through damping process exponentially very fast without oscillations.
For fixed time τ=0.1 psec, around the vicinity of exciton-polariton resonance ω_t, we plot total reflectivity $|R_1(\omega_0)+R_2(\omega_0)|$ versus laser frequency ω_0 for CdS and CuCl crystals respectively (see Figs. 3.6.3 and 3.6.4, pages 62 and 63). Spatial dispersion reduces the total amplitude for all ABCs, while local part still dominates. A remarkable result for CuCl material is the combined effect of local and non-local parts which enhances even more the double peak we find for local transient reflectivity for all ABCs and local case (δ=0). In contrast, in CdS which does not show any double peak for local transient reflectivity case, now shows it only for Pekar's ABC. Results for CdS, assigned this double peak behavior

to the specific form of Pekar's ABC, but CuCl shows that this qualitative behavior prevails for all ABCs and even for local case (δ=0). A possible explanation for this phenomenon could be the broader gap for CuCl (ω_{LT}=5.7 meV) compared to CdS case (ω_{LT}=2 meV) that permits one to see the richer structure of transient reflectivity in the vicinity of ω_t. This structure could be assigned to exciton-polariton group velocity decrease in the gap. Exciton-polaritons are heavily damped in this region, which slows down their motion. For this reason, CuCl is a good candidate to investigate transient reflectivity in the vicinity of ω_t.

3.7 THE DEAD-LAYER PROBLEM

Certain authors [6, 31, 32, 45] have found that for high quality CdS and CdSe crystals, the experimental reflectivity measurements show a spike of the reflectivity at ω_ℓ which is recovered by incorporating the "dead-layer" concept. Due to surface repulsion of the excitons, one can define an exciton-free region of thickness Δ where the excitons are forbidden to enter. The layer Δ can be described by ε_0 the non-resonance part of the dielectric function $\varepsilon(\mathbf{k}, \omega)$. Other authors [53, 54] have not found such a correlation between the quality of the crystals and the existence of the spike in the reflectivity spectra. Since, the problem is still open, a possible extension of our work, would be to incorporate the model of surface "dead layer" in our calculations. The reflection coefficient for the geometry: vacuum - surface "dead" layer - non-local semi-infinite medium is given by the following expression [6]:

$$\rho(\omega) = \frac{r_{12} + r_{23} \exp[2ik_0\sqrt{\varepsilon_0}\,\Delta]}{1 + r_{12}\, r_{23} \exp[2ik_0\sqrt{\varepsilon_0}\,\Delta]} \qquad (3.7.1)$$

with

$$r_{12} = \frac{1-\sqrt{\varepsilon_0}}{1+\sqrt{\varepsilon_0}} \quad \text{and} \quad r_{23} = \frac{\sqrt{\varepsilon_0} - \bar{n}(n_1, n_2)}{\sqrt{\varepsilon_0} + \bar{n}(n_1, n_2)} \tag{3.7.2}$$

where r_{12} is the reflection coefficient for the vacuum - dead layer interface, r_{23} is the reflection coefficient for the dead layer - non-local medium interface, and $k_0=\omega/c$. The transient reflectivity for an incident square pulse of unit intensity and duration T at frequency ω_0, (see Eq. 3.2.1), is given by Eq. (3.2.6), where now the reflection coefficient $\rho(\omega)$ is described by Eq. (3.7.1). The derivation of local and non-local parts of transient reflectivity is straightforward. It can lead to analytical expressions for the tail of the reflected pulse for various dead layer thicknesses Δ. The dead layer thickness Δ is an external parameter in our theory, and has not been calculated through a microscopic model, but it is chosen in such a way to agree with the experimental reflectivity data. But, Δ is an additional parameter in the problem (in addition to damping factor Γ) and will complicate the simple model of transient reflection from the interface vacuum - non-local medium. It will be important to investigate the influence of dead layer to the reflectivity spectra and compare them with experiments, since Δ is widely used in fitting data.

3.8 CONCLUSIONS

We have carried out analytical and numerical calculations for the reflectivity of an E-M pulse of duration T from a spatial dispersive semi-infinite medium in the case of normal incidence. We investigated the role of different ABCs on the steady-state reflectivity and transient reflectivity. Especially, in the time domain, after the pulse dies out, the medium continues emitting energy in damped oscillatory form for the case of long relaxation times

($\Gamma/\omega_t << 1$). Different ABCs influence the decay process in a different quantitative way especially for laser frequency ω_0 very close to the exciton-polariton resonance frequency ω_t, where spatial dispersion effects are dominant. In the frequency domain, the transient reflectivity amplitude shows a double peak at ω_t and ω_ℓ, for some or all ABCs depending on the choice of material. The reflection of the incident field (see Eq. (3.2.1)), changes the frequency spectrum of the reflected field. Starting with the Fourier spectrum of the incident field near resonance ($\omega_0 \approx \omega_t$)

$$E_{INC}(\omega) = \frac{1}{2\pi} \frac{1 - \exp[i(\omega - \omega_t)T]}{\omega_t - \omega - i\eta} \tag{3.8.1}$$

the Fourier transform of the reflected field consists of 2 parts in the case of local optics (see Eq. (3.3.6)): the first term comes from the Fourier transform of the steady-state reflectivity in Eq. (3.3.7) and it is given by the following expression:

$$E_S(\omega) = -\frac{\rho(\omega_t)}{2\pi} \exp[i\omega \frac{2L}{c}] \frac{1 - \exp[i(\omega - \omega_t)T]}{\omega_t - \omega - i\eta} \tag{3.8.2}$$

while the second term corresponds to the contribution of the transient part in Eq. (3.5.4):

$$E_T(\omega) = \frac{2i}{\sqrt{\varepsilon_0}} \exp[i\omega(\frac{2L}{c} + T)] \begin{cases} \frac{1}{\sqrt{p\omega_t \Gamma}}, & \omega = \omega_\ell \\ \frac{1}{\sqrt{\omega|\omega - \omega_\ell|}}, & \omega \neq \omega_\ell \end{cases} \tag{3.8.3}$$

The Fourier spectrum of the reflected field is qualitatively different than that of the incident field. The main signal changes the magnitude (proportional to reflectivity coefficient $\rho(\omega \approx \omega_t)$) and phase (because of the time delay in the round trip of distance 2L/c).

Furthermore, the reflected field frequency spectrum acquires an additional term from the transient contribution, which has a peak at $\omega=\omega_\ell$.

As a consequence of the theoretical analysis in this Chapter and taking into account that the transient reflectivity "informs" us about the decay dynamics of the polarization inside the crystal, we have distinguished three different channels for transient reflectivity. After the main incident pulse is cut-off, all the energy that has been stored inside the dielectric, partially is reemitted backwards due to oscillating dephasing process, which is characterized by the polarizability $\beta^2=4\pi\alpha_0$ of the resonance (coupling of light and dipoles), partially dissipates due to the phenomenological damping constant Γ in an exponential time decay form, and partially propagates mechanically in a non-exponential time decay form due to polarization propagation, which is characterized by the spatial dispersion coefficient δ. The different ABCs influence the polarization propagation for transient reflectivity in a different manner, which has to do with the assumptions underlying the derivation of each ABC.

Our results are obtained under certain simplifying assumptions: The finite length crystal is replaced by a semi-infinite non-local medium. Furthermore we have simplified our calculations by assuming dimensionless parameters, $p=\beta^2/2\varepsilon_0$, Γ/ω_t, $\delta=(\hbar\omega_t/m^*c^2)^{1/2}$ to be small. For CdS and CuCl crystals each one of them is $\leq 10^{-3}$.

Regarding the comparison of our theoretical results with the analysis of experiments done by Aaviksoo et al. [44], we have to point out that there is a disagreement between our results and theirs. According to their analysis, they observe a distinct reduction of the transient reflectivity due to the introduction of spatial dispersion. We would like to point out that is not very clear that spatial dispersion reduces the reflectivity transients all the times. Our figures indicate that for different times spatial dispersion either reduces or increases the transients relative to the local optics result. Further measurements and theoretical analysis should clarify this discrepancy.

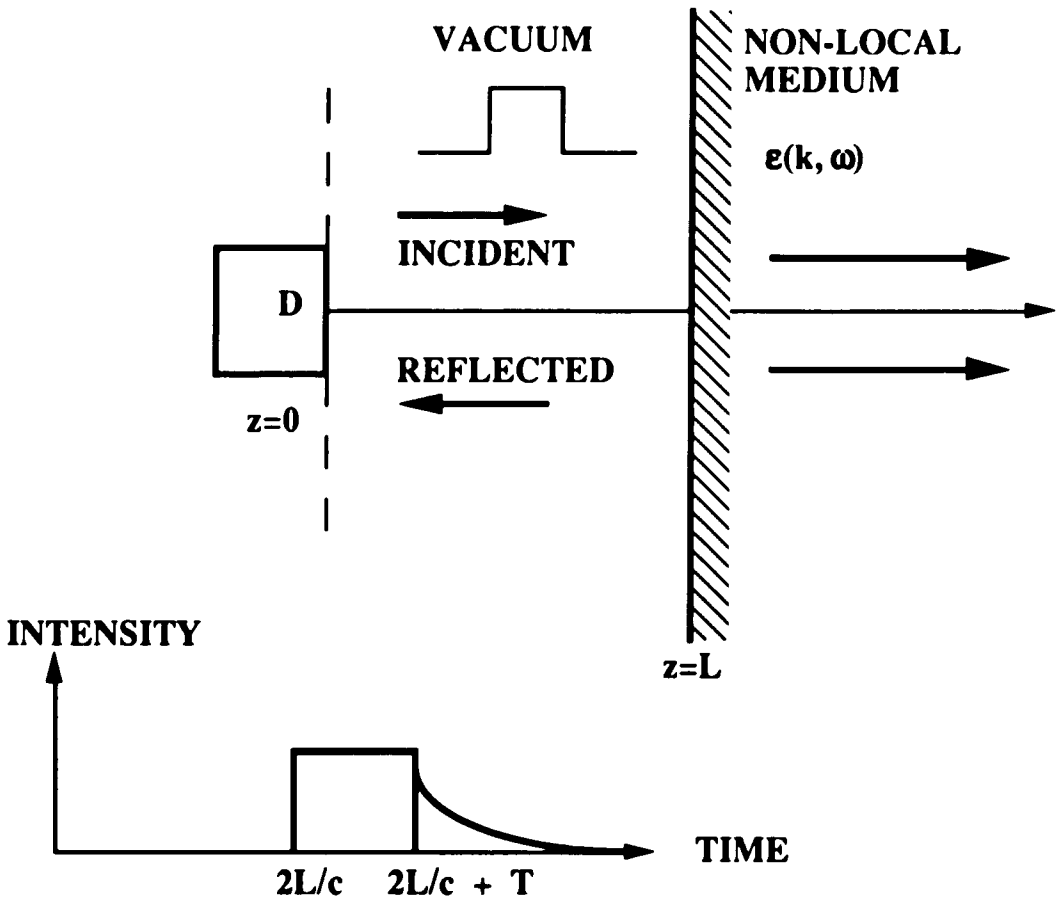

Figure 3.2.1 Schematic illustration of the geometry and the notation used. At time t=0 a square pulse of duration T is emitted from the plane z=0 where a detector is placed to monitor the reflectivity. For $2L/c < t < 2L/c+T$ the steady-state signal and for $\tau = t-2L/c-T \geq 0$ the transient signal is detected.

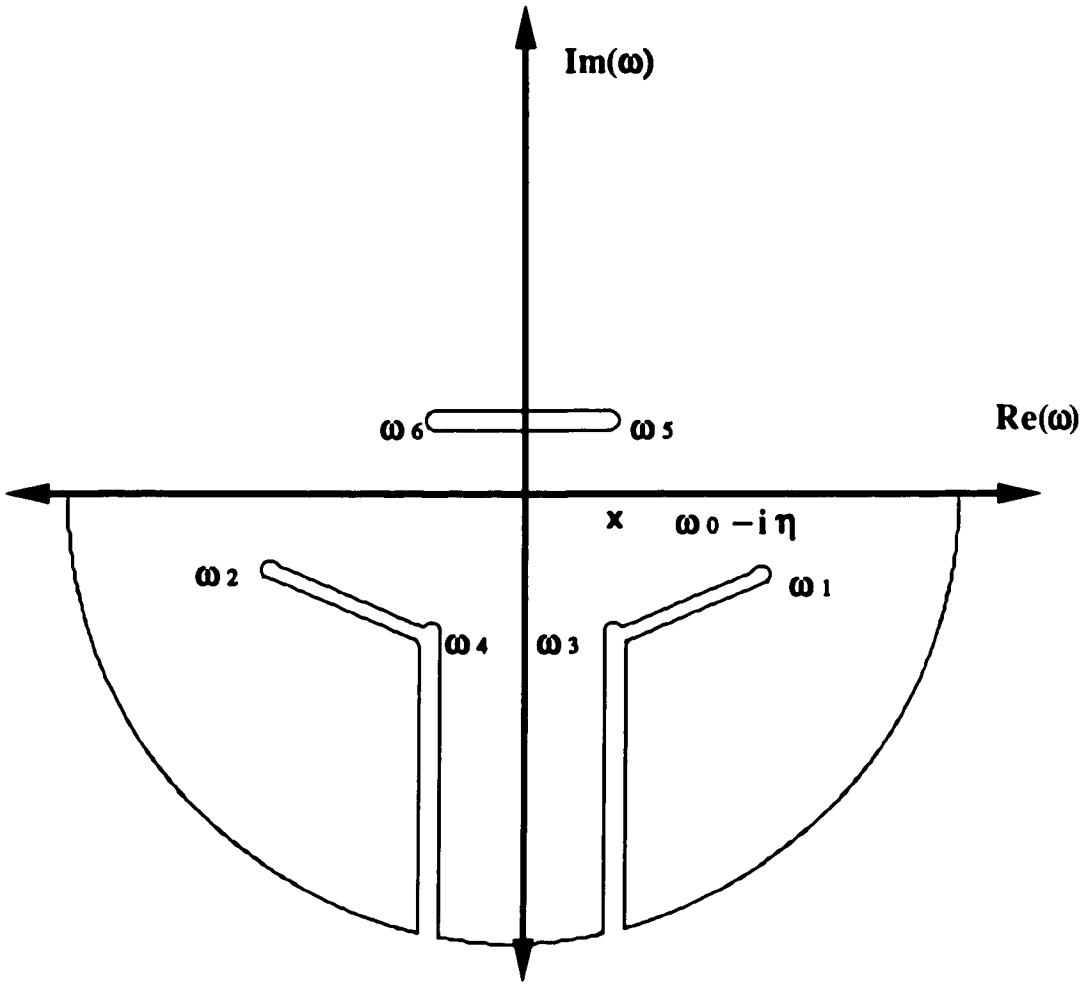

Figure 3.3.1(a) Schematic illustration of the contour in the complex ω plane needed to evaluate the reflected for Pekar, Ting and Kiselev's ABC. A pole at ω-iη and six branch-point singularities ω_j, j=1 to 6 give rise to the steady-state and transient reflectivity, respectively.

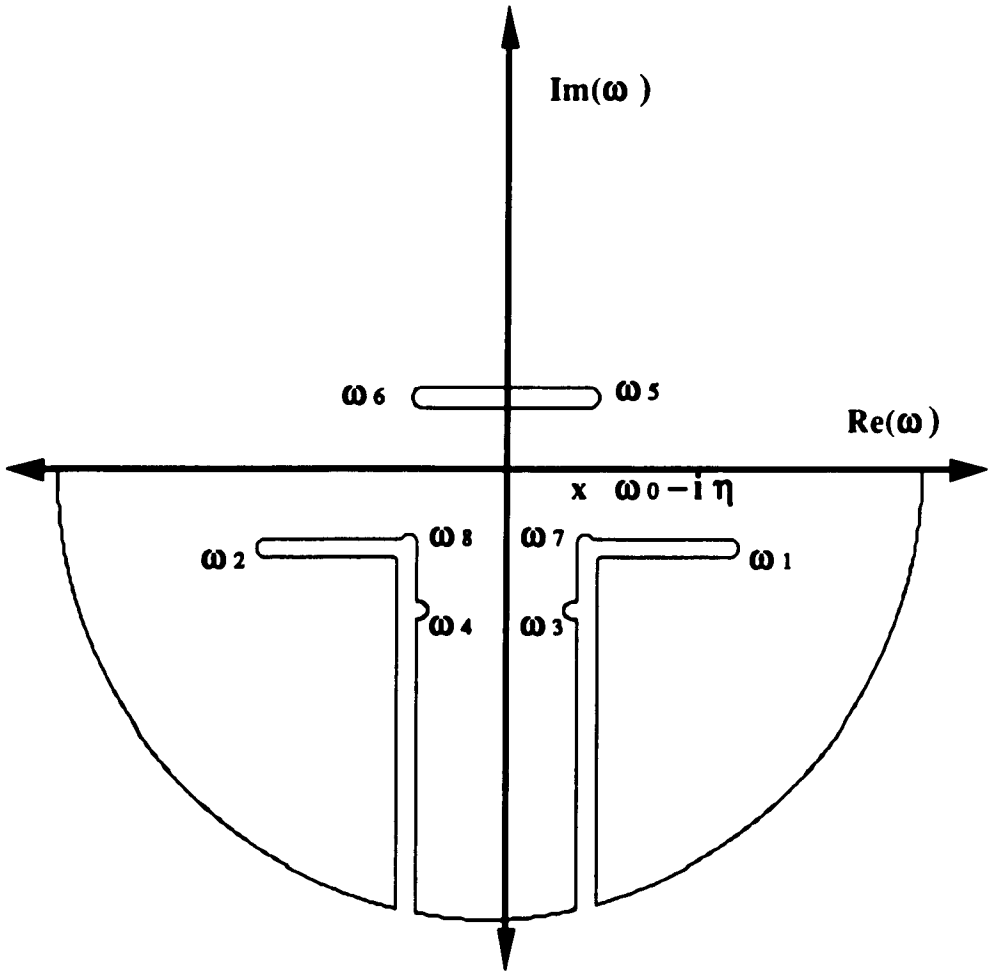

Figure 3.3.1(b) Schematic illustration of the contour in the complex ω plane needed to evaluate the reflected for Birman's ABC. A pole at ω-iη and eight branch-point singularities ω_j, j=1 to 8 give rise to the steady-state and transient reflectivity, respectively.

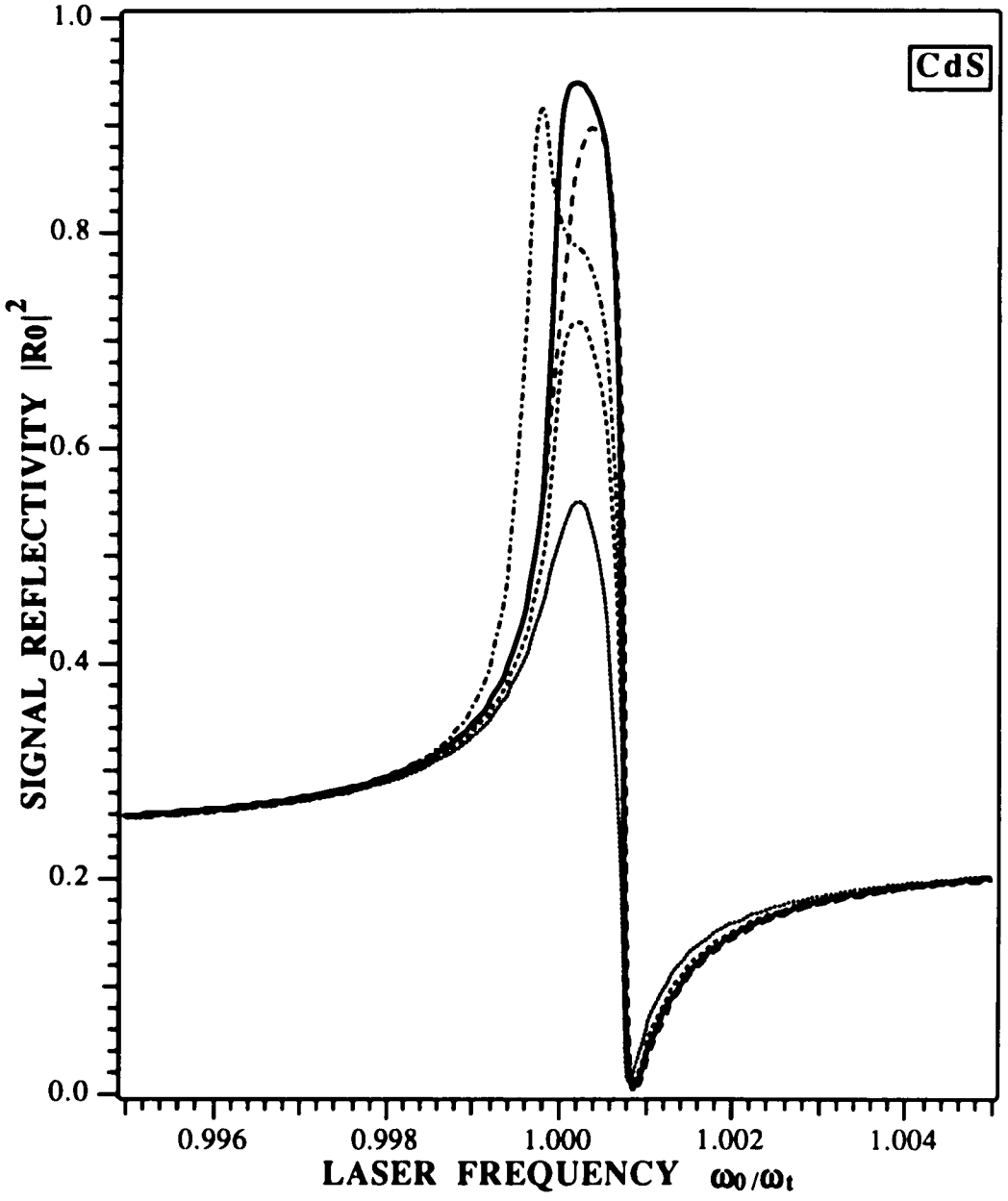

Figure 3.3.2 Resonance enhancement of steady-state reflectivity $|R_0|^2$ which persists for $2L/c < t < 2L/c+T$. The parameters are chosen appropriate to a CdS crystal with $\varepsilon_0=8$, $\hbar\omega_t=2.55$ eV, $m^*=0.9m_e$, $\Gamma/\omega_t=5\times10^{-5}$, $\beta^2=0.0125$ and $\gamma=10^{-1}$. For comparison each curve is represented by an ABC as follows: Local Optics ———, Pekar ·····, Birman - - - - -, Ting – – – – –, Kiselev ·····.

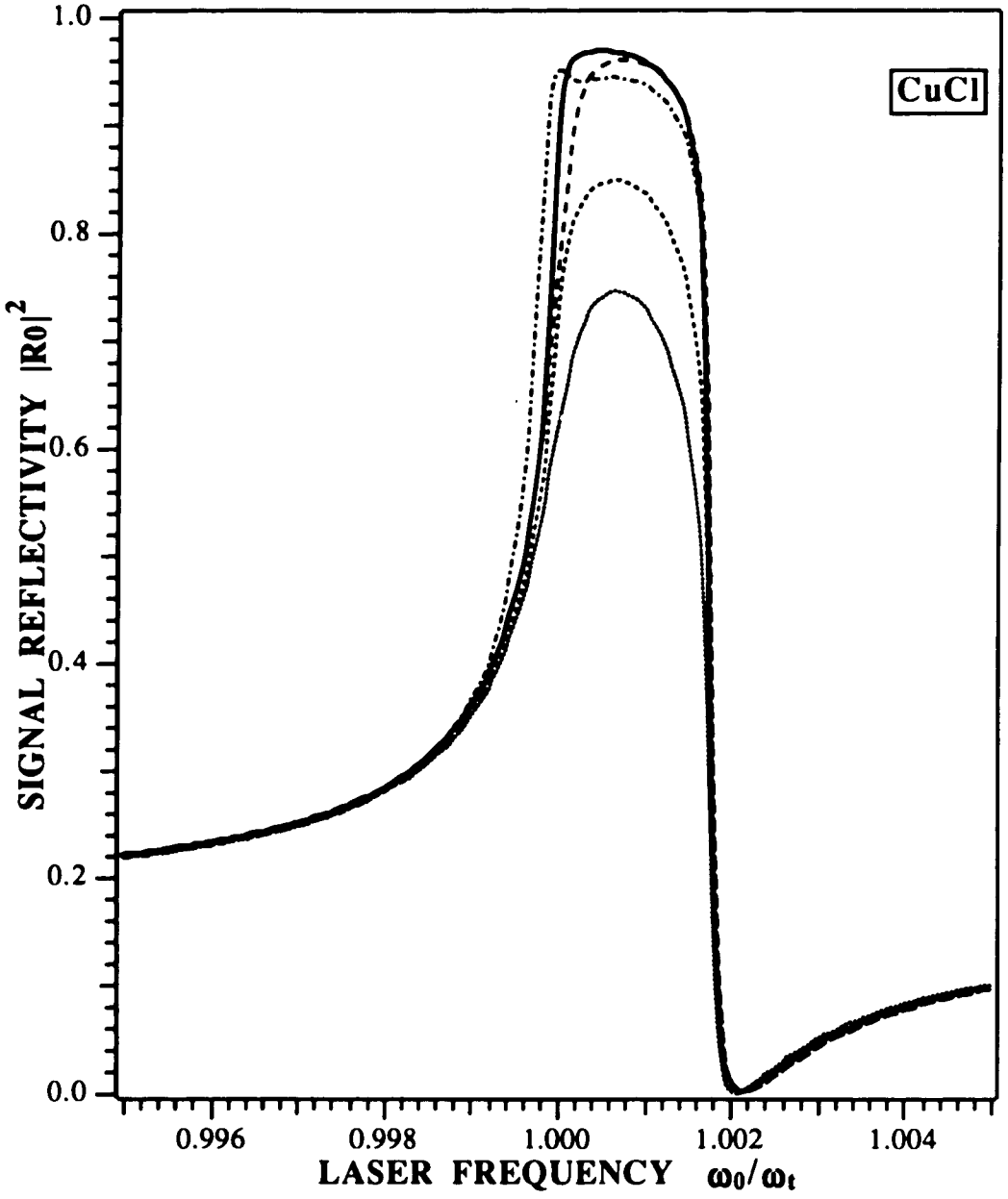

Figure 3.3.3 Resonance enhancement of steady-state reflectivity $|R_0|^2$ which persists for $2L/c < t < 2L/c+T$. The parameters are chosen appropriate to a CuCl crystal with $\varepsilon_0=5.59$, $\hbar\omega_t=3.2022$ eV, $m^*=2.3m_e$, $\Gamma/\omega_t=5\times10^{-5}$, $\beta^2=0.0199$ and $\gamma=10^{-1}$. For comparison each curve is represented by an ABC as follows: Local Optics ———, Pekar ·····, Birman - - - - -, Ting – – – – –, Kiselev ·····.

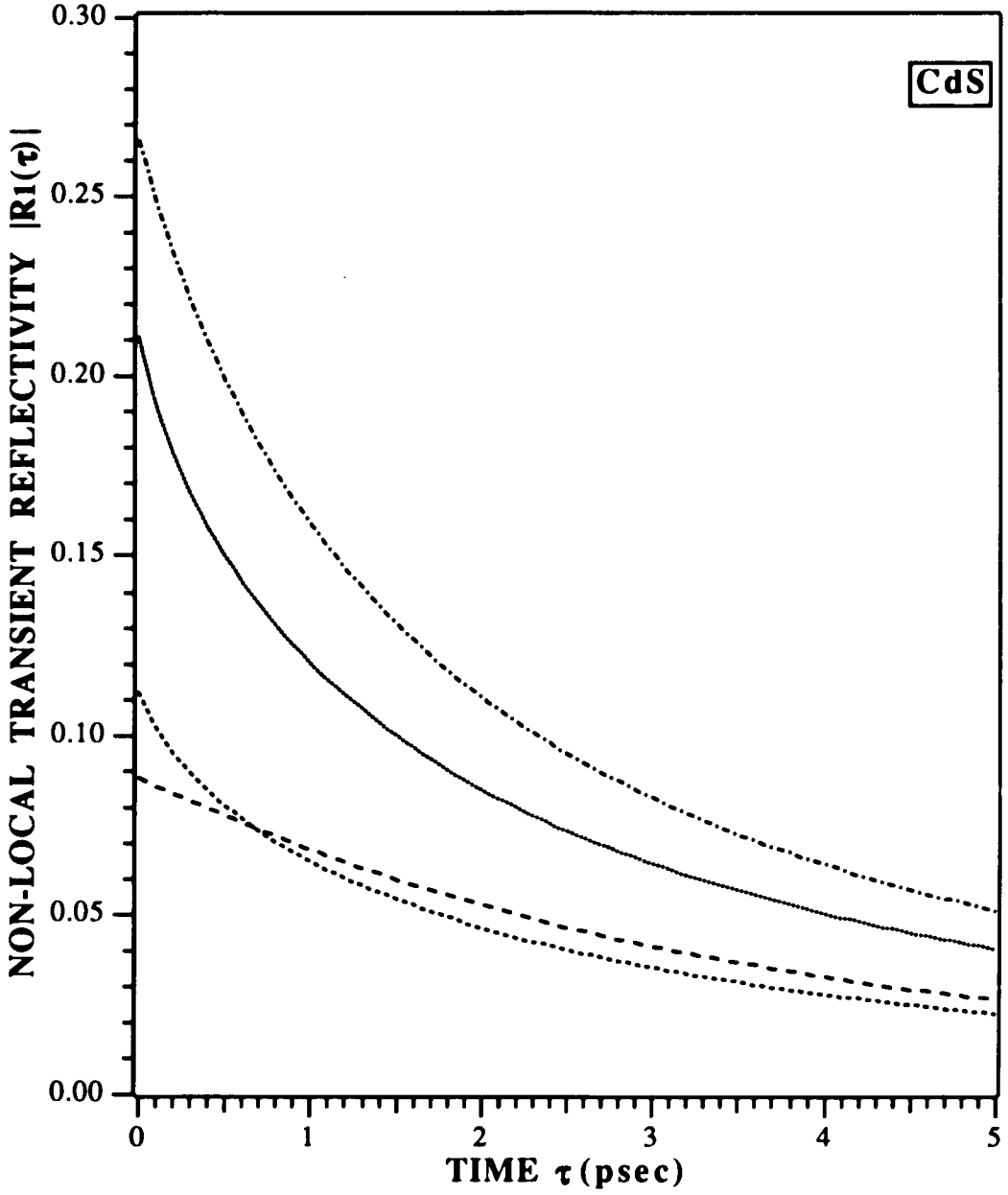

Figure 3.4.1 Time decay of the non-local part of transient reflectivity $|R_1(\tau)|$ for various ABCs for the case of exact resonance $\omega_0=\omega_t$. The parameters for CdS are the same as in Figure 3.3.2.

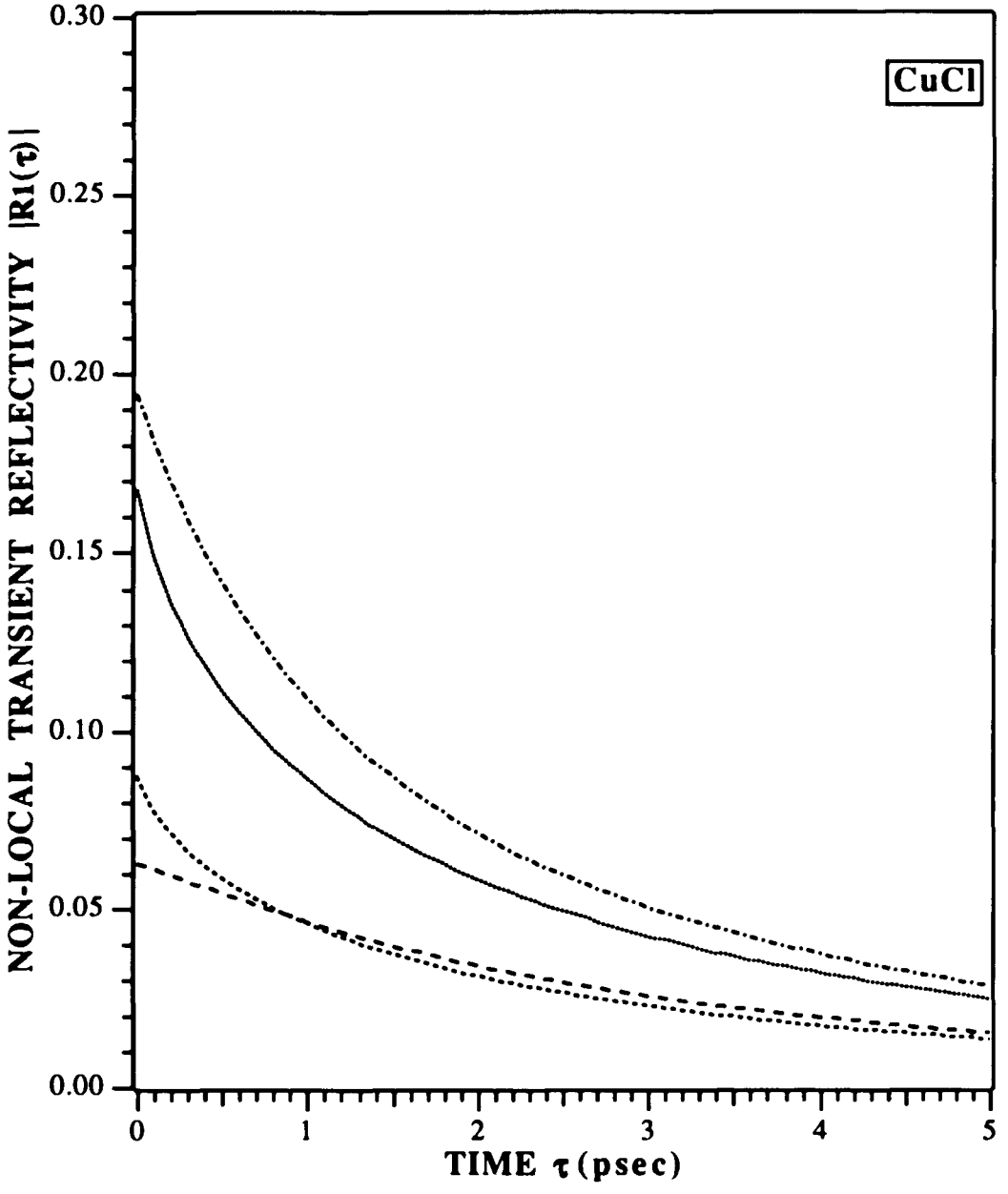

Figure 3.4.2 Time decay of the non-local part of transient reflectivity $|R_1(\tau)|$ for various ABCs for the case of exact resonance $\omega_0=\omega_t$. The parameters for CuCl are the same as in Figure 3.3.3.

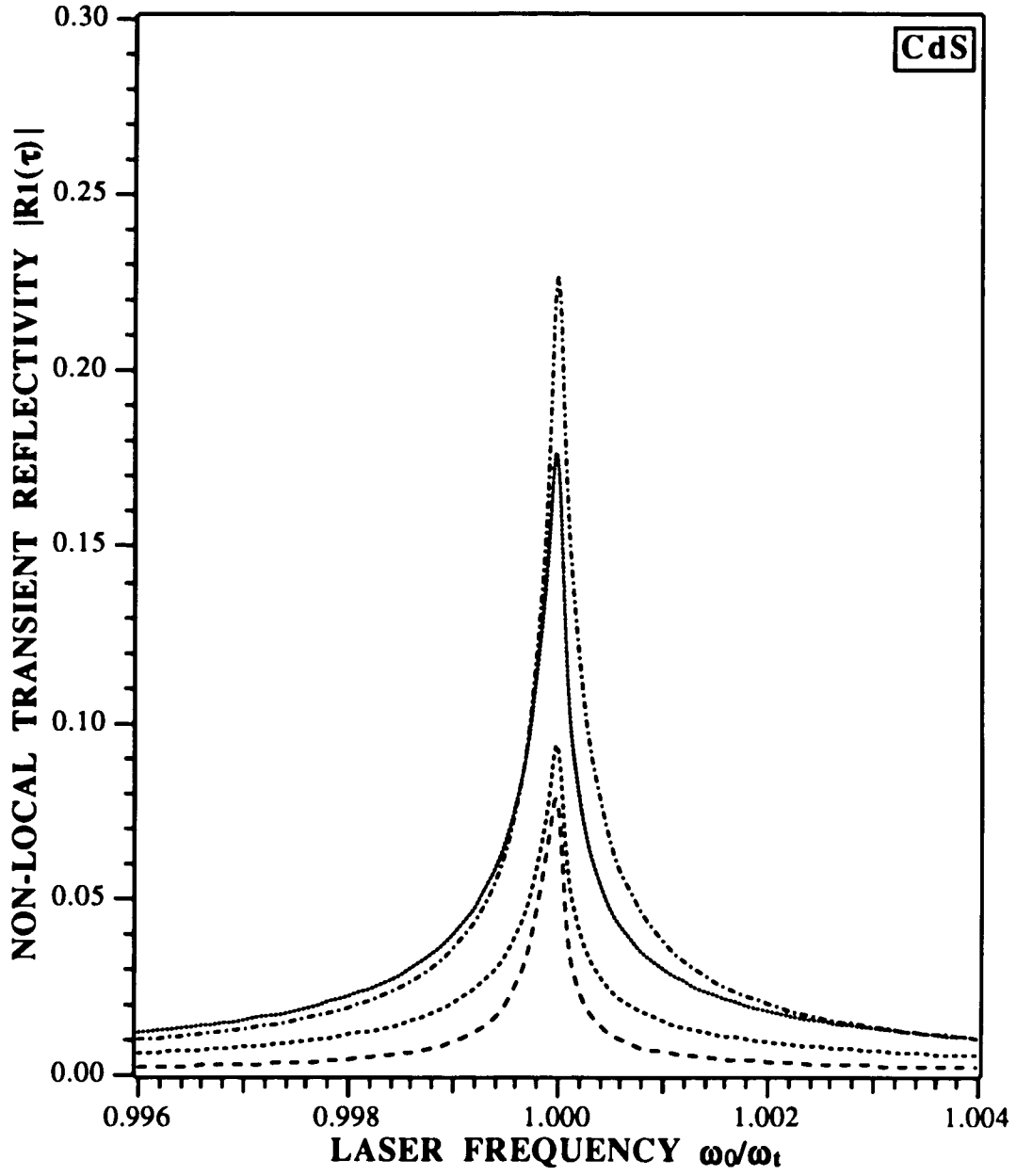

Figure 3.4.3 Resonance enhancement of the non-local part of transient reflectivity $|R_1(\omega_0)|$ for various ABCs at fixed time $\tau = 0.1$ psec. The parameters for CdS are the same as in Figure 3.3.2.

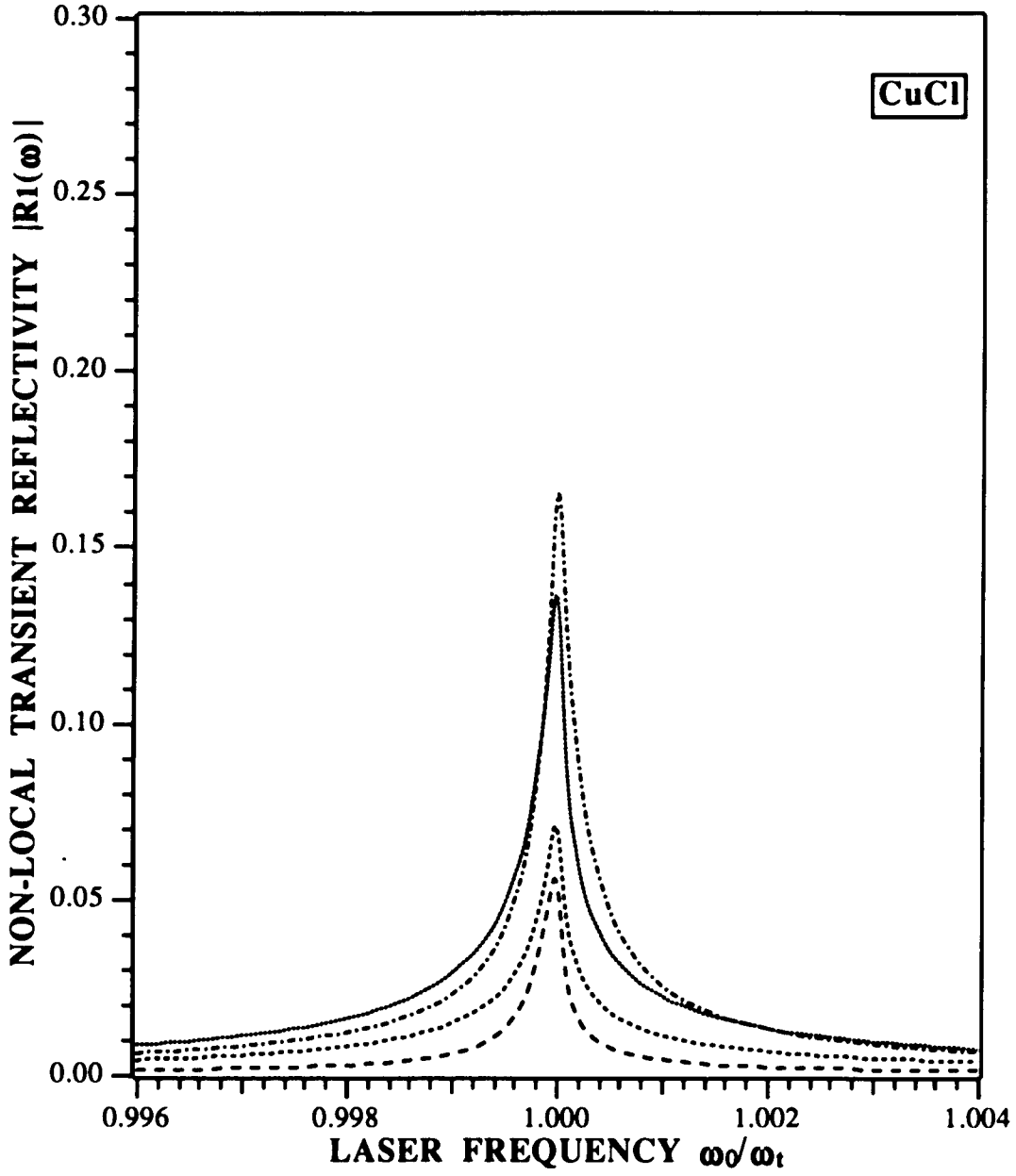

Figure 3.4.4 Resonance enhancement of the non-local part of transient reflectivity $|R_1(\omega_0)|$ for various ABCs at fixed time $\tau = 0.1$ psec. The parameters for CuCl are the same as in Figure 3.3.3.

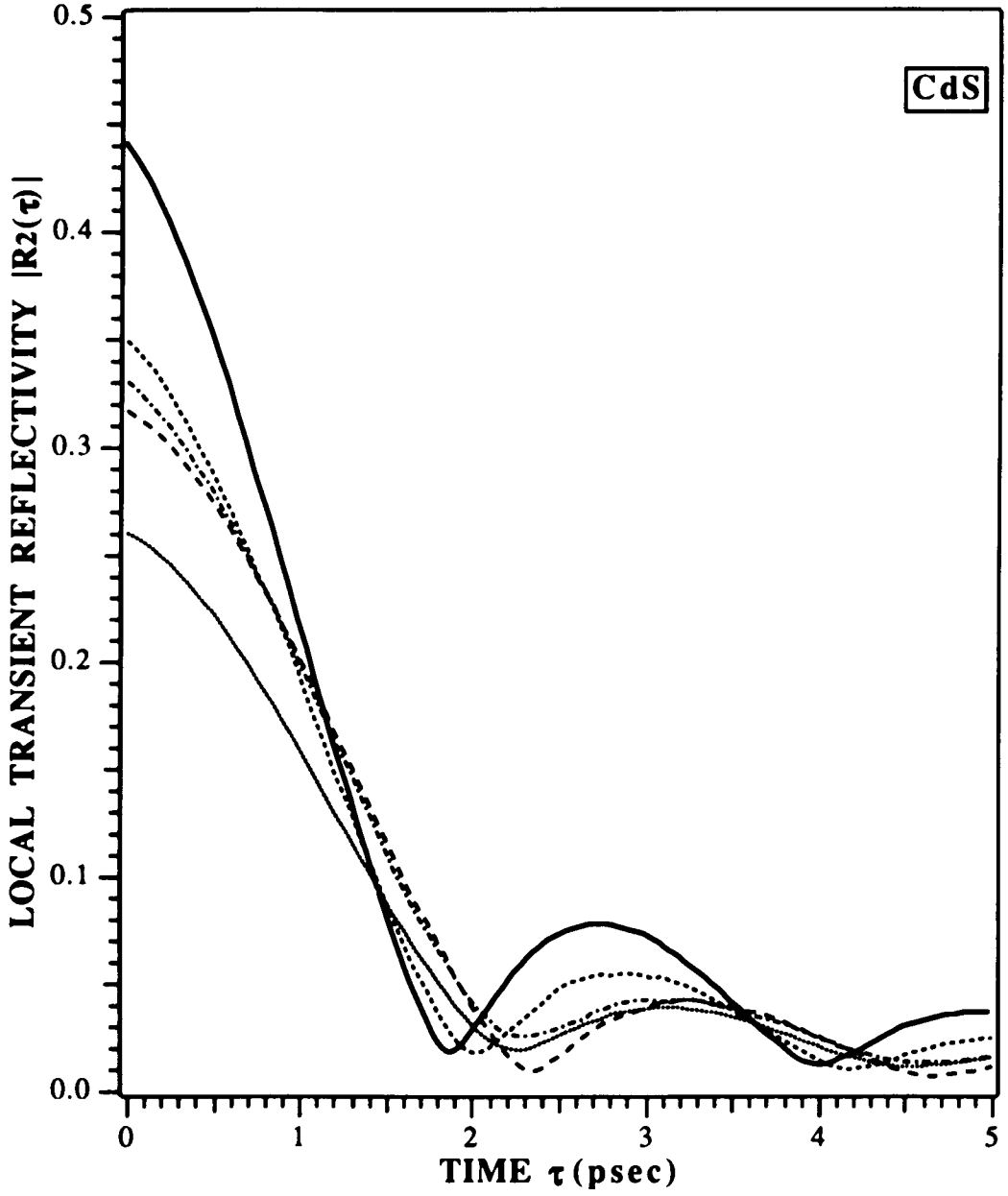

Figure 3.5.1 Time oscillatory decay of the local part of transient reflectivity $|R_2(\tau)|$ for various ABCs for the case of exact resonance $\omega_0=\omega_t$. The parameters for CdS are the same as in Figure 3.3.2.

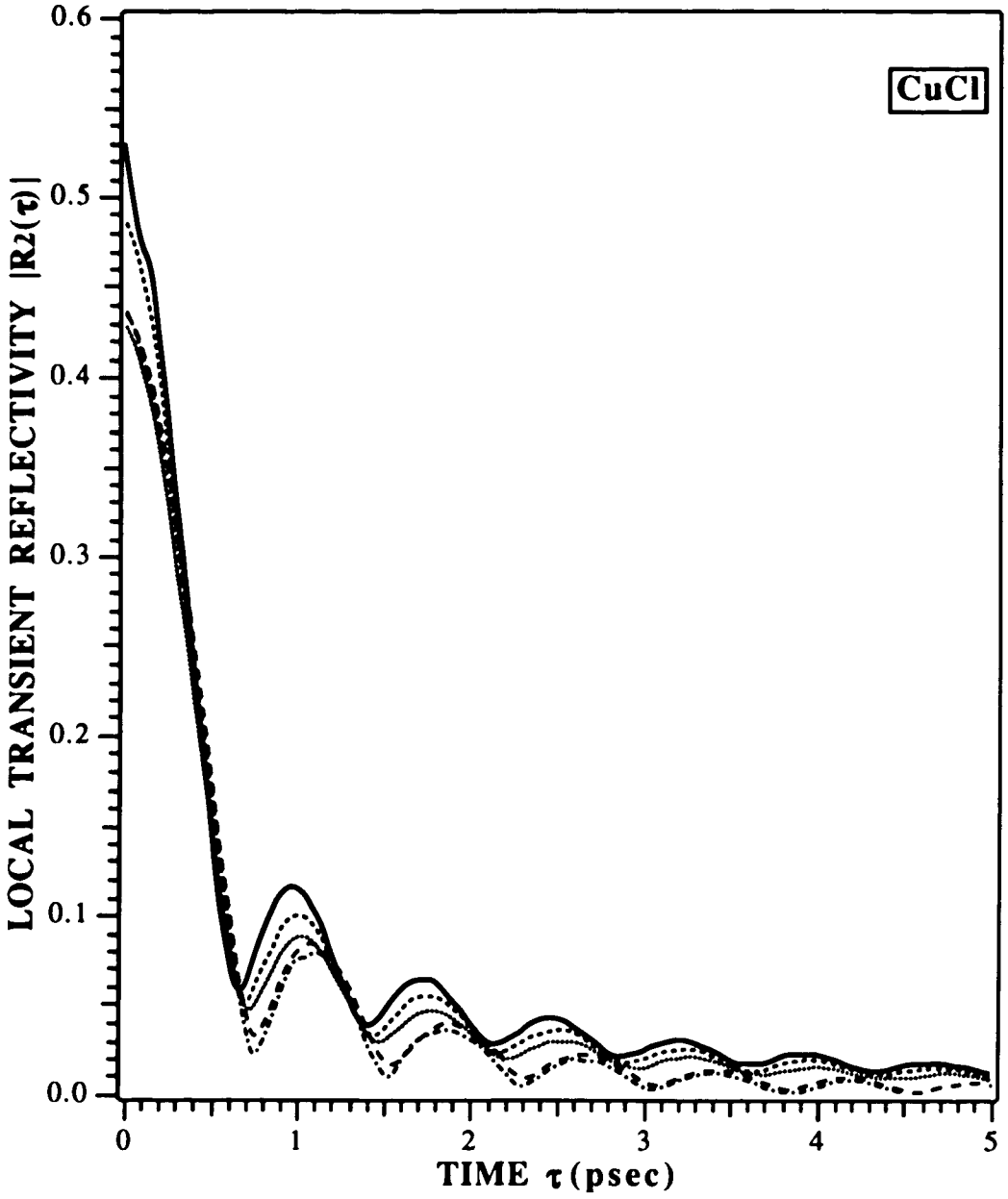

Figure 3.5.2 Time oscillatory decay of the local part of transient reflectivity $|R_2(\tau)|$ for various ABCs for the case of exact resonance $\omega_0=\omega_t$. The parameters for CuCl are the same as in Figure 3.3.3.

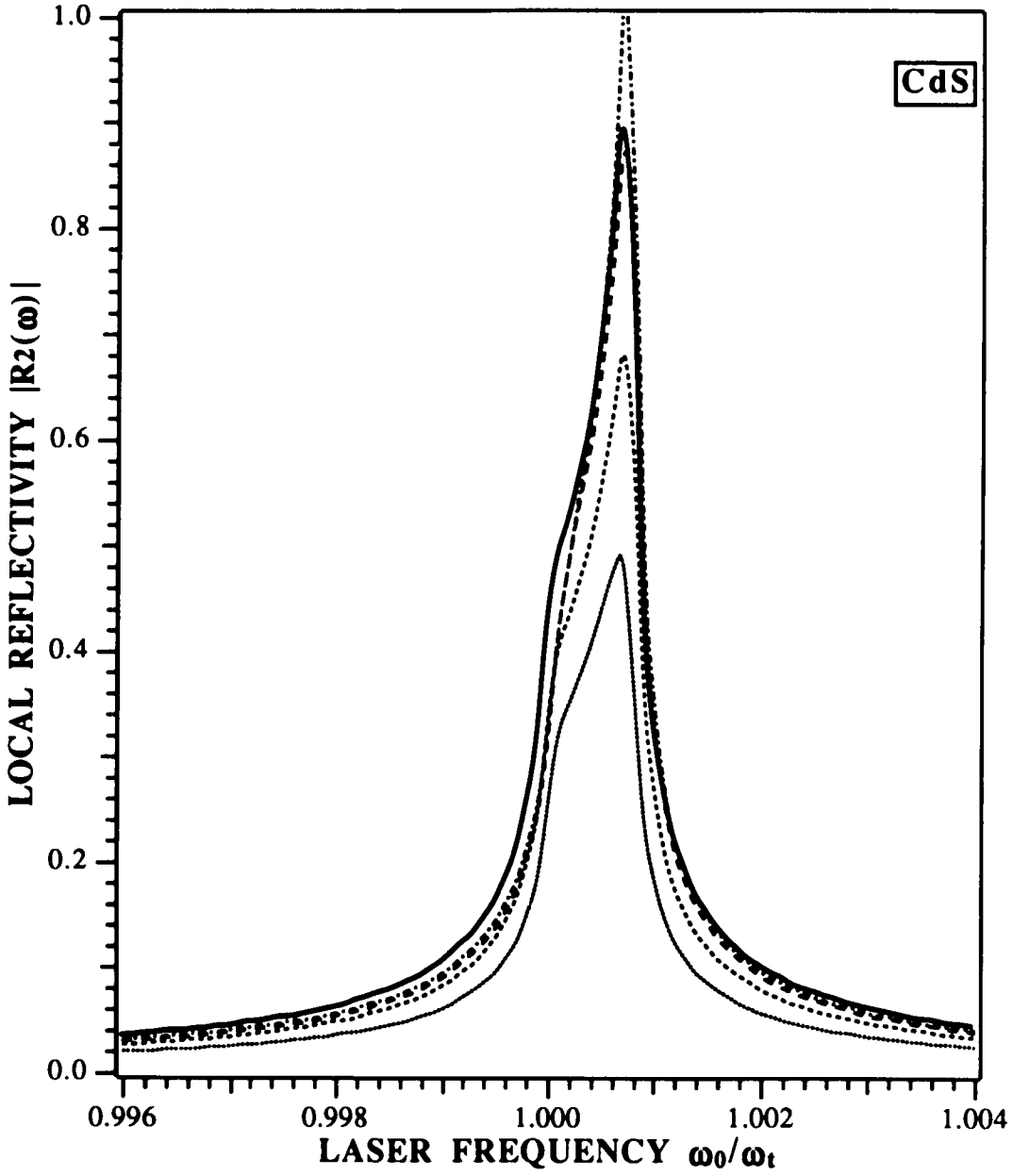

Figure 3.5.3 Resonance enhancement of the local part of transient reflectivity $|R_2(\omega_0)|$ for various ABCs at fixed time τ=0.1 psec. The parameters for CdS are the same as in Figure 3.3.2.

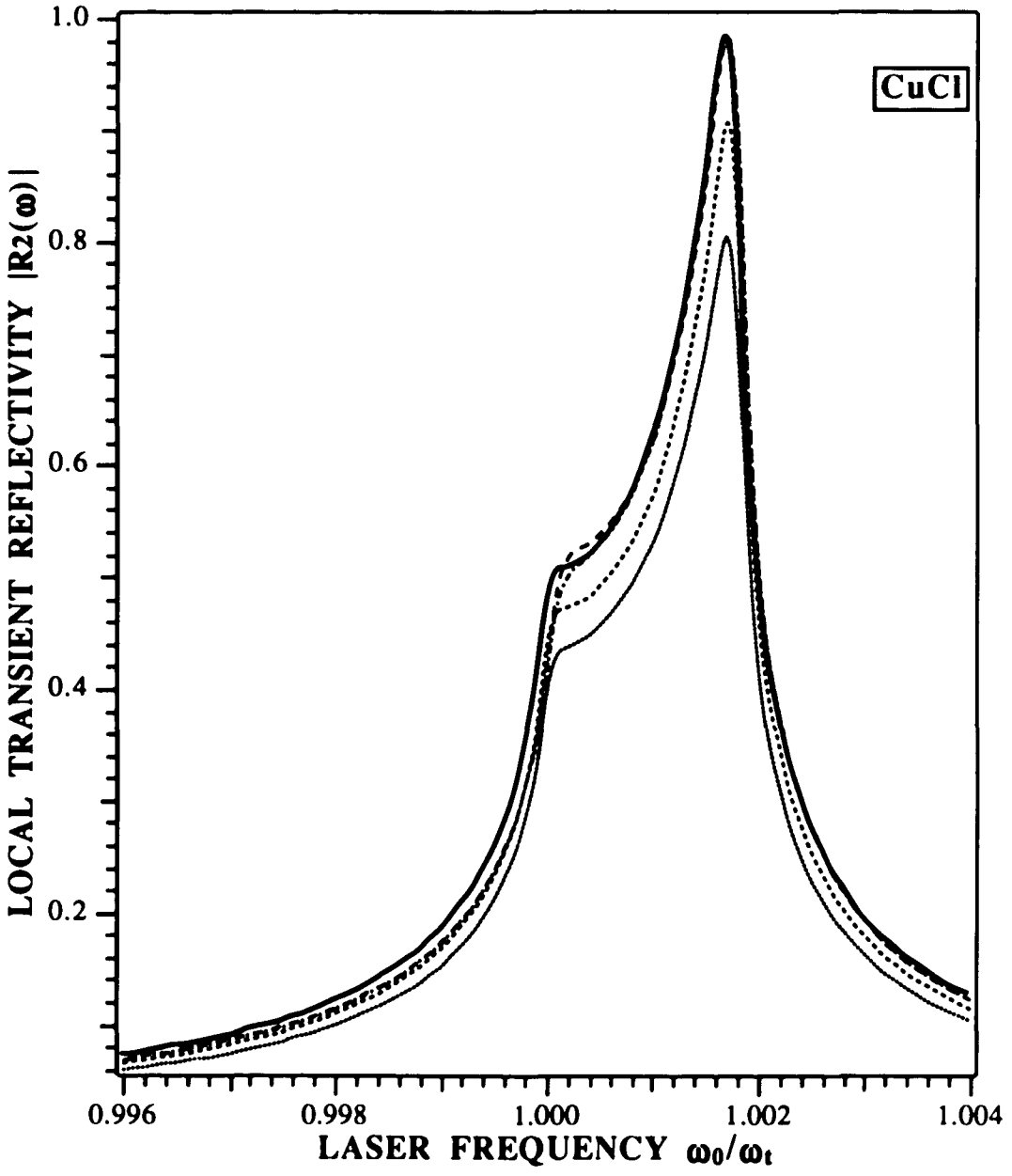

Figure 3.5.4 Resonance enhancement of the local part of transient reflectivity $|R_2(\omega_0)|$ for various ABCs at fixed time τ=0.1 psec. The parameters for CuCl are the same as in Figure 3.3.3.

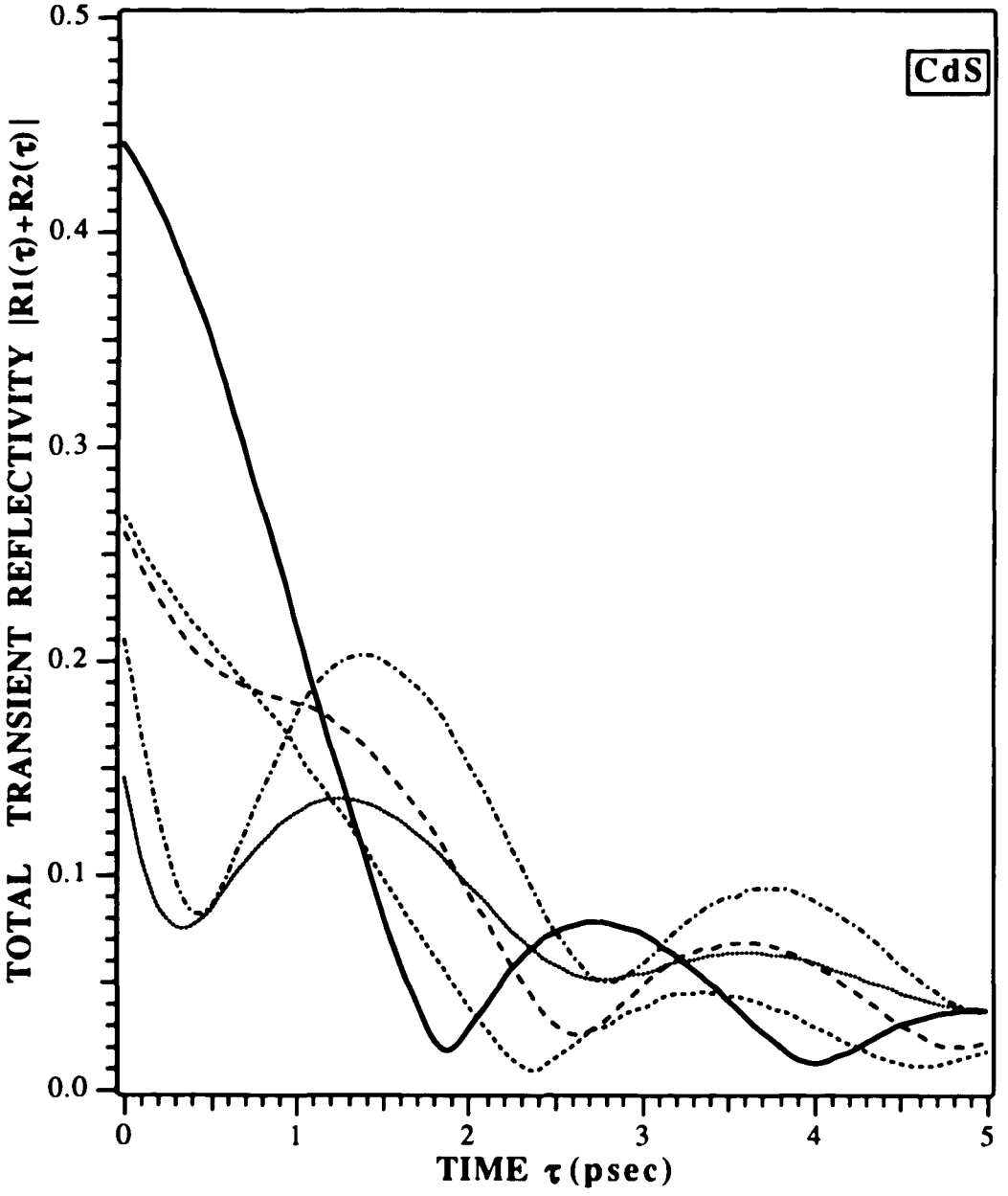

Figure 3.6.1 Time oscillatory decay of the total transient reflectivity $|R_1(\tau)+R_2(\tau)|$ for various ABCs for the case of exact resonance $\omega_0=\omega_t$. The parameters for CdS are the same as in Figure 3.3.2.

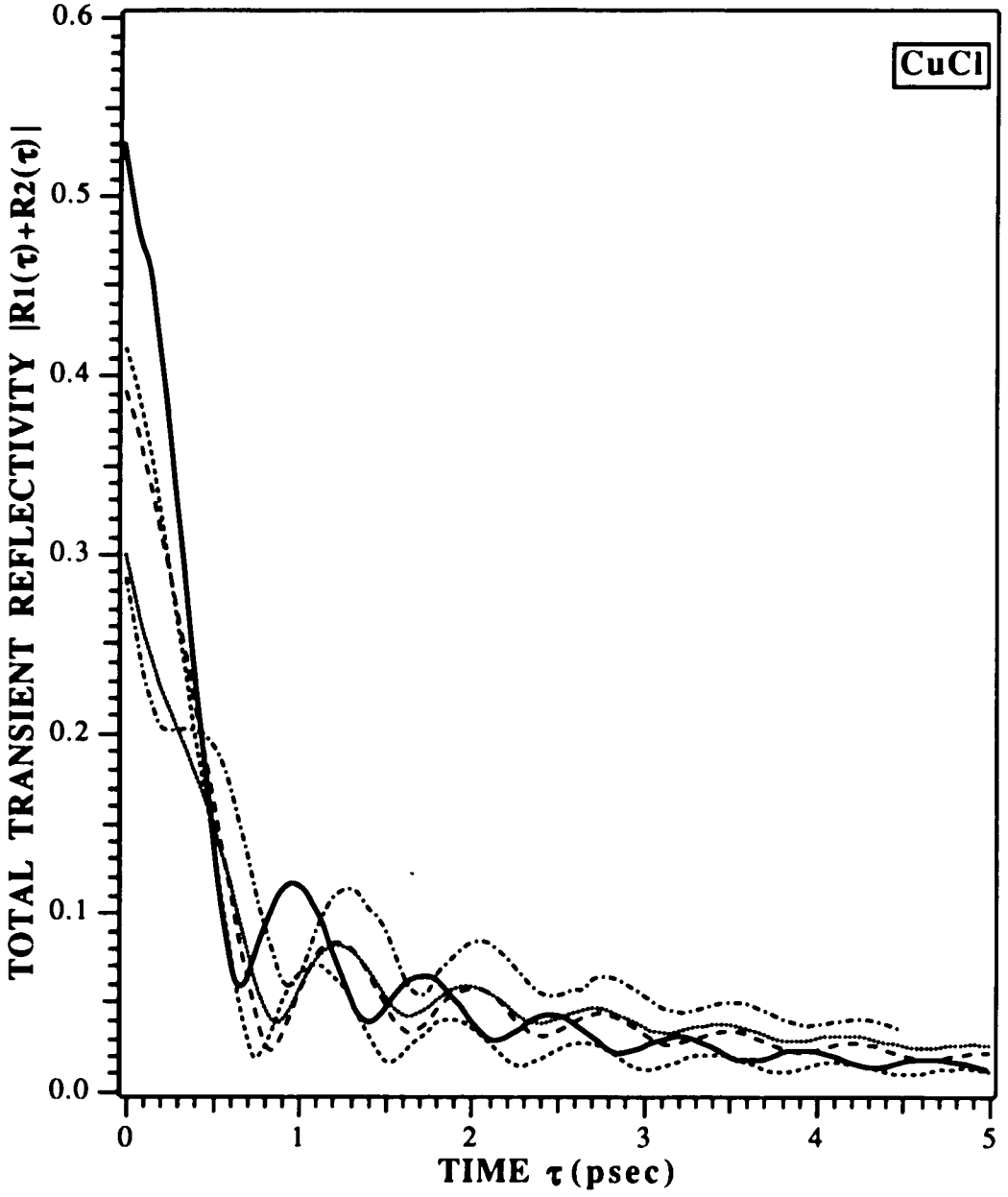

Figure 3.6.2 Time oscillatory decay of the total transient reflectivity $|R_1(\tau)+R_2(\tau)|$ for various ABCs for the case of exact resonance $\omega_0=\omega_t$. The parameters for CuCl are the same as in Figure 3.3.3.

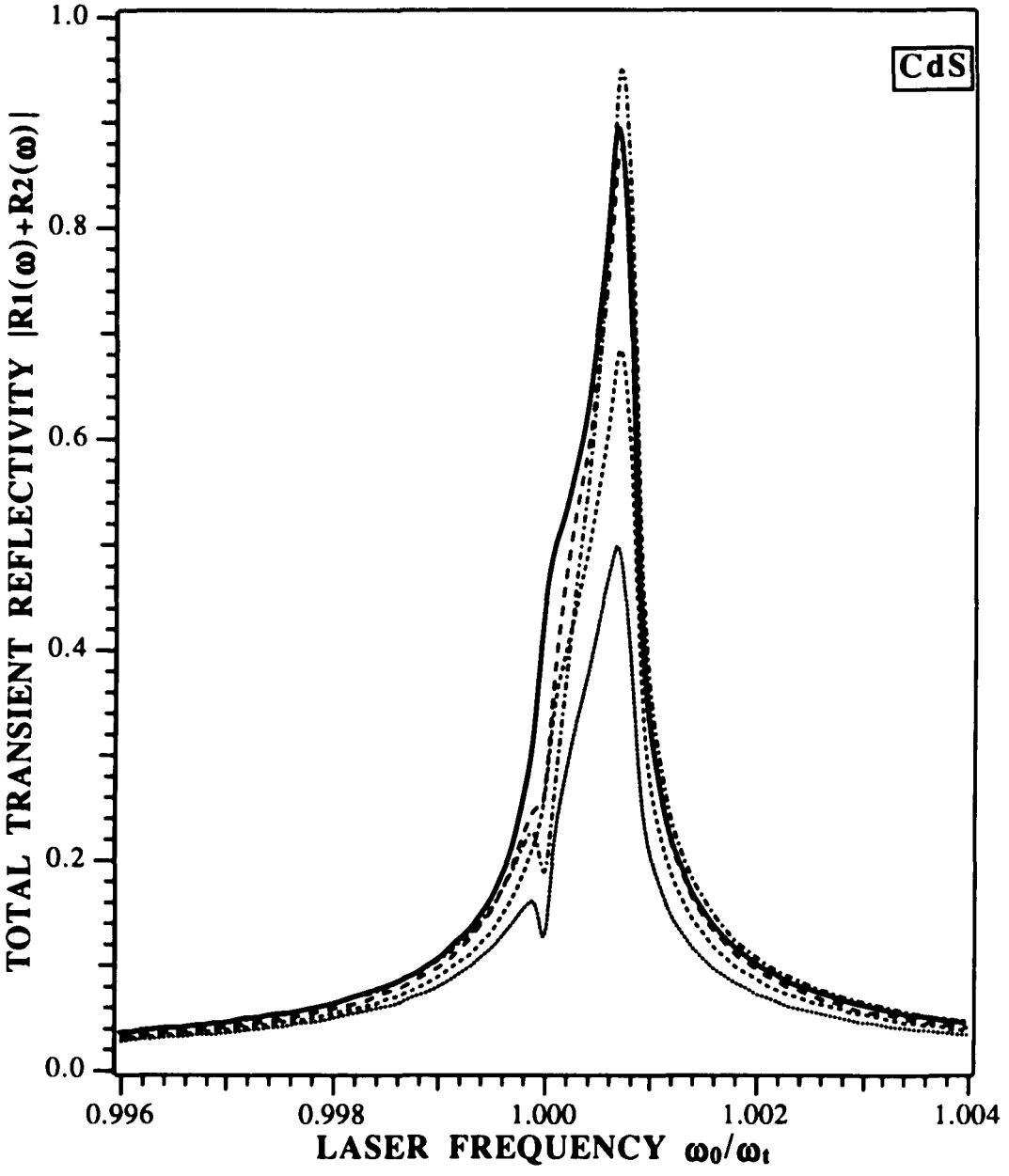

Figure 3.6.3 Resonance enhancement of the total transient reflectivity $|R_1(\omega_0)+R_2(\omega_0)|$ for various ABCs at fixed time $\tau = 0.1$ psec. The parameters for CdS are the same as in Figure 3.3.2.

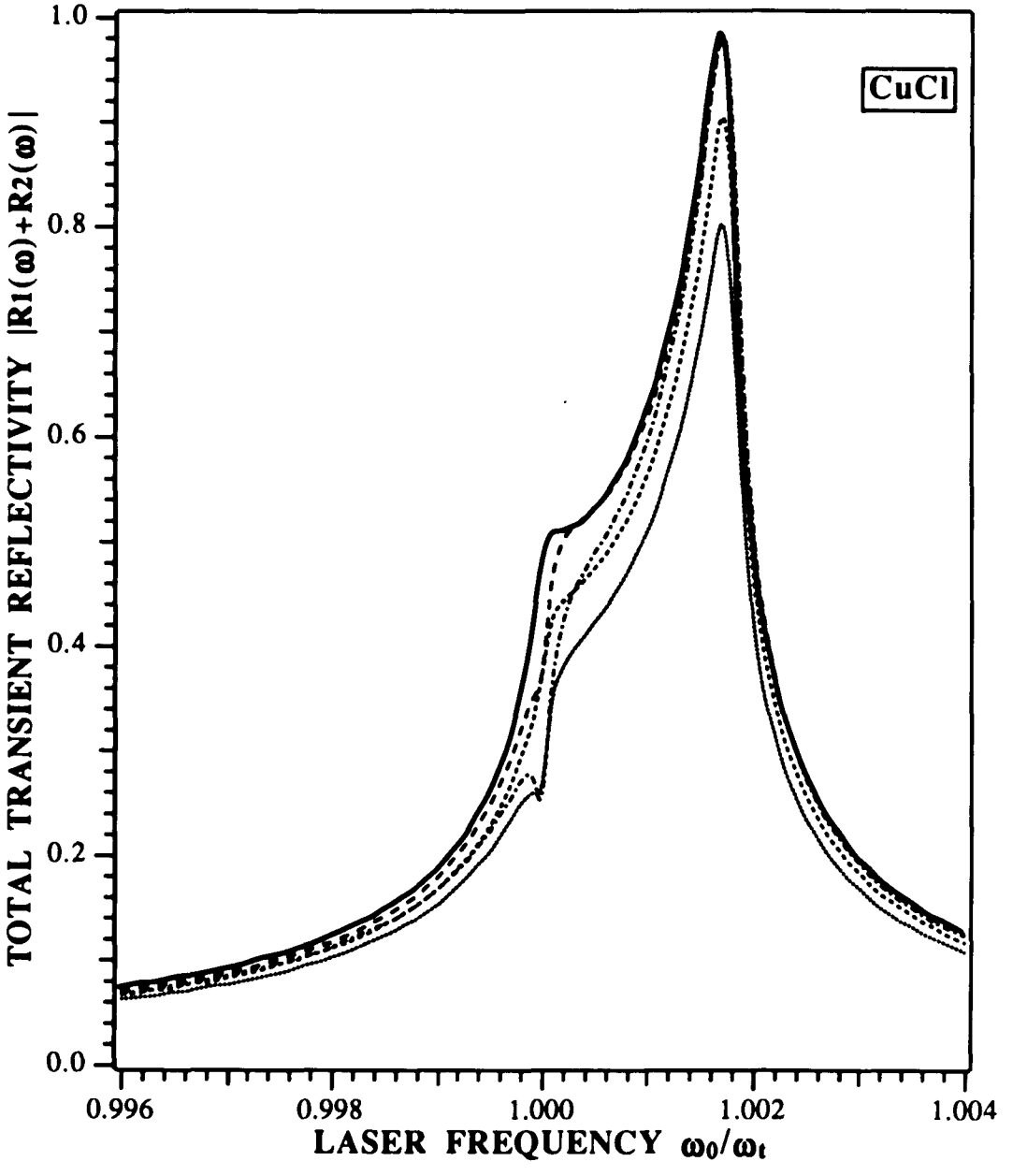

Figure 3.6.4 Resonance enhancement of the total transient reflectivity $|R_1(\omega_0)+R_2(\omega_0)|$ for various ABCs at fixed time τ = 0.1 psec. The parameters for CuCl are the same as in Figure 3.3.3.

CHAPTER 4

INTENSE PULSE PROPAGATION IN LOCAL RESONANT MEDIA

The least parts of almost all natural Bodies are in some measure transparent: And the Opacity of those Bodies ariseth from the multitude of Reflexions caused in their internal Parts.

Newton, **Opticks**, Book II, Part III, Prop. II

4.1 INTRODUCTION

In this Chapter, we will review the intense optical pulse propagation in gases and dielectrics. The discovery of self-induced transparency (SIT) by McCall and Hahn [55] in 1969 focused attention on the very old problem of light propagation in dielectrics. The investigations of Sommerfeld and Brillouin [56] gave a complete picture in the framework of the classical Lorentz linear model of resonant dielectrics. However, this model is adequate only if the light intensity is low, or if the light frequency is far from any of the atomic resonances of the dielectric medium. Since the nineteen-sixties, intense and practically coherent monochromatic laser light has been available as a probe of optically resonant systems. The response of such systems near resonance is not satisfactorily described by the Lorentz model of harmonically oscillating charges. Nonlinearities arise in the light-dielectric interaction, producing a wide range of nonclassical effects such as SIT, photon echoes, optical nutation, saturation phenomena etc. A pedagogical introduction to the various phenomena associated with the nonlinearities is given by Allen and Eberly [57].

Self-induced transparency (SIT) phenomena originated from the study of the propagation of intense coherent laser pulses in resonantly absorptive media. Above a threshold pulse intensity for a given pulse width, a pulse is observed to propagate with anomalously low energy loss: the highly absorptive medium becomes transparent. In this limit, the pulse velocity in the lossless propagation region can be many orders of magnitude slower than the velocity of light in vacuum.

These spectacular effects are the result of a coherent coupling of the E-M wave fields to the resonant atoms of the absorptive medium. Any change in the state of the absorbers which is incoherent with the optical pulse will destroy the SIT phenomena described above. Therefore several restrictions are applied in the analysis of the SIT phenomenon. Incoherent processes like spontaneous radiation from the excited state of the absorber, and

phonon or defect coupling to absorbers in solids place an upper limit on the pulse width τ which can permit SIT propagation.

4.2 SELF INDUCED TRANSPARENCY (SIT) IN DILUTE GASES

The phenomenon of self-induced transparency (SIT) for short intense optical pulses propagating in a liquid-helium-cooled ruby rod was experimentally and theoretically first demonstrated by McCall and Hahn [55] and has been reviewed by Lamb [58] and Slusher [59]. Experimental confirmation of SIT theory for gaseous absorbers was reported by Patel and Slusher [60], and Slusher and Gibbs [61, 62]. Patel and Slusher were the first to present results for a dilute gas. They demonstrated delay times of about 0.2 μsec in SF_6, and found output pulses that appeared more symmetric than the input pulses produced from a CO_2 laser. Gibbs and Slusher have described detailed experiments on the propagation of coherent optical pulses in dilute Rb vapor, a non-degenerate resonant absorber and observed non-linear transmission. Their input 2π pulse was not transmitted completely, because the input pulse from a ^{202}Hg II laser did not have a hyperbolic secant profile so it had to be reshaped by the medium. Large pulse delays were observed without pulse energy loss. The delays observed were in agreement with the theoretical prediction by McCall and Hahn.

The theoretical analysis of SIT can be derived using a semiclassical description which involves a number of assumptions. The absorbing medium is composed of a two-level non-degenerate system of non-interacting atoms. For optical atomic transitions near room temperature, the probability of thermal excitation from ground state to excited state is very small, i.e., $k_B T << \hbar\omega_t$, where ω_t is the resonant frequency for the absorbing transition. This permits us to assume that all absorbers are in the ground state prior to the excitation by a coherent radiation pulse.

Self-induced transparency, which accounts for the low energy loss, can be analyzed by treating the E-M field classically and the two-level systems semi-classically. For simplicity, one takes fields which are x and y independent (one-dimensional problem); then the Maxwell wave equation can be written as follows:

$$\left(\frac{\partial^2}{\partial z^2}-\frac{1}{c^2}\frac{\partial^2}{\partial t^2}\right)\mathbf{E}(t,z)=\frac{4\pi}{c^2}\frac{\partial^2}{\partial t^2}\mathbf{P}(t,z) \tag{4.2.1}$$

The medium has a dipole density N which makes it polarizable. Each dipole moment has strength d. A true quantum dipole (an atom in a gas, an exciton in a semiconductor) has a series of energy levels. For resonant problems of interest, one can restrict oneself to the ground state and first excited state of each dipole. For such a two-level system, the state can be represented by a two component vector $|\Psi(a, b)>$ where a is the amplitude to be in the excited state and b to be in the ground state. One can then define the pseudo-spin vector:

$$\begin{aligned} s_1 &= <\Psi|\hat{\sigma}_1|\Psi> = a^* b + a b^* \\ s_2 &= <\Psi|\hat{\sigma}_2|\Psi> = -i(a^* b - a b^*) \\ s_3 &= <\Psi|\hat{\sigma}_3|\Psi> = a^* a - b^* b \\ s_1^2 + s_2^2 + s_3^2 &= (|a|^2 + |b|^2)^2 = 1 \end{aligned} \tag{4.2.2}$$

where $<\Psi/\hat{\sigma}_j/\Psi>$ is the averaging over Pauli matrix $\hat{\sigma}_j$ (j=1, 3). The semi-classical approximation corresponds to neglecting fluctuations about these averages which is consistent if the dipoles are in a coherent state. The dynamical equations associated with the components of s(t) may be written:

$$\dot{s}_1(t) = -\omega_t s_2(t) + \frac{2}{\hbar} < \mathbf{d}_i \cdot \mathbf{E}(t) > s_3(t)$$

$$\dot{s}_2(t) = \omega_t s_1(t) + \frac{2}{\hbar} < \mathbf{d}_r \cdot \mathbf{E}(t) > s_3(t) \qquad (4.2.3)$$

$$\dot{s}_3 = -\frac{2}{\hbar} < \mathbf{d}_i \cdot \mathbf{E}(t) > s_1(t) - \frac{2}{\hbar} < \mathbf{d}_r \cdot \mathbf{E}(t) > s_2(t)$$

where ω_t is the resonant frequency of the medium, and $\hat{\mathbf{d}} = \mathbf{d}_r\hat{\sigma}_1 - \mathbf{d}_i\hat{\sigma}_2$ is the Hermitian dipole operator. For many purposes, it is adequate to assume that the states *a* and *b* are connected by a $\Delta m = \pm 1$ transition. Then it is useful to adjust the phases in such a way that the dipole component $\mathbf{d}_i$, vanishes, and simultaneously define $(2/\hbar)\mathbf{d}_r \cdot \mathbf{E} = (2d/\hbar)\mathbf{u}_d \cdot \mathbf{E} = \kappa\mathcal{E}$, where $\mathbf{u}_d$ is the unit vector in the **E** direction.

The semiclassical Eqs. (4.2.3) then take a simpler form:

$$\dot{s}_1 = -\omega_t s_2 \qquad \dot{s}_2 = \omega_t s_1 + \kappa\mathcal{E} s_3 \qquad \dot{s}_3 = -\kappa\mathcal{E} s_2 \qquad (4.2.4)$$

The pseudospin Eqs. (4.2.4) have the same structure as the magnetic resonance equations derived by Bloch [63]. In a frame rotating with $\mathcal{E}$, the pseudospin vector has components u, v, and w:

$$\begin{pmatrix} u \\ v \\ w \end{pmatrix} = \begin{pmatrix} \cos\Theta(t) & \sin\Theta(t) & 0 \\ -\sin\Theta(t) & \cos\Theta(t) & 0 \\ 0 & 0 & 1 \end{pmatrix} \begin{pmatrix} s_1 \\ s_2 \\ s_3 \end{pmatrix} \qquad (4.2.5)$$

One can then obtain the Bloch equations [64] for the two-level system of dipoles

$$\dot{u} = (\dot{\Theta}(t) - \omega_t)v \qquad \dot{v} = -(\dot{\Theta}(t) - \omega_t)u + \kappa\mathcal{E}w \qquad \dot{w} = -\kappa\mathcal{E}v \qquad (4.2.6)$$

where u and v are the in-phase (dispersive) and out of phase (absorptive) components relative to E of the macroscopic polarization **P**, and w is the population inversion of the medium. For very small electric fields (linear optics), $w \approx -1$, the atoms are mainly in the ground state, practically unexcited, and they behave as Lorentzian oscillators. For larger electric field intensities, the nonlinearities of the Bloch equations become important.

McCall and Hahn considered a circularly polarized pulse with a carrier wave of frequency ω. On the time and length scale of this carrier wave, the envelope is slowly varying. Thus it is natural to separate out the fast and the slow variables. The slowly varying envelope approximation (SVEA) consists in taking an envelope function **E**(t, z) which satisfies:

$$\left|\frac{\partial \mathcal{E}}{\partial z}\right| << \left|\frac{\mathcal{E}}{\lambda}\right| \quad \text{and} \quad \left|\frac{\partial \mathcal{E}}{\partial t}\right| << \omega|\mathcal{E}| \tag{4.2.7}$$

By using Eq. (4.2.7), second order derivatives and products of first order and higher these are dropped in the Maxwell wave equation. McCall and Hahn took the envelope **E**(t, z) as follows:

$$\mathbf{E}(t,z)=\mathcal{E}(t,z)\,\hat{\mathbf{a}} \quad , \quad \hat{\mathbf{a}}= \begin{bmatrix} \cos\theta & 0 \\ 0 & \sin\theta \end{bmatrix} \begin{pmatrix} \hat{\mathbf{x}} \\ \hat{\mathbf{y}} \end{pmatrix} \tag{4.2.8}$$

where $\theta=\omega t-Kz+\phi(z)$ and K is the wavenumber of the pulse inside the medium. No phase modulation ($d\phi/dt=0$) was considered in accordance with the SVEA approximation.

The polarization of the medium **P**(t, z) is most easily expressed in the frame rotating with **E**:

where u and v are the in-phase (dispersive) and out of phase (absorptive) components relative to E of the macroscopic polarization P, and w is the population inversion of the medium. For very small electric fields (linear optics), $w \approx -1$, the atoms are mainly in the ground state, practically unexcited, and they behave as Lorentzian oscillators. For larger electric field intensities, the nonlinearities of the Bloch equations become important.

McCall and Hahn considered a circularly polarized pulse with a carrier wave of frequency ω. On the time and length scale of this carrier wave, the envelope is slowly varying. Thus it is natural to separate out the fast and the slow variables. The slowly varying envelope approximation (SVEA) consists in taking an envelope function E(t, z) which satisfies:

$$\left|\frac{\partial \mathcal{E}}{\partial z}\right| << \left|\frac{\mathcal{E}}{\lambda}\right| \quad \text{and} \quad \left|\frac{\partial \mathcal{E}}{\partial t}\right| << \omega|\mathcal{E}| \tag{4.2.7}$$

By using Eq. (4.2.7), second order derivatives and products of first order and higher these are dropped in the Maxwell wave equation. McCall and Hahn took the envelope E(t, z) as follows:

$$\mathbf{E}(t,z)=\mathcal{E}(t,z)\,\hat{\mathbf{a}} \quad , \quad \hat{\mathbf{a}}=\begin{bmatrix}\cos\theta & 0\\ 0 & \sin\theta\end{bmatrix}\begin{pmatrix}\hat{\mathbf{x}}\\ \hat{\mathbf{y}}\end{pmatrix} \tag{4.2.8}$$

where $\theta=\omega t-Kz+\phi(z)$ and K is the wavenumber of the pulse inside the medium. No phase modulation ($d\phi/dt=0$) was considered in accordance with the SVEA approximation.

The polarization of the medium P(t, z) is most easily expressed in the frame rotating with E:

$$\mathbf{P}(t,z)=\frac{1}{2}N\hbar\kappa\left\{u(t,z)\,\hat{\mathbf{a}}+v(t,z)\hat{\mathbf{b}}\right\}\qquad \hat{\mathbf{b}}=\begin{bmatrix}-\sin\theta & 0\\ 0 & \cos\theta\end{bmatrix}\begin{pmatrix}\hat{\mathbf{x}}\\ \hat{\mathbf{y}}\end{pmatrix} \tag{4.2.9}$$

Self-Induced Transparency results as a novel consequence of the non-linear interaction of an intense electric field with the two level resonance atoms of a medium and was observed by McCall and Hahn in computer solutions of the coupled Maxwell-Bloch equations and later confirmed experimentally [55]. The nature of the effect is based on the fact that after the pulse has propagated a few classical absorption lengths into the medium the initial pulse evolves into the shape of a symmetric hyperbolic-secant travelling pulse, and has the area under the pulse envelope equal to 2π ("2π pulse"). The pulse solution of the Maxwell-Bloch equations in the SVEA approximation is of the form:

$$\mathcal{E}(t,z)=\frac{2}{\kappa\tau}\operatorname{sech}\left[\frac{t-z/V}{\tau}\right]\qquad \text{with}\quad \int_{-\infty}^{+\infty}\mathcal{E}(t,z)\,dt=2\pi \tag{4.2.10}$$

which corresponds to a family of solitary waves of arbitrary pulse width τ travelling with velocity $V=c/(1+2\pi\kappa\omega N d\tau^2)$.

The physical picture that corresponds to SIT is shown in Fig. 4.2.1 (page 77). The front part of a short pulse coherently excites the atoms in the medium up to the state of complete inversion. The macroscopic polarization formed in this process then interacts with the remaining part of the pulse and emits coherent radiation which joins the back part of the pulse. If the atoms return to the ground state after this stimulation process, steady-state propagation is realized.

4.3 SELF-INDUCED TRANSPARENCY IN SEMICONDUCTORS

The possibility of analogous SIT effects in semiconductors was studied for the first time by Poluektov and Popov [65], and by Tzoar and Gersten [66], both studies being in the SVEA. Experiments on materials like CdS_xSe_{1-x} and GaAs [67-70] showed that powerful light pulses (~100MW/cm^2) of duration shorter than the relaxation times connected with the exciton motion can propagate above a threshold intensity with anomalously small losses near the absorption resonance; significant delays (~100 psec) in time (larger than the pulse widths) were observed for these pulses. In addition, the propagation velocity of these pulses depends on the level of excitation, and the behavior of the pulse shape in space and time. These features of nonlinear absorption of ultrashort optical pulses were identified with SIT for excitons in semiconductors.

The implementation of the SIT picture presented special difficulties for semiconductors. While SIT was understood for dilute gases by McCall and Hahn, the extension of this picture to crystals is not obvious since complete inversion of the atoms can hardly be achieved even for intense light; instead of this, the formation of polaritons is significant. The polariton, being a mixed mode of the E-M field and the polarization wave in crystals, has a dispersion (in the case of local medium) which varies steeply near the resonance frequency ω_t accompanied by a gap in which any propagation is forbidden (polariton gap) in the "local optics " picture. Haken and Schenzle [71] showed that the effect of SIT can be expected for Frenkel excitons despite the fact that excitons are not localized states, but delocalized excitations of the crystal as a whole. They derived the photon dispersion relation of the carrier wave and the pulse velocity in the strong field case.

Hanamura [72] and Inoue [73] derived the dispersion relation for polaritons for weak fields for the case of Wannier and Frenkel excitons, respectively, and argued that SIT cannot occur, since it is prevented by the polariton effect of excitons. Akimoto and Ikeda

[74] investigated the solution of the Maxwell-Bloch equations beyond the SVEA; they derived the dispersion relation and the pulse velocity in connection with the steady-state pulse solutions in a self-consistent manner, which disagrees with the previous investigations of the dispersion relation. They showed that dispersion for a light-exciton pulse and its velocity are functions of the frequency ω and the pulse width τ. Similar results were presented by Goll and Haken [75] using quantum mechanical approaches.

The SIT phenomenon was also investigated for the case of spatially dispersive media. Agranovich and Rupasov [76] generalized the Maxwell-Bloch equations to include media with spatial dispersion in the SVEA. Additional work by Belkin et al. [77, 78] in the SVEA considered saturation and phase modulation which lead to the spreading of pulses.

4.4 EXTENSION OF SELF-INDUCED TRANSPARENCY BEYOND THE (SVEA)

For dilute gases, Matulic and Eberly [79] generalized the work of McCall and Hahn to include phase modulation (chirping). By including phase modulation in the SVEA, they found multi-pulse chirped steady-state wave trains. However their ansatz was too limited to lead to any solutions for single steady-state pulses. Propagation of the linearly chirped pulses in absorbers was studied by numerical integration of the equations of motion by Crisp [80]. Marth, Holmes, and Eberly [81] went beyond the SVEA for the on resonance case, and developed a method of approximation based on a series expansion in powers of a small parameter which is related to the electric field amplitude. In this way, they studied very short pulses for the complete set of Maxwell-Bloch equations. Corrections to the results of McCall and Hahn were found; they are significant only for picosecond and shorter pulses. Bialynicka-Birula [82] confirmed the results by Marth et al. by introducing a systematic perturbation expansion in the small parameter $(\omega\tau)^{-1}$.

Akimoto and Ikeda [74] investigated non-linear steady-state propagation of a coherent light pulse in resonant, local and non-local dielectric media for infinite relaxation times. They developed a systematic perturbative expansion method - beyond the SVEA - for various types of pulses based on a power-series expansion in a small parameter which is related to the pulse width. Their results can be summarized as follows. Besides the usual SIT with full inversion, steady pulse solutions were also found in the case when the pulse width is much longer than the reciprocal of the polariton gap frequency ω_{LT} with only partial inversion. A long pulse outside the gap (i.e. with peak frequency outside the gap) behaves as a weak polariton-soliton wave in the picosecond regime. A long pulse inside the gap propagates very slowly as a sort of standing wave of a non-linear polariton. A short pulse of strong intensity realizes the usual SIT. The stability of these solutions was not studied. The derived pulse shapes depend continuously on the pulse width τ which is an arbitrary parameter in the problem, just as McCall and Hahn found in the SVEA. Mathematical details and plots will be presented in Section 5.4, where we will re-derive their results from a uniform perturbation analysis and compare our new results to theirs.

Ikeda and Akimoto went beyond the SVEA and generalized the coupled system of Maxwell-Bloch equations to spatially dispersive media [83] and solved these equations by a power series expansion developed by them in Ref. [74]. They showed that two kinds of steady-state pulse solutions propagate in the medium: one propagates in the medium as an E-M radiation field and the other by excitation transfer between the dipoles. The former solution is SIT-like in the short pulse limit, while in the long pulse limit it becomes a polariton-soliton or a standing wave of non-linear polariton.The latter is an exciton-polariton containing little photon component. When the pulse width is extremely long, there appears a polariton-soliton of a new type in which the two propagation mechanisms are mixed. They found that spatial dispersion in this case prevents polariton-soliton solutions from existing in a certain frequency range.

4.5 SOLITARY WAVES VERSUS SOLITONS

A travelling wave ϕ is a disturbance which depends only upon z and t through ζ = t-z/V, where V is a fixed constant, the velocity of the wave. A solitary wave ϕ_{SW} is a localized travelling wave, i.e. it is a travelling wave that decays to zero as $\zeta \rightarrow \pm \infty$. The concept of a solitary wave was introduced in hydrodynamics by Russell over a century ago, while the mathematical foundation for the study of solitary waves was provided by Korteweg-deVries [84]. Travelling wave solutions of the Korteweg-deVries (KdV) equation can be obtained by assuming $\phi(z, t) = \phi(\zeta)$ where ζ = t-z/V represents the position in a coordinate system moving at a velocity V from which the wave appears stationary. For such travelling waves, the original partial differential equation (PDE) can be reduced to an ordinary differential equation (ODE). For the KdV the solution consists of an infinite periodic train of localized "humps" for which the velocity V of the train and the spacing between the humps d are continuously variable. The solitary wave is obtained simply by letting $d \rightarrow \infty$.

A special subclass of solitary waves is the soliton class of solutions for dispersive wave equations. A working definition for solitons is the following one: A soliton ϕ_S is a solitary wave solution of a wave equation which asymptotically preserves its shape and velocity upon collisions with other solitary waves [85].

The simplest example of a soliton is a pulse-like travelling wave solution of the dispersionless linear wave equation:

$$\frac{\partial^2 \phi}{\partial z^2} - \frac{1}{c^2}\frac{\partial^2 \phi}{\partial t^2} = 0 \qquad (4.5.1)$$

If we introduce dispersion without non-linearity into Eq. (4.5.1), this destroys the possibility of solitary waves because the various Fourier components of any initial

conditions propagate at different velocities. By the same token the introduction of non-linearity without dispersion again removes the possibility of solitary waves because the pulse energy is continuously injected via harmonic generation into higher frequency modes. In the time domain this often appears as the formation of shock waves. But with both dispersion and non-linearity, solitary waves can again be formed. The solitary wave can be qualitatively understood as representing a balance between the effect of non-linearity and that of dispersion.

In a SIT review paper, Lamb [58] pointed out that the propagating isolated hyperbolic secant pulses found by McCall and Hahn are in fact solitons. The Maxwell-Bloch equations in the SVEA form an exactly integrable system, just like the Korteweg-deVries and the Sine-Gordon equations. Such exactly integrated systems possess an infinite number of conservation laws, preventing solitons from disintegrating during collisions. The solutions of Maxwell-Bloch equations break into a sequence of isolated coherent optical pulses as McCall and Hahn had demonstrated. The amplitude of each of these solitons can be predicted from the conservation laws derived by Lamb. The analytical technique for carrying out this procedure is known as the inverse scattering transform (IST). In 1973, Lamb [86] showed using a series of variable transformations that the SIT equations reduced to one of the standard equations of IST, the Zakharov-Shabat equations [87]. A general review of the IST as applied to SIT in the SVEA was given by Hauss [88]. More generally, the IST solves the initial value problem for PDEs which have an infinite number of conservation laws. These are the integrable questions.

The problem which we will discuss in the following Chapter 5 is the following: What happens if one adds a small perturbation to an integrable system? For example, in the case of Maxwell-Bloch equations, what happens if one goes beyond the SVEA by keeping higher order terms in Maxwell wave equation? A generic perturbation destroys exact integrability. Thus one expects that as soon as one goes beyond the SVEA, solitons should disappear, but one might still expect there to be solitary waves. In other words, the

polariton-soliton and SIT solutions derived by Akimoto and Ikeda in their perturbation analysis in various pulse width limits should not be solitons, only solitary waves. However, it will turn out that the solitary waves also disappear except for a discrete set of solutions, and that this cannot be seen at any finite order in a perturbative expansion about the SVEA.

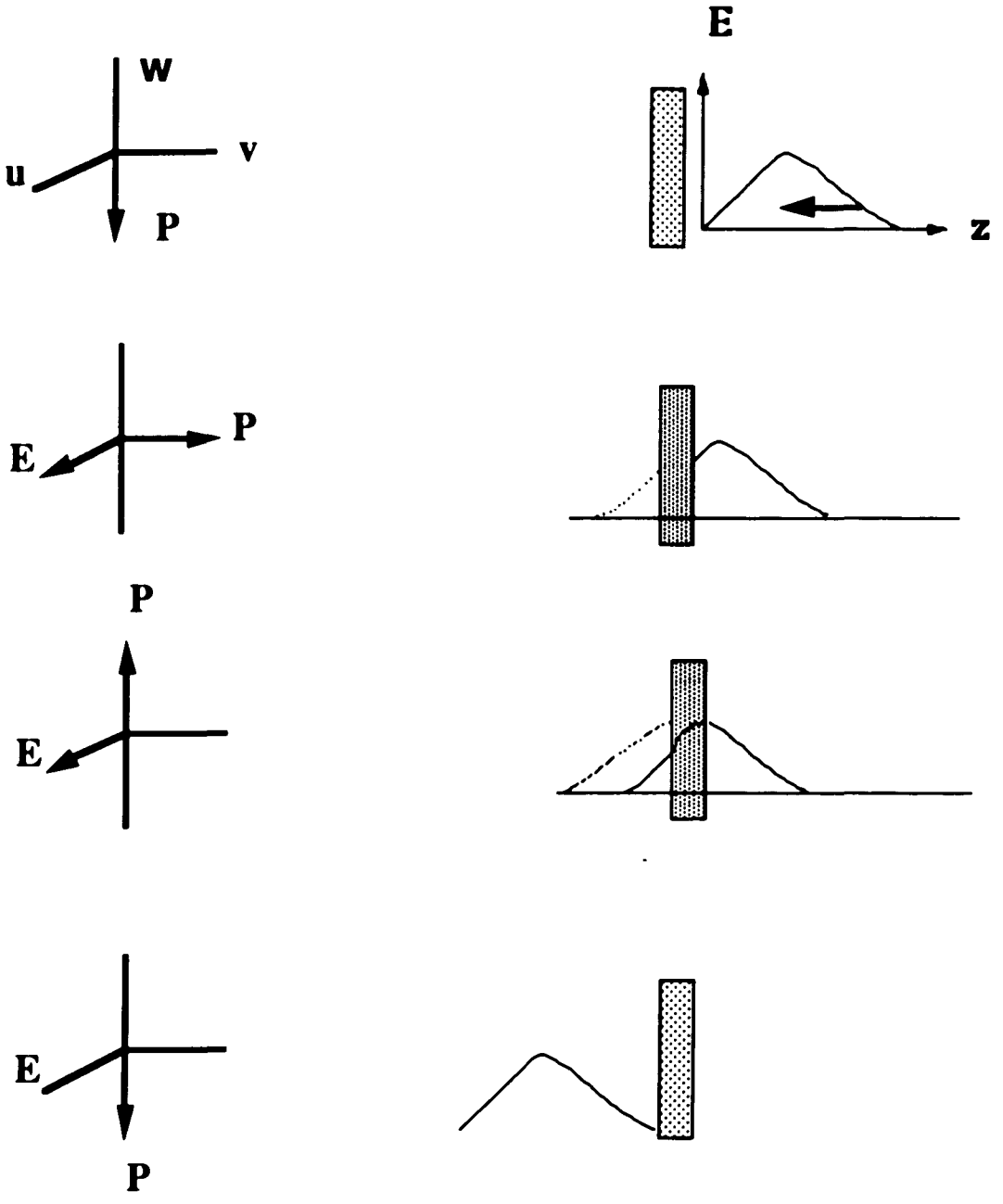

Figure 4.2.1 Pictorial description of the rotation of the macroscopic pseudo-polarization vector **P=Nd** by a 2π hyperbolic secant pulse as the pulse is transmitted through an absorber. The pulse is delayed one pulse length for each absorption length as the pulse is coherently absorbed and re-emitted.

CHAPTER 5

STEADY-STATE PROPAGATION OF INTENSE OPTICAL PULSES IN UNBOUNDED LOCAL DIELECTRIC MEDIA

O say! What is this thing called Light?

Colley Cibber

5.1 INTRODUCTION

Atomic electric dipole transitions in crystals and gases typically produce radiation in the optical region of the E-M spectrum. Consequently, in almost every experiment involving the interaction of E-M radiation with electric dipoles, one must take into account the E-M propagation through the dipole medium. Over the last 25-30 years, intense, coherent light pulses have been available for the study of optically resonant systems. The response of such systems, when strongly probed near resonance, is of non-linear nature.

Self-induced transparency (SIT) is a strongly non-linear phenomenon. It can be analyzed by simultaneously solving the Maxwell wave equation and the optical Bloch equations which govern the dynamics of the electric dipoles of a two-level system of atoms in an E-M field. In this case, the dipoles and the E-M radiation field do not couple directly to each other: they couple to each other parametrically through population inversion. It is the non-linearity inherent in such a coupling that plays an essential role in the formation of a solitary pulse. On the other hand, in dense dielectric media like crystals, complete inversion of the atoms can hardly be achieved for high light intensities; instead of this, the formation of polaritons is significant. The polariton, being a mixed mode of the E-M field and the polarization wave in the dielectric, (or in quantum mechanical terms an exciton-polariton quasiparticle), has a dispersion which varies steeply near the resonance frequency ω_t, accompanied by the presence of a gap (in the case of no spatial dispersion) in which no real propagating mode exists (polariton gap).

Akimoto and Ikeda investigated the steady-state (soliton-like) propagation of a coherent light pulses in resonant, local [74] and non-local dielectric media [83] for infinite relaxation times (no damping), and no surface effects. They developed a method which unifies the two complementary concepts, SIT and polaritons and presented a systematic perturbative expansion method - beyond the SVEA - for various types of pulses based on a power-series expansion in a small parameter which is related to the pulse width τ. They argued

that if the Fourier frequency spectrum of a finite width pulse covers the polariton gap completely, the pulse does not "see" the existence of the gap. The pulse is then called short. In the opposite case, when the Fourier frequency spectrum lies completely inside or completely outside the polariton gap, the pulse is called long. A long pulse behaves differently outside and inside the gap.

The purpose of this chapter is to go beyond Akimoto and Ikeda's perturbation expansion using a uniform approximation approach and to prove that Akimoto and Ikeda's steady-state pulses do not exist for arbitrary pulse widths τ, but only for selected pulse widths. In Section 5.2, following Akimoto and Ikeda [74], the complete set of Maxwell-Bloch equations is derived beyond the SVEA, together with the dispersion relation of the carrier wave and the pulse velocity. In Section 5.3, the coupled system of Maxwell-Bloch equations is solved perturbatively, based on a series expansion in powers of a small parameter which is related to the electric field amplitude. This method has already been presented for the on resonance case by Marth, Holmes, and Eberly [81] for the SIT problem in dilute gases. General expressions for the solitary waves and their phase modulations are derived for any incident carrier frequency ω and arbitrary pulse width τ. In particular, these expressions include Akimoto and Ikeda's results for short and long pulses inside and outside the polariton gap.

In Section 5.4, the breakdown of the perturbation expansion developed in Section 5.3 is explained: this uniform expansion and Akimoto and Ikeda's expansions for short and long pulses are only locally valid: they are not uniformly valid on the whole domain $(-\infty, +\infty)$, and thus these expansions *cannot* determine whether there exist solitary wave solutions. Under these circumstances, a tuning of the pulse width τ for each given frequency detuning ω-ω_t is required for the boundary conditions at $\pm\infty$ to be satisfied. In other words, a fine tuning of non-linearity and dispersion is needed to obtain solitary solutions. Numerical results from the integration of Maxwell-Bloch equations are presented in Section 5.5. We find that selected solitary branch solutions (mainly inside the polariton

gap) are generated: the competition between non-linearity and dispersion leads to a selection mechanism for the pulse width and velocity inside the dielectric. The numerical results are discussed in Section 5.6 where it is shown that only a very restricted parameter space exists for which solitary solutions occur, contrary to the implications of Akimoto and Ikeda's previous work. Note that the results are applicable to the Maxwell-Bloch model in which damping and spatial dispersion effects are neglected.

5.2 THE MAXWELL-BLOCH EQUATIONS BEYOND THE SVEA

Let us assume that the dielectric medium can be described by an unbounded continuum system of non-interacting two-level atoms and the coherent E-M field can treated classically. It is assumed that the atoms have only one possible transition, that incoherent scattering from impurities, back scattering, and nonresonant losses are absent, multimode and diffractive effects can be ignored, while relaxation times are infinite (no damping, Γ=0). No spatial dispersion effects ($m^* = 0$) and no surface effects are included.

Without assuming the slowly varying envelope approximation (SVEA) in dielectrics, we are looking for 'traveling wave' solutions for the electric field $\mathbf{E}(t, z)$ and the polarization density $\mathbf{P}(t, z)$ which depends only on the variable $\zeta=(t-z/V)$, where V is a velocity to be determined. However this does not lead to any solutions, so we must look for special solutions which are self-similar. A function is self-similar if it is unchanged under a combination of dilations, and translations of both the dependent and independent variables.

Mathematically speaking, given a partial differential equation (PDE), let us consider its symmetry group G. In general, G will be an m parameter group. One looks for special solutions which are self-similar: they are typically singlets of a one-parameter subgroup of

G. For example, by using a one parameter transformation: z → z+A and t → t+B and applying it to Helmholtz equation

$$(\nabla^2 - \frac{1}{c^2}\frac{\partial^2}{\partial t^2})\phi(z,t) = 0 \tag{5.2.1}$$

we can choose a one parameter subgroup: z → z+λA and t → t+A. The parameter λ is determined trivially: it is just the velocity in the equation.

In the case of Maxwell-Bloch equations, the symmetry group is now translation in space and time, z → z+VA and t → t+A and rotations of the form:

$$\begin{pmatrix}\hat{\mathbf{x}}\\ \hat{\mathbf{y}}\end{pmatrix} = \begin{pmatrix}\cos\Theta(t) & \sin\Theta(t)\\ -\sin\Theta(t) & \cos\Theta(t)\end{pmatrix}\begin{pmatrix}\hat{\mathbf{x}}\\ \hat{\mathbf{y}}\end{pmatrix}$$

Again, one can choose a one parameter subgroup: t → t+A and z → z+VA and θ → θ+(ω–KV)A. Then if we go to the frame rotating with **E**, we can look for solutions of the form:

$$\mathbf{E}(t,z) = \mathcal{E}(t - z/V)\hat{\mathbf{a}}(t,z)$$

$$\mathbf{P}(t,z) = \frac{1}{2}N\hbar\kappa\left\{u(t-z/V)\,\hat{\mathbf{a}}(t,z) + v(t-z/V)\hat{\mathbf{b}}(t,z)\right\} \tag{5.2.2}$$

where the rotating orthogonal unit vectors,

$$\hat{\mathbf{a}}(t,z) = \begin{bmatrix}\cos\theta & 0\\ 0 & \sin\theta\end{bmatrix}\begin{pmatrix}\hat{\mathbf{x}}\\ \hat{\mathbf{y}}\end{pmatrix} \qquad \hat{\mathbf{b}}(t,z) = \begin{bmatrix}-\sin\theta & 0\\ 0 & \cos\theta\end{bmatrix}\begin{pmatrix}\hat{\mathbf{x}}\\ \hat{\mathbf{y}}\end{pmatrix}$$

$$\theta=\omega t-Kz+\phi(t-z/V) \tag{5.2.3}$$

contain phase modulation (chirping) ϕ for the electric field, explicitly. The almost circularly polarized electric field E(t, z) is factorized into the slow varying pulse envelope $\hat{E}$ and the rapidly oscillating carrier wave $\hat{\mathbf{a}}$, in which $\hat{\mathbf{x}}$ and $\hat{\mathbf{y}}$ are the unit vectors of polarization. The envelope is a function of (t-z/V) where V is the steady-state velocity in the +z-direction. The magnitude of the carrier wave vector K is generally not equal to the magnitude of the vacuum wave vector $k_0=\omega/c$; the dispersion relation for K versus ω will be determined later in a self-consistent manner in the tail of the pulse. The polarization density P(t, z) is the sum of the in-phase (dispersive) component u and the out of phase (absorptive) component v; each one of them is also assumed to have the same functional behavior as E(t, z). In Eq. (5.2.2) N is the volume density of resonant atoms, and κ is the common dipole matrix d element divided by $\hbar/2$, i.e. $\kappa=2d/\hbar$.

The electric field vector E(t, z) obeys the Maxwell wave equation:

$$\left(\frac{\partial^2}{\partial z^2}-\frac{1}{c^2}\frac{\partial^2}{\partial t^2}\right)\mathbf{E}(t,z)=\frac{4\pi}{c^2}\frac{\partial^2}{\partial t^2}\mathbf{P}(t,z) \tag{5.2.4}$$

where we have used the fact that none of the fields depends on x or y. By taking its components along $\hat{\mathbf{x}}$ and $\hat{\mathbf{y}}$ separately the vector wave equation turns into two-second order coupled scalar equations:

$$\left(\frac{1}{V^2}-\frac{1}{c^2}\right)\ddot{\mathcal{E}}-\left[(K^2-k_0^2)+2\left(\frac{K}{V}-\frac{k_0}{c}\right)\dot{\phi}+\left(\frac{1}{V^2}-\frac{1}{c^2}\right)\dot{\phi}^2\right]\mathcal{E}$$
$$=\frac{2\pi N\hbar\kappa}{c^2}\left[\ddot{u}-(\omega+\dot{\phi})^2u-\ddot{\phi}v-2(\omega+\dot{\phi})\dot{v}\right] \tag{5.2.5}$$

$$\left(\frac{1}{V^2}-\frac{1}{c^2}\right)\ddot{\phi}\mathcal{E}+2\left[\left(\frac{K}{V}-\frac{k_0}{c}\right)+\left(\frac{1}{V^2}-\frac{1}{c^2}\right)\dot{\phi}\right]\dot{\mathcal{E}}$$
$$=\frac{2\pi N\hbar\kappa}{c^2}\left[\ddot{v}-(\omega+\dot{\phi})^2 v+\ddot{\phi}u+2(\omega+\dot{\phi})\dot{u}\right] \tag{5.2.6}$$

Here the dots mean d/dζ, where ζ=t-z/V is the local time coordinate. In the SVEA, the phase modulation $\dot{\phi}\equiv 0$ vanishes identically, and the terms ü and v̈ are discarded in comparison to ω^2u and ω^2v. One can eliminate all but the lowest derivative term on each side of Eqs. (5.2.5) and (5.2.6) and then one obtains the usual SIT equations [55] for a sharp line resonance.

The atomic Schrödinger equation, allowing for phase modulation, and assuming no effective broadening for the resonance line, leads to the Bloch equations [64] for u and v, together with the population difference between the ground and excited states, w (see Chapter 4, Section 4.2). They form a classical pseudo-spin vector in the rotating frame, assuming that no higher frequencies are included.

$$\dot{u}=(\omega-\omega_t+\dot{\phi})v \tag{5.2.7}$$

$$\dot{v}=-(\omega-\omega_t+\dot{\phi})u+\kappa\mathcal{E}w \tag{5.2.8}$$

$$\dot{w}=-\kappa\mathcal{E}v \tag{5.2.9}$$

where ω_t is the resonant frequency of the medium, while the product $\kappa\mathcal{E}$ has the dimensions of frequency, and may be called the instantaneous Rabi frequency for the pulse. All the relaxation times have been assumed to be infinite, which leads to a conservation law for the components of the pseudo-spin Bloch vector (see Eq. (4.2.2)):

$$u^2+v^2+w^2=1 \tag{5.2.10}$$

This conservation law relates to "excitation energy" like [probability of excitation + probability of deexcitation + probability of population inversion = 1].

The system of Maxwell-Bloch eqs. can be rewritten for convenience in dimensionless form. Introducing the dimensionless electric field amplitude $E = \kappa\mathcal{E}/2\pi N\hbar\kappa^2 = \kappa\mathcal{E}/\omega_{LT}$ where $\omega_{LT} = 2\pi N\hbar\kappa^2 = 8\pi Nd^2/\hbar$ is the polariton gap frequency, and the dimensionless time $\xi = \zeta/\tau = (t-z/V)/\tau$ (τ is arbitrary, but it will chosen to be essentially the pulse width), one can obtain the following systems of equations, in which from now on the dots mean $d/d\xi = \tau\, d/d\zeta$:

$$\gamma\ddot{E}-(\alpha+\beta\dot{\phi}+\gamma\dot{\phi}^2)E=s^2\ddot{u}-(1+s\dot{\phi})^2u-s^2\ddot{\phi}v-2(1+s\dot{\phi})s\dot{v} \tag{5.2.11}$$

$$\gamma\ddot{\phi}E+(\beta+2\gamma\dot{\phi})\dot{E}=s^2\ddot{v}-(1+s\dot{\phi})^2v+s^2\ddot{\phi}u+2(1+s\dot{\phi})s\dot{u} \tag{5.2.12}$$

$$\Lambda\dot{u}=(\Delta+\Lambda\dot{\phi})v \tag{5.2.13}$$

$$\Lambda\dot{v}=-(\Delta+\Lambda\dot{\phi})u+Ew \tag{5.2.14}$$

$$\Lambda\dot{w}=-Ev \tag{5.2.15}$$

Also Δ is the dimensionless frequency detuning, Λ is the reciprocal pulse width, and s depends on the material parameters. They are defined as

$$\Delta=(\omega-\omega_l)/2\pi N\hbar\kappa^2 = (\omega-\omega_l)/\omega_{LT} \tag{5.2.16a}$$

$$\Lambda=\tau^{-1}/2\pi N\hbar\kappa^2=1/\omega_{LT}\tau \tag{5.2.16b}$$

$$s = 1/\omega\tau=\Lambda/[\Delta+\omega_l/\omega_{LT}] \tag{5.2.16c}$$

The coefficients α, β and γ are defined as

$$\alpha=(K/k_0)^2-1 \tag{5.2.16d}$$

$$\beta=2s[(cK/Vk_0)]-1] \tag{5.2.16e}$$

$$\gamma=s^2[(c/V)^2-1] \tag{5.2.16f}$$

and they are functions of the three dimensionless parameters Δ, Λ and s. As pointed out by Akimoto and Ikeda [74], the wavenumber K and the pulse envelope velocity V can be derived as functions of ω and τ by linearizing the set of Maxwell-Bloch ODEs (Eqs. 5.2.11-15) and setting $\dot{\phi}=0$ and w=-1 which corresponds to defining ω and K in the pulse tail where the excitation is very weak. One can obtain exponential solutions $\mathcal{E} \sim \exp[\pm\xi]$, besides the plane wave solution which corresponds to the usual polariton. Even though these solutions are divergent and therefore meaningless, they are meaningful in the tail of a steadily propagating pulse since the exponential form can describe a growing (or decaying) wave locally. In the presence of nonlinearity, the divergence of the linear solution will be suppressed and a pulse is formed. At the same time, the dispersion relation around the pulse peak will be modulated through the non-zero phase modulation $\dot{\phi}$. The growth (or decay) rate τ gives a measure of the pulse width, since the pulse shape has been assumed to be a slowly varying function in space and time. One can determine K and V as functions of ω and τ:

$$\left(\frac{K}{k_0}\right)^2=\frac{1}{2}\left[(1-s^2)-\frac{(1-s^2)\Delta+2s\Lambda}{\Delta^2+\Lambda^2}+(1+s^2)\left(\frac{(\Delta-1)^2+\Lambda^2}{\Delta^2+\Lambda^2}\right)^{1/2}\right] \tag{5.2.17}$$

$$\left(\frac{c}{V}\right)^2 = \frac{s^{-2}}{2}\left[-(1-s^2)+\frac{(1-s^2)\Delta+2s\Lambda}{\Delta^2+\Lambda^2}+(1+s^2)\left(\frac{(\Delta-1)^2+\Lambda^2}{\Delta^2+\Lambda^2}\right)^{1/2}\right] \qquad (5.2.18)$$

from which one can obtain the expressions for α and γ in terms of Δ, Λ and s through Eq. (5.2.16); the coefficient β is given by:

$$\beta = \frac{\Lambda(1-s^2)}{\Delta^2+\Lambda^2} - \frac{2s\Delta}{\Delta^2+\Lambda^2} \qquad (5.2.19)$$

The polariton gap corresponds to the range $0 < \Delta < 1$. The dependence of the dispersion relation upon pulse width is given by Eq. (5.2.17) and is plotted in 3-D in Fig. 5.2.1 (page 108). For very short pulses ($\Lambda >> 1$), the dispersion relation approaches that of the photon (photon-like). As the pulse becomes longer ($\Lambda \rightarrow 0$) , the dispersion relation outside the gap approaches that of the polariton (polariton-like). The wave vector K remains real inside the gap and tends to zero like $K \approx k_0\Lambda[4\Delta^3(1-\Delta)]^{-1/2}$.

The pulse velocity is plotted in Fig. 5.2.2 (page 108). For very short pulses ($\Lambda >> 1$), the pulse velocity V tends to c. As the pulse becomes longer ($\Lambda \rightarrow 0$), the pulse velocity outside the gap approaches $c(s/\Lambda)[4\Delta^3(1-\Delta)]^{1/2}$, which is equal to the group velocity $v_g = d\omega/dK$ calculated from the dispersion relation of the polariton in Eq. (5.2.17). The pulse velocity remains real inside the gap and tends to zero like $c\Lambda(\omega_{LT}/\omega_t)[\Delta/(1-\Delta)]^{1/2}$. The material parameter ω_{LT}/ω_t was taken to be equal to 10^{-3} for these plots.

Now, the problem is to solve the Maxwell-Bloch Eqs. (5.2.11-15) simultaneously under the boundary condition that in the limit $\zeta \rightarrow \pm\infty$, the electric field vanishes, E=0, and the dipoles of the dielectric are in the ground state, w=-1.

The two second-order Maxwell Eqs. (5.2.11-12) are both non-linear and are not solvable by known methods. Their complexity can be reduced somewhat by using the

Bloch Eqs. (5.2.13-15) to eliminate all the derivatives of u, and v. This step is simply algebraic. One finds for the two Maxwell equations:

$$\gamma\ddot{E}-[\alpha+\beta\dot{\phi}+\gamma\dot{\phi}^2+\frac{s}{\Lambda}(\frac{s\Delta}{\Lambda}-2)w+\frac{s^2}{\Lambda}\dot{\phi}w]E=-(\frac{s\Delta}{\Lambda}-1)^2u \tag{5.2.20a}$$

$$\gamma\ddot{\phi}E+(\beta+2\gamma\dot{\phi}-\frac{s^2}{\Lambda}w)\dot{E}=-[(\frac{s\Delta}{\Lambda}-1)^2+(\frac{s}{\Lambda})^2E^2]v \tag{5.2.20b}$$

The phase equation (5.2.20b) is a first-order linear differential equation for $\dot{\phi}$, from which one can derive a first integral [81]:

$$\gamma\dot{\phi}E^2=-\frac{\beta}{2}E^2+\Lambda(\frac{s\Delta}{\Lambda}-1)^2(w+1)+\frac{s^2}{\Lambda}E^2w-\frac{s^2}{\Lambda}\int_0^E E'w(E')dE' \tag{5.2.21}$$

Eq. (5.2.21) shows that if one knows the functional relation between the dimensionless energy of the dipoles w and the pulse amplitude E, i.e, if the relation w=w(E) can be found, then $\dot{\phi}$(E) is determined. Furthermore, if both w(E) and $\dot{\phi}$(E) are known, then one can determine, at least formally by using Bloch eqs., the functional relation u=u(E). This turns the amplitude equation (5.2.20a) into a non-linear second order differential equation for E alone. Thus the system is reduced to quadratures in principle if w=w(E) is known.

5.3 THE ELECTRIC FIELD AMPLITUDE EXPANSION

In order to carry out the procedure of integration of the Bloch Eqs. (5.2.13-15), the amplitude Eq.(5.2.20a), and the phase Eq. (5.2.20b), one simply needs to adopt a

sufficiently general form for the relation w(E). The ansatz used for w(E) is a power series expansion about the origin:

$$w(E) = \sum_{i=0}^{\infty} w_{2i} \cdot (\frac{\kappa \mathcal{E}}{\omega_{LT}})^{2i} = \sum_{i=0}^{\infty} w_{2i} \cdot E^{2i} \qquad (5.3.1)$$

The choice of the dimensionless electric field amplitude $E = \kappa\mathcal{E}/\omega_{LT}$ as the expansion parameter, and the restriction to even powers of the parameter E, are both suggested by the McCall and Hahn theory of SIT in the SVEA [55]. All the coefficients w_{2i} are to be determined self-consistently except w_0 which must be equal to -1 in order that the dipoles of the dielectric are in their ground state when pulse amplitude E is zero.

The convergence of the series in Eq. (5.3.1) is a rather subtle mathematical question and can not been answered precisely, since as will be shown later, the coefficients w_{2i} depend in complicated ways, on the parameters Δ, Λ, and s. However, there are good reasons for expecting high accuracy of using just a few terms in w(E). In the first place, the relation between population inversion w and field energy E^2 must be mathematically analytic. Moreover, there is a simple physical argument that requires that the expansion parameter $E = \kappa\mathcal{E}/\omega_{LT}$ be smaller than unity: the eigen-energies of the dipoles are of order of $\hbar\omega_t$, and the perturbative dipole-E-M field interaction energy is $\mathbf{d}\cdot\mathbf{E} \sim d\mathcal{E} \sim \hbar\kappa\mathcal{E}$. Thus one is forced to assume $\kappa\mathcal{E} << \omega_t$ and even more $\kappa\mathcal{E} << \omega_{LT}$, (since $\omega_{LT}/\omega_t \sim 10^{-3}$ for dielectrics), if the interaction is to be significantly weaker than the unperturbed energy.

An additional problem arises when one has to decide how many terms should be kept in the power series expansion in Eq. (5.3.1) to obtain finer approximate solutions for the electric field amplitude E. In this procedure, the expansion is carried out up the fourth power of the small parameter $E = \kappa\mathcal{E}/\omega_{LT} << 1$. This will lead to an ODE for the electric field amplitude E, which will represent the lowest level of approximation for the power

series expansion. Any higher order terms like w_6 can properly be expected to give only a small correction to the terms preceding it.

The power series in w(E) [Eq. (5.3.1)] is truncated as follows:

$$w(E) = -1 + w_2 E^2 + w_4 E^4 \qquad \text{for } E << 1 \tag{5.3.2}$$

Given w(E) , the desired expression for the phase modulation for $\dot{\phi}$ is found immediately from Eq. (5.2.21) by evaluating the definite integral. One obtains:

$$\gamma\dot{\phi} = \left\{-\frac{\beta}{2} - \frac{s^2}{2\Lambda} + \Lambda\,(\frac{s\Delta}{\Lambda} - 1)^2 w_2\right\} + \left\{\Lambda\,(\frac{s\Delta}{\Lambda} - 1)^2 w_4 + \frac{3s^2}{4\Lambda} w_2\right\} E^2 + \ldots. \tag{5.3.3}$$

When $\xi \rightarrow \pm\infty$ there is no phase modulation so that the E independent field term is zero. This leads to an expression for w_2, and for ϕ_2 in terms of Δ, Λ, s, w_2, and w_4:

$$w_2 = \frac{1}{2\Lambda} \frac{(\beta + \frac{s^2}{\Lambda})}{(\frac{s\Delta}{\Lambda} - 1)^2} = \frac{1}{2(\Delta^2 + \Lambda^2)} \tag{5.3.4}$$

$$\dot{\phi} = \phi_2 E^2 + \ldots. \qquad \text{where } \phi_2 = \frac{\Lambda\,(\frac{s\Delta}{\Lambda} - 1)^2 w_4 + \frac{3s^2}{4\Lambda} w_2}{\gamma} \tag{5.3.5}$$

Since the functional form of w(E) and $\dot{\phi}(E)$ is known to lowest order, the functional form for u(E) and v(E) can be derived with the help of the Bloch equations (5.2.13-15). This gives

$$u(E) = u_1 E + u_3 E^3 \tag{5.3.6}$$

where

$$u_1 = -2\Delta w_2 \quad \text{and} \quad u_3 = -\frac{1}{3}[4\Delta w_4 + 2\Lambda \phi_2 w_2] \tag{5.3.7}$$

and

$$v = v_1 \dot{E} \qquad \text{where} \qquad v_1 = -2\Lambda w_2 \tag{5.3.8}$$

Now, one can integrate the corresponding amplitude Maxwell equation (5.2.20a), by multiplying it by $\dot{E}$ after using Eqs. (5.3.2, 5.3.4-7) for w(E), $\dot{\phi}(E)$, and u(E). All the terms in Eq. (5.2.20a) except $\dot{\phi}^2$ contribute at this order of the approximation. The result of the integration is the following ODE for the electric field amplitude E:

$$\ddot{E} = E + \frac{(\beta + \frac{s^2}{\Lambda})\phi_2 + \frac{s}{\Lambda}(\frac{s\Delta}{\Lambda} - 2)w_2 - (\frac{s\Delta}{\Lambda} - 1)^2 u_3}{\gamma} E^3 \tag{5.3.9}$$

This implies at the envelope of the electric field amplitude E is a hyperbolic secant at this level of approximation, the coefficient w_4 is unknown for the moment. In order to derive w_4, another independent equation for E can be obtained from the conservation law in Eq. (5.2.10) by using the lowest order terms for u(E), v(E), and w(E) from Eqs. (5.3.2, 5.3.6-8). This leads to another ODE for the electric field amplitude E with the unknown w_4:

$$\ddot{E} = E + 2[\frac{2w_4 - w_2^2 - 2u_1 u_3}{v_1^2}]E^3 \tag{5.3.10}$$

By equating the coefficients of E^3 in Eqs. (5.3.9-10), an equation of first degree for w_4 is obtained. The coefficient w_4 is rather a complicated expression of the parameters Δ, Λ, and s. A detailed formula for w_4 and for the other lowest order coefficients in the case $s\neq 0$, is given in Appendix D. For the case s=0 (since for semiconductors $\omega_{LT}/\omega_t \sim 10^{-3}$ this is good approximation).

$$w_4 = \frac{-3\gamma^2 w_2^2}{2[-3\gamma^2 + 8(\Delta\gamma)^2 w_2 + 8\Delta\gamma(\Lambda w_2)^2 + 3\beta\Lambda^3 w_2^2 + 2\Lambda^4 w_2^3]} \qquad (5.3.11)$$

The solution of the non-linear ODEs in Eqs. (5.3.9-10) is given by [89]

$$E = C\,\mathrm{sech}[\xi] = C\,\mathrm{sech}[\frac{t - z/V}{\tau}] \qquad \text{where } \ddot{E} = E - \frac{2}{C^2}E^3 \qquad (5.3.12)$$

and

$$C^2 = \frac{4[-3\gamma^2 + 8(\Delta\gamma)^2 w_2 + 8\Delta\gamma(\Lambda w_2)^2 + 3\beta\Lambda^3 w_2^2 + 2\Lambda^4 w_2^3]}{w_2[4\Delta\gamma + 3\beta\Lambda + 2\Lambda^2 w_2]} \qquad (5.3.13)$$

The other w_4 - dependent coefficients ϕ_2 and u_3 can be derived also:

$$\phi_2 = \frac{-3\gamma\Lambda w_2^2}{2[-3\gamma^2 + 8(\Delta\gamma)^2 w_2 + 8\Delta\gamma(\Lambda w_2)^2 + 3\beta\Lambda^3 w_2^2 + 2\Lambda^4 w_2^3]} \qquad (5.3.14)$$

and

$$u_3 = \frac{\gamma w_2^2(2\Delta\gamma + \Lambda^2 w_2)}{[-3\gamma^2 + 8(\Delta\gamma)^2 w_2 + 8\Delta\gamma(\Lambda w_2)^2 + 3\beta\Lambda^3 w_2^2 + 2\Lambda^4 w_2^3]} \qquad (5.3.15)$$

In this way, a unification of the various limits of Akimoto and Ikeda's can be derived:

(i) Long pulses outside the gap. The following inequalities are then satisfied: $\Lambda << \Delta$ and $\Lambda << |\Delta\text{-}1|$ (in Akimoto and Ikeda's paper [74] the expansion parameter is $\varepsilon=\Lambda/\Delta<<1$). Explicit forms of the lowest order solutions are:

$$E = \Lambda\left(\frac{4\Delta-3}{\Delta-1}\right)^{1/2}\operatorname{sech}\xi \qquad \dot{\phi} = -\frac{3\Lambda}{2\Delta(4\Delta-3)}\operatorname{sech}^2\xi \tag{5.3.16a-b}$$

$$u = -\frac{\Lambda}{\Delta}\left(\frac{4\Delta-3}{\Delta-1}\right)^{1/2}\operatorname{sech}\xi + \frac{\Lambda^3}{2\Delta^2[(4\Delta-3)(\Delta-1)]^{1/2}(\Delta-1)}\operatorname{sech}^3\xi \tag{5.3.16c}$$

$$v = \left(\frac{\Lambda}{\Delta}\right)^2\left(\frac{4\Delta-3}{\Delta-1}\right)^{1/2}\operatorname{sech}\xi\tanh\xi \tag{5.3.16d}$$

$$w = -1+\left(\frac{\Lambda}{\Delta}\right)^2\frac{(4\Delta-3)}{2(\Delta-1)}\operatorname{sech}^2\xi - \frac{3}{8}\left(\frac{\Lambda}{\Delta}\right)^4\frac{1}{(\Delta-1)^2}\operatorname{sech}^4\xi \tag{5.3.16e}$$

(ii) Long pulses inside the gap. The expansion parameter $\varepsilon = \Lambda/\Delta$ is the same as outside the gap.The lowest order solutions are:

$$E = 2\Delta\sqrt{1-\Delta}\operatorname{sech}\xi \qquad \dot{\phi} = -\frac{3}{2}\frac{\Lambda}{\Delta}\operatorname{sech}^2\xi \tag{5.3.17a-b}$$

$$u = -2\sqrt{1-\Delta}\operatorname{sech}\xi + 4(1-\Delta)^{3/2}\operatorname{sech}^3\xi \tag{5.3.17c}$$

$$v = \frac{2\Lambda}{\Delta}\sqrt{1-\Delta}\,\mathrm{sech}\,\xi\tanh\xi \qquad (5.3.17d)$$

$$w = -1 + 2(1-\Delta)\mathrm{sech}^2\xi - 6(1-\Delta)^2\mathrm{sech}^4\xi \qquad (5.3.17e)$$

(iii) At resonance, i.e. Δ=0 or ω=ω_t. For a long pulse the expansion parameter is ε=Λ, and the results are:

$$E = \Lambda\,\mathrm{sech}\,\xi \qquad \dot{\phi} = -\frac{3}{4}\mathrm{sech}^2\xi \qquad (5.3.18a\text{-}b)$$

$$u = \frac{1}{4}\mathrm{sech}^3\xi \qquad v = \mathrm{sech}\,\xi\tanh\xi \qquad (5.3.18c\text{-}d)$$

$$w = -1 + \frac{1}{2}\mathrm{sech}^2\xi - \frac{3}{8}\mathrm{sech}^4\xi \qquad (5.3.18e)$$

(iv) Long pulses at Δ=1, or ω=ω_t+ω_{LT}. In this case, the expansion parameter is ε=Λ and the results are:

$$E = \sqrt{2\Lambda}\,\mathrm{sech}\,\xi \qquad \dot{\phi} = -\frac{3\Lambda}{2}\mathrm{sech}^2\xi \qquad (5.3.19a\text{-}b)$$

$$u = -\sqrt{2\Lambda}\,\mathrm{sech}\,\xi + \sqrt{2\Lambda^3}\,\mathrm{sech}^3\xi \qquad v = \sqrt{2\Lambda^3}\,\mathrm{sech}\,\xi\tanh\xi \qquad (5.3.19c\text{-}d)$$

$$w = -1 + \Lambda\,\mathrm{sech}^2\xi - \frac{3\Lambda^2}{2}\mathrm{sech}^4\xi \qquad (5.3.19e)$$

(v) Short pulses. The following conditions are satisfied: $\Lambda >> 1$ and $\Lambda >> \Delta$ (in Akimoto and Ikeda's paper [74], $\varepsilon=1/\Lambda<<1$). The solutions are given as follows:

$$E = 2\Lambda \operatorname{sech}\xi \qquad \dot{\phi} = -\frac{3}{8\Lambda}\operatorname{sech}^2\xi \tag{5.3.20a-b}$$

$$u = -2\frac{\Delta}{\Lambda}\operatorname{sech}\xi + \frac{1}{4\Lambda}\operatorname{sech}^3\xi \qquad v = 2\operatorname{sech}\xi\tanh\xi \tag{5.3.20c-d}$$

$$w = -1 + 2\operatorname{sech}^2\xi - \frac{3}{8\Lambda^2}\operatorname{sech}^4\xi \tag{5.3.20e}$$

For $\Lambda \rightarrow \infty$, one obtains complete inversion and no phase modulation, as found by McCall and Hahn [55].

The results in the various limits of Akimoto and Ikeda's analysis can been confirmed numerically. Figs. 5.3.1 and 5.3.2 (page 109) show C and ϕ_2 versus Δ and Λ when s=0 . For long pulses outside the polariton gap, the amplitude of the hyperbolic secant pulse is proportional to Λ and goes to zero as $\Lambda \rightarrow 0$. Inside the gap ($0 < \Delta < 1$), for a long pulse, the amplitude is proportional to Δ, while outside the gap the amplitude is smaller. This difference disappears as the pulse becomes shorter. When $\Lambda \rightarrow \infty$, the pulse does not "see" the polariton gap and it is not sensitive to Δ. The phase coefficient ϕ_2 has finite negative values for long pulses and tends to zero for short pulses (no phase modulation) in agreement with the McCall and Hahn's results. The product $\phi_2 \cdot C$ is proportional to Λ for long pulses and to $1/\Lambda$ for short pulses. In Figs. 5.3.3 and 5.3.4 (page 110), the coefficients w_2 and w_4 are plotted versus Δ and Λ when s=0. It is clear that the uniform expansion of the population inversion w converges very fast, since for both long and short pulses $|w_4| << |w_2|$. Especially for short pulses ($\Lambda \rightarrow \infty$), the coefficient w_4 goes to zero, and leads to complete population inversion. For long pulses inside and outside the polariton

gap ($\Lambda \rightarrow 0$), population inversion is not attainable. In Figs. 5.3.5 and 5.3.6 (page 111), we plotted the two lowest order coefficients u_1 and u_3 for the dispersive part of the macroscopic polarization, versus Δ and Λ when s=0. For long pulses both coefficients have finite values inside and outside the gap, while for short pulses, both tend to zero in accordance with SIT in SVEA since in this case the medium completely absorbs the pulse energy. This can be seen in the plot of the lowest correction for the absorptive part v_1 of the macroscopic polarization P in Fig. 5.3.7 (page 112). For long pulses ($\Lambda \rightarrow 0$), the absorption part tends to zero, while for short pulses v_1 tends to a finite value $-1/\Lambda$ which together with $C=2\Lambda$ leads to Eq. (5.3.20d).

5.4 BREAKDOWN OF PERTURBATION THEORY: NON-EXISTENCE OF SOLITARY WAVE SOLUTIONS

The previous expansion of the population inversion w in a power series of the amplitude E in Section 5.3 is locally valid, but it is not uniformly valid on the whole domain $(-\infty, +\infty)$. In order to clarify this statement, one can start with two simple examples from singular perturbation theory.

Consider the first order linear equation: $Ax+B=0$. The solution is $x=-B/A$. Now, introducing a small perturbation with $\varepsilon << 1$, consider the equation of second degree: $\varepsilon x^2+Ax+B=0$. The two solutions are:

$$x = \frac{-A \pm \sqrt{A^2 - 4B\varepsilon^2}}{2\varepsilon} \qquad = \begin{cases} -\dfrac{B}{A} + O(\varepsilon^2) \\ -\dfrac{2A}{\varepsilon} + O(\varepsilon) \end{cases} \tag{5.4.1}$$

The second solution is not analytic (i.e. singular) in ε at $\varepsilon=0$: $\varepsilon \cdot x^2$ is a singular perturbation.

As a second example, consider the case of a first order ODE:

$$\dot{y} + y = 0 \qquad \text{with solution} \quad y = C\exp[-x] \tag{5.4.2}$$

With the introduction of a small perturbation $\varepsilon << 1$, consider the new ODE:

$$\varepsilon\ddot{y} + \dot{y} + y = 0 \tag{5.4.3}$$

Its solutions are

$$y = A\exp[(-1 + O(\varepsilon^2))x] + B\exp[-(\varepsilon^{-1} + O(\varepsilon))x] \tag{5.4.4}$$

There are two families of solutions, but one of them is not analytic in ε at ε=0. Again, $\varepsilon\cdot\ddot{y}$ is a singular perturbation.

This singular perturbation argument can be applied to the case of the Maxwell-Bloch equations, in particular for the perturbation scheme used by Akimoto and Ikeda [74]. Let us take for example a long pulse case outside the gap; the expansion parameter is $\varepsilon=\Lambda/\Delta<<1$. The system of Maxwell-Bloch equations for steady-state solutions can be in principle transformed to a sixth-order ODE for the amplitude E. Schematically, this could give

$$\underbrace{\varepsilon^{(..)}\{E^{(6)}+.....\}}_{\substack{\text{singular}\\ \text{perturbation}}} + \ddot{E} - E + \frac{2}{C^2}E^3 = 0 \tag{5.4.5}$$

For ε=0, the zeroth order equation has a constant of motion and describes an integrable system. As soon as $\varepsilon\neq0$, the conservation law is broken and the equation is no longer

integrable. A pictorial analogy for this situation (see Fig. 5.4.1, page 113) is to analyze the case of a ball rolling down a potential V(E) for which the conserved quantity is:

$$E_{\mathrm{TOTAL}} = \frac{\dot{E}^2}{2} + V(E) \text{ where } V(E) = -\frac{E^2}{2} + \frac{E^4}{4} \tag{5.4.6}$$

A solitary pulse corresponds to a trajectory from $E(\xi=-\infty)=0$ to $E(\xi=+\infty)=0$ which has total energy $E_{\mathrm{TOTAL}}= 0$. For small amplitude E~0, the E^4 term can be dropped, so the potential can be written as $V(E) \sim - E^2/2$, and the ODE is approximated as follows:

$$\dot{E}^2 - E^2 = 0 \quad \text{with solutions } E \sim \exp[\pm\xi] \tag{5.4.7}$$

This form correspond to the tails of the solitary wave at $\xi=\pm\infty$. The peak of the solitary solution E_{max} corresponds to $\dot{E}=0$. Because of conservation of energy, the trajectory leaving $E=\dot{E}=0$ is guaranteed to return to this point. However, as soon as $\varepsilon\neq0$, this is not the case, and in general, the returning trajectory misses the $E=\dot{E}=0$ point.

Now, we return to our problem. We are looking for the validity of Akimoto and Ikeda's perturbation expansions in the whole domain $(-\infty, +\infty)$. In the general case $\varepsilon\neq0$, the boundary conditions are over-specified for the Eq. (5.4.5): there is a unique trajectory (up to translational symmetry $\xi \rightarrow \xi+c$) which comes out of $E=\dot{E}=0$ point at $\xi=-\infty$. In general, there is no reason to expect the continuation of this solution not to have any of the growing solutions as $\xi=+\infty$. Under these circumstances, one expects to have to tune the parameters Λ, Δ, and s to come back to the $E=\dot{E}=0$ point at $\xi=+\infty$. This is the condition for a solitary solution to exist. The competition between dispersion and nonlinearity has to be controlled simultaneously by the laser frequency ω and the width of the pulse τ.

In Akimoto and Ikeda's analysis [74], the non-existence of solitary wave solutions cannot be seen perturbatively in the small parameter ε expansion. In their perturbative

analysis, at each order of iteration ($E=\Sigma\varepsilon^n E_n$), for $n \geq 1$, the electric field amplitude E_n satisfies a linear second-order ODE. In this case, there is always at least one solution which satisfies the boundary conditions for $E_n \to 0$ at $\xi = \pm \infty$. The terms E_n can be calculated iteratively and never signal any problem. This explains why Akimoto and Ikeda never realized that the expansion was misleading and that solitary waves generally do not exist. They believed that their hyperbolic secant solutions were soliton solutions like in the case of McCall and Hahn. Similar remarks apply to our expansion of the population inversion w(E) in powers of E given in Section 5.3. All these expansions all locally valid, but they are not uniformly valid on the whole domain $(-\infty, +\infty)$.

5.5 NUMERICAL RESULTS: SELECTED SOLITARY PULSES

In the previous section, it was argued that the fine tuning of Λ, Δ, and s was required for the existence of solitary waves propagating inside the unbounded dielectric for pulse widths shorter than the relaxation times of the medium.

To find whether there are solitary waves, we first make the problem well-posed. The Maxwell-Bloch equations have translational symmetry in ξ and ϕ, and are invariant under $\xi \to -\xi$, $v \to -v$ (see Eqs. (5.2.20a) and (5.2.13-15)). Also, changing the sign of E, u, and v is a symmetry. Since the boundary conditions at $\xi = -\infty$ define the solution everywhere modulo the above translations and modulo the sign symmetry, it is not difficult to see that solitary wave solutions (after shifting ξ so that the pulse peak is at $\xi = 0$) have w and ϕ even in ξ, and E must be either even or odd. The standard hyperbolic secant 2π–pulses are even, so we will restrict ourselves to E even. Then u is even and v is odd. Let us thus consider the ODEs on the interval $(-\infty, 0]$ with the same boundary conditions at $\xi = -\infty$ and the condition $v=0$ at $\xi = 0$. This new boundary value problem is well posed, having in general a unique solution. If $\dot{E}=0$ at $\xi = 0$ also, it is easy to see that one can construct a

solitary wave solution on the whole ξ-axis by reflection of the solution on the half-line with a change of sign for v. Since we had to translate ξ to have v(0)=0, we see that the condition for existence of a solitary wave solution is that $\dot{E}=0$ at the ξ where v=0. This condition can be interpreted as forbidding any cusp in E. Let us define ξ_{tip} to be the value of ξ where v=0. In general $\dot{E}\neq 0$ at $\xi_{tip}= 0$, corresponding to a solution which has some amount of growing (bad) modes as $\xi \rightarrow +\infty$. The amount of these bad modes is zero to all orders in perturbation theory, but nonetheless can be non-zero.

We numerically integrated the system of Maxwell-Bloch equations (see Appendix E, Eqs. E1-7) from $\xi \rightarrow -\infty$. For ξ in the tail, the solution can be obtained from the perturbative expressions for E, $\dot{E}$, $\dot{\phi}$, u, v, and w; these are used as initial conditions on the fields. We evolve forward and find ξ_{tip}, and determine $\dot{E}$ there. Call this value $\dot{E}_{tip}(\Delta, \Lambda, s)$. As expected on the basis of the arguments in the previous section, in general $\dot{E}_{tip}\neq 0$, and solitary waves do not exist for those values of Δ, Λ, s. However, we found that $\dot{E}_{tip}$ changes sign when the parameters are varied, and that there are surfaces in the Δ, Λ, s space on which $\dot{E}_{tip}=0$. These are the surfaces for which solitary wave solutions exist; they determine the selected velocities for steady-state pulse propagation.

The numerical analysis shows that one can tune the parameters Λ, Δ, and s so as to obtain $\dot{E}_{tip} = 0$ at least in the gap $0 \leq \Delta \leq 1$. Using a root solver, we determined the locus of the curves (Λ, Δ) for which there are solitary solutions at fixed $\omega_{LT}/\omega_t=10^{-3}$. As can be seen in Fig. 5.5.1 (page 114), various branches of solutions rise from $\Delta=0$, and set at $\Delta=1$; these are special points just as in the linear theory. Other branches actually stop inside the gap due to the appearance and disappearance of multiple solutions to v=0. We have followed some of these branches after the appearance of multiple solutions to v=0. Usually, the pulse shapes continue to develop more and more oscillations, eventually looking nothing like the original hyperbolic secant shapes. In Fig. 5.5.2 (page 115), we plot the mismatch function for the value of the cusp of the solution $\dot{E}_{tip}$ at the tip for the parameters given by the dashed line of Fig. 5.5.1 (page 114). The oscillations are difficult

to resolve all the way down to small Λ, but it is likely that there are an infinite number of branches (but not dense set of solutions) coming out of the point $(\Delta, \Lambda)=(1, 0)$. The point $(\Delta, \Lambda)=(1, 0)$ is an accumulation point, as probably is the whole line: $\Lambda=0, 0\leq \Delta \leq 1$.

The numerical analysis indicates that for $\varepsilon=\Lambda/\Delta \rightarrow 0$, outside the polariton gap, the functional behavior of $\dot{E}_{tip}$ is $\dot{E}_{tip} \sim \exp[-\lambda(\Delta)/\varepsilon]$ (λ is function of Δ which was calculated numerically), which is non-analytic as expected. This implies that there are no solitary pulse solutions far from the gap. In Fig. 5.5.3 (page 116), the formal behavior of $\dot{E}_{tip}$ is shown versus Δ/Λ for two different values of Δ.

Because of this fine tuning, solitary pulses do not exist for arbitrary pulse width τ, but only for selected values. This selection appears to be dominant inside the polariton gap, where the dispersion and non-linearity strongly compete against each other.

5.6 CONCLUSIONS

In this Chapter, a uniform perturbation expansion for the population inversion w in a power series of the small electric field amplitude E was used to solve the coupled Maxwell-Bloch equations in the lowest orders of approximation. General expressions for the solitary waves and their phase modulations were derived for an arbitrary incident carrier frequency ω and an arbitrary pulse width τ. The expressions derived confirmed Akimoto and Ikeda's results for short and long pulses, inside and outside the polariton gap. However such perturbation expansions are in general only asymptotic. In particular, our uniform expansion and Akimoto and Ikeda's perturbation expansions for short and long pulses are only locally valid: they are not uniformly valid on the whole domain $(-\infty, +\infty)$, and thus cannot be used to determine whether there exist solitary wave solutions. Note that even when there are solutions for the electric field amplitude E which satisfy the boundary conditions, they are not soliton solutions as for SIT in the SVEA. Rather they are solitary waves since the system of Maxwell-Bloch equations beyond the SVEA is not integrable.

The existence of solitary waves requires the fine tuning of the pulse width τ for a given frequency detuning ω-ω_t. Numerical results from the integration of Maxwell-Bloch equations showed that selected solitary branch solutions especially inside the polariton gap are generated. This indicates that the competition between non-linearity and dispersion leads to a pulse width selection mechanism for the pulse propagation inside the dielectric.

Even going beyond the SVEA and including phase modulation (chirping) for the envelope of the electric field amplitude does not affect the probability conservation for two-level atoms in the Bloch space, (Maxwell-Bloch equations acquire new non-linearities). The derived solutions in various pulse widths for frequencies inside and outside the polariton gap, indicated that only in the case of very short pulses ($\Lambda \rightarrow \infty$) is the phase modulation zero, and this corresponds to complete inversion ("2π pulse"). In the other cases, the inversion of the atoms is not realized and they remain in the ground state.

The explanation is fairly simple. In the presence of frequency modulation the identity between the pulse area and the dipole turning angle in Bloch space is no longer true. The most dramatic consequence, is the failure of the area theorem. As soon as frequency modulation of the driving field is permitted, the usual area theorem cannot be derived, and there is no replacement for it. This can been seen more clearly, by writing down the Maxwell-Bloch equations in SVEA where the system is integrable

$$\begin{aligned} &\alpha E = u && \beta \dot{E} = -v \\ &\Lambda \dot{u} = \Delta v && \Lambda \dot{v} = -\Delta u + E w && \Lambda \dot{w} = -E v \end{aligned} \tag{5.6.1}$$

and compare it with the complete set in Eqs. (5.2.11)-(5.2.15). From Eqs. (5.6.1), an energy relation between the inversion population w and the electric field amplitude E can be derived

$$w = -1 + \frac{\beta}{2\Lambda} E^2 \tag{5.6.2}$$

that leads to an ODE for the electric field amplitude E of the form:

$$\ddot{E} = \left(\frac{1}{\Lambda\beta} - \frac{\alpha^2}{\beta^2} \right) E - \frac{1}{2\Lambda^2} E^3 \tag{5.6.3}$$

In the short pulse limit ($\alpha \rightarrow 0, \beta \rightarrow 1/\Lambda$, $s << 1$), one obtains McCall and Hahn's solutions and the area theorem (see Eq. 4.2.10). Therefore, in the short pulse limit, McCall and Hahn's assumption of no phase modulation is justified, allowing area theorem to hold. Our results differ qualitatively from the results in SVEA, since our system of ODEs contains all the higher derivatives for the envelope of the electric field and its phase modulation (see Eqs. (5.2.20a, b) and (5.2.13-15)). By including the higher order terms, the solution of the system of complete Maxwell-Bloch ODEs becomes complicated and has been outlined in Section 5.3. The solutions beyond SVEA differ qualitatively from the solutions in SVEA. In SVEA approximation, the steady-state solutions are in fact solitons, while without making the SVEA, the solutions are solitary waves and they are not realized for arbitrary pulse width. The area theorem is not valid anymore for arbitrary pulse widths, but only in the short pulse limit. The possibility of solitary pulse solutions requires a special selection mechanism between detuning and non-linearity (pulse width), which becomes very important inside the polariton gap.

Comparison of the above results with experiments will be of major interest. By tuning the laser frequency ω inside the polariton gap for a specific pulse width τ, it should be possible to observe which kind of pulses propagate with low loss in the medium and to measure their velocities. It will of great interest to investigate whether solitary wave pulse propagation is feasible in principle in the resonant excitation of excitons in semiconductors

inside the polariton gap for discrete pulse widths. The physical picture is mathematically similar to the description of transitions in two-level atoms with a sharp absorption line. Our most important prediction, that of pulse shape and velocity selection, requires that one should be able to resolve the gap. Thus line broadening must be kept at a minimum. In addition, one must have a system of width equal to several Beer absorption lengths before one can expect the propagation to become steady-state. There have been to date no experimental verification of steady-state shapes, nor careful determinations of velocities. Similarly the perturbative corrections to the SVEA have not been investigated experimentally. The corrections to the leading order should be measurable if selection is. Note that the lowest order does not correspond to linear theory. Linear theory corresponds to $E<<1$, which is not true for the whole domain $(-\infty, +\infty)$ for ξ. The first step is thus to do velocity measurements to see if the velocity reaches an asymptotic value as the sample thickness increases. Steady state velocities can drop to 10^3 to 10^4 times less than the velocity of the light in the medium away from resonance, so this may be a feasible measurement. If one can show that there is steady-state propagation, the velocity should correspond to the selected one as determined by our theory, given ω and the material parameters. In addition, if the pulse shape is measurable, it can be compared with the theoretical prediction, providing a further check on the steady-state nature of the propagation. Since steady-state pulses exist only inside the gap, one will need to be able to experimentally resolve the gap rather well; in particular any line broadening must be small compare to ω_{LT}. This pretty much rules out doing experiments with gases (e.g. Rb, [61, 62]).

However the gap is large enough in many semiconductors to permit an experiment to test our theory. Consider for instance a local optics ($m^* = \infty$) semiconductor with parameters like CdS. Take $\hbar\omega_t$=2.55 eV and $\hbar\omega_{LT}$=2.0 meV, and assume (as in the case of CdS) that the line broadenings due to the finite relaxation times T_1 and T_2 are small enough so that the structure inside the gap is not washed out. Then we find that the top

branch at Δ=0.3 corresponds to a pulse of width τ=0.95 psec, leading to a pulse velocity $V/c=3.4\times10^{-4}$. On the same branch at Δ=0.9, we find τ=2.5 psec, and $V/c=3.65\times10^{-4}$. These velocities should be measurable. Spatial dispersion effects ($m^* < \infty$) will be important, but should not change the results much as long as the selected velocities are not too small.

A first experiment has to do with the measurement of the delay of a intense optical pulse passing through the crystal relative to the time of a reference pulse in the vacuum. The velocity V of the propagation of the light in the sample can be estimated from the formula $c/V=1+c(\delta t / \ell)$, where ℓ is the thickness of the sample, and δt is the delay time between the two pulses. Velocities are expected to drop 10^3-10^4 times less than the velocity of the light in the medium away from resonance.

Another experiment should measure the transmitted power versus incident one, and reveal a sharp increase of the transparency of the crystal by more than two to three orders of magnitude relative to the linear case. The duration of exciton relaxation times T_1 (longitudinal), T_2 (transverse) must be longer than the pulse width τ, and this has to be checked experimentally by a weak pulse being applied to the semiconductor with continuously variable time delay Δt relative to the main intense pulse, at a small angle (~1°). The intensity of the weak pulse is insufficient to induce transparency in the crystal. For small delays $\Delta t \leq T_2$ the transmission varies in a wide range since the medium can be in practically in any state (we have two pulses of different intensities). For $\Delta t \geq T_2$ the interaction is not longer coherent and the absorption of the weak pulse is determined by the process of T_1 relaxation. The number of excitons decreases with the relaxation time T_1 and at the same time the absorption of the weak pulse increases. By this we try to disconnect the solitary wave propagation for exciton-polaritons from saturation phenomena, collision processes, exciton-phonon interactions etc.

For observation of solitary wave pulses various factors have to taken into account: the crystals have to be pure, otherwise impurities would introduce dephasing collisions which

might destroy the coherence of the pulse and the pulse duration τ has to be less than any of the relaxation times, which include the spontaneous recombination time T_1, polarization decay time T_2, electron-electron collision time T_{ee}, and electron-phonon collision time T_{ep}; (this is equivalent to $\tau \leq T_2$ for two-level transitions). The experiment has to be done in low temperatures below liquid-nitrogen temperature (77°K) to increase the transverse relaxation time T_2. The crystal can a thick slab (~mm), while he pulses are ultrashort of duration from fsec to few psecs, while the pulse power can range around 10-100 MW/cm^2.

A possible extension of this work will be to investigate intense pulse propagation in local media with finite relaxation times (damping $\Gamma \neq 0$) The Bloch equations are modified to include the relaxation times T_1 and T_2:

$$\Lambda \dot{u} = (\Delta + \Lambda \dot{\phi}) v - \Gamma_2 u \tag{5.6.4}$$

$$\Lambda \dot{v} = -(\Delta + \Lambda \dot{\phi}) u - \Gamma_2 v + E w \tag{5.6.5}$$

$$\Lambda \dot{w} = -E v - \Gamma_1 (w + 1) \tag{5.6.6}$$

where $\Gamma_2 = 1/(\omega_{LT} T_2)$ is the dimensionless transverse relaxation time, and $\Gamma_1 = 1/(\omega_{LT} T_1)$ the dimensionless longitudinal relaxation time. Dissipation, as an additional factor enters the competition between dispersion and non-linearity, and expected to influence the locus of the solitary solutions inside the polariton gap.

By taking into account the finiteness of the exciton mass, it is possible then to extend our analysis to spatially dispersive media. Until now, the analysis has been done in local dielectric medium (without damping) where the dipoles are assumed not to interact with each other. Spatial dispersion arises from the dipole-dipole interaction in the dielectrics. A generalization of Ikeda and Akimoto's work [83] for spatially dispersive media along the lines of this work will unify their perturbation expansion for various pulse limits and lead

to numerical search of existence of either E-M or spatial dispersive solitary waves for selected laser frequencies and pulse widths.

Finally, in practice, one has to deal with the fact that there has to be an incident pulse from vacuum into the medium. This requires solving for the boundary effects due to the vacuum-dielectric interface (for discussion of the space-time Maxwell boundary conditions, see Appendix F). It would be worthwhile to investigate the shape of the incident pulses which efficiently generate solitary waves inside the medium after a few absorption lengths. As the incident pulse shape changes, one should see a discontinuous jump in the velocity of the steady-state pulse transmitted into the medium as one switches from one branch of solitary waves to another (c.f. Fig. 5.5.1, page 114).

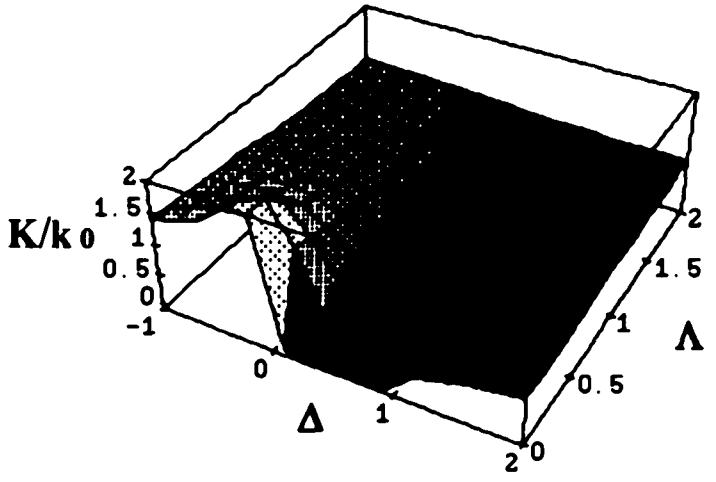

Figure 5.2.1 Dispersion relation for the carrier wave $K/k_0 = cK/\omega$ at the pulse tail versus frequency detuning $\Delta = (\omega-\omega_0)/\omega_{LT}$ and inverse pulse width $\Lambda = 1/\omega_{LT}\tau$ scaled by the polariton gap frequency $\omega_{LT} = 2\pi N\hbar\kappa^2$ for $\omega_{LT}/\omega_t = 10^{-3}$.

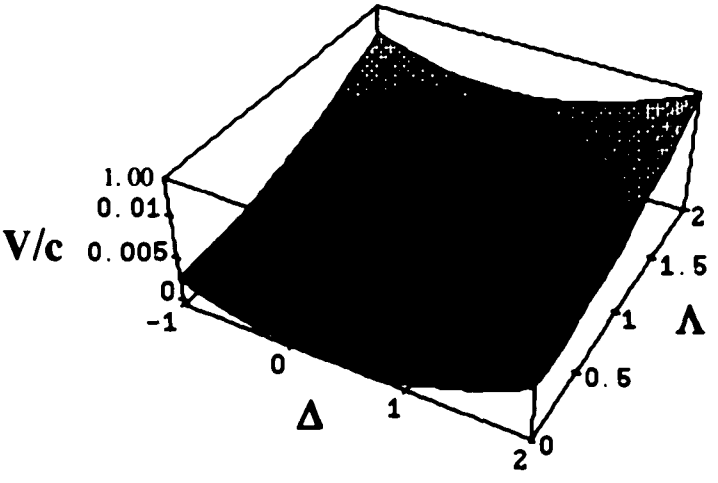

Figure 5.2.2 Propagation velocity of the pulse envelope as a function of Δ and Λ for $\omega_{LT}/\omega_t = 10^{-3}$.

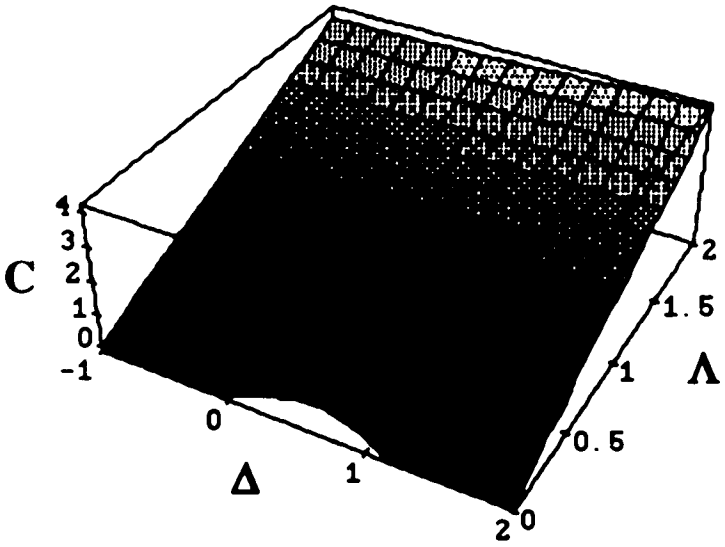

Figure 5.3.1 Coefficient C for the hyperbolic secant pulse solution as a function of Δ and Λ for s=0.

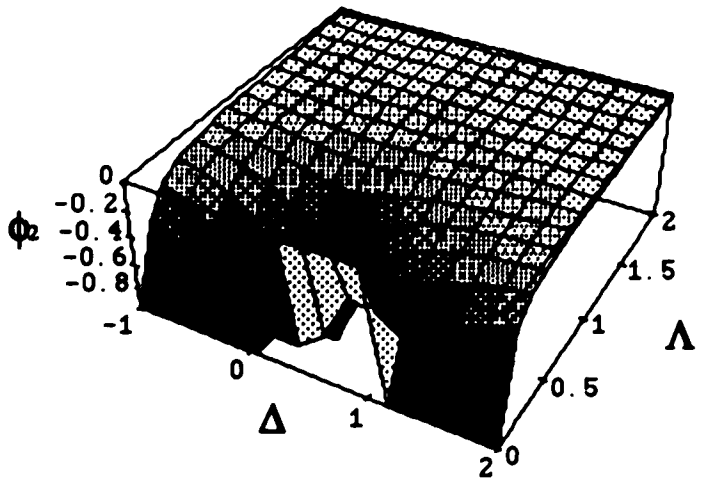

Figure 5.3.2 Coefficient ϕ_2 for the phase modulation of the hyperbolic secant pulse solution as a function of Δ and Λ for s=0.

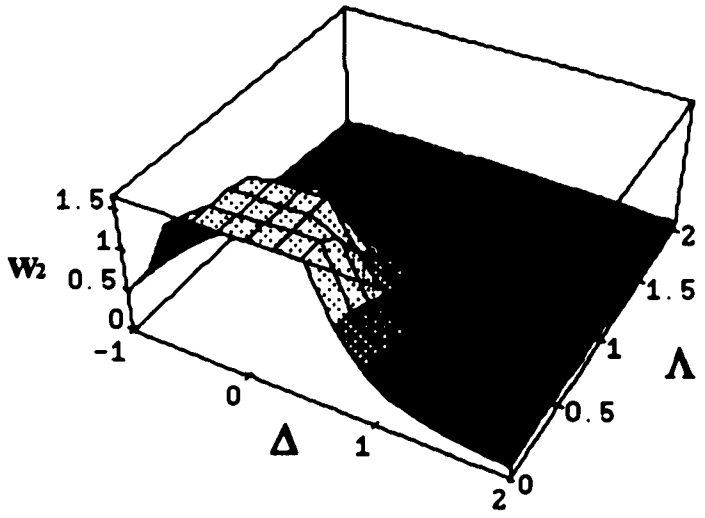

Figure 5.3.3 Coefficient w_2 for the population inversion w of the dielectric medium as a function of Δ and Λ for s=0.

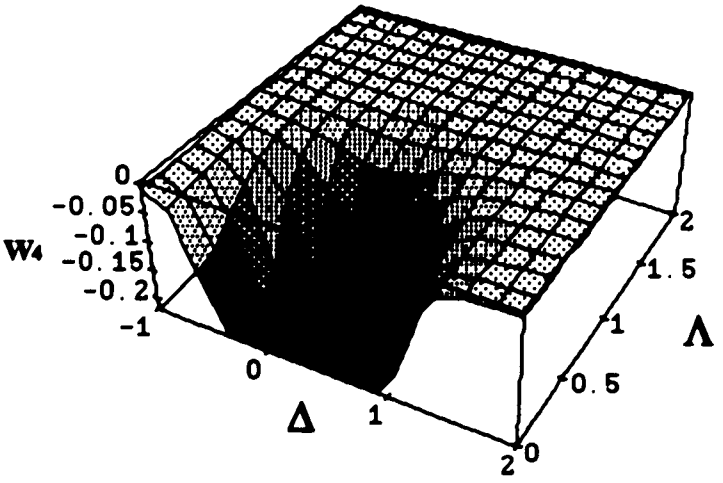

Figure 5.3.4 Coefficient w_4 for the population inversion w of the dielectric medium as a function of Δ and Λ for s=0.

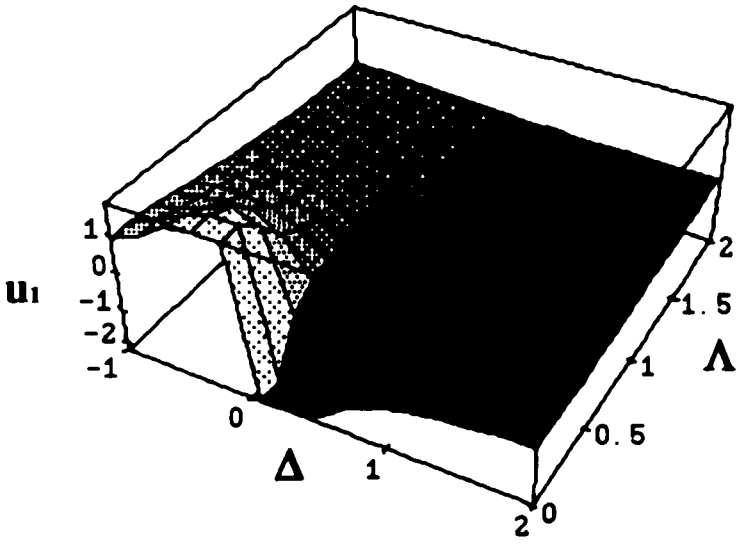

Figure 5.3.5 Coefficient u_1 for the dispersive part of the macroscopic polarization **P** as a function of Δ and Λ for s=0.

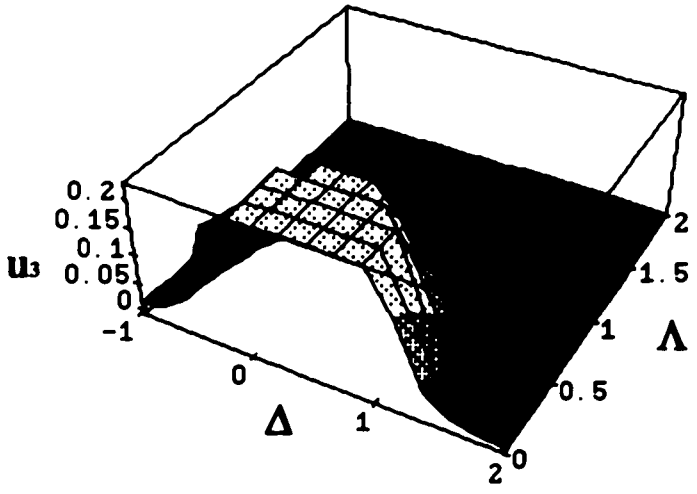

Figure 5.3.6 Coefficient u_3 for the dispersive part of the macroscopic polarization **P** as a function of Δ and Λ for s=0.

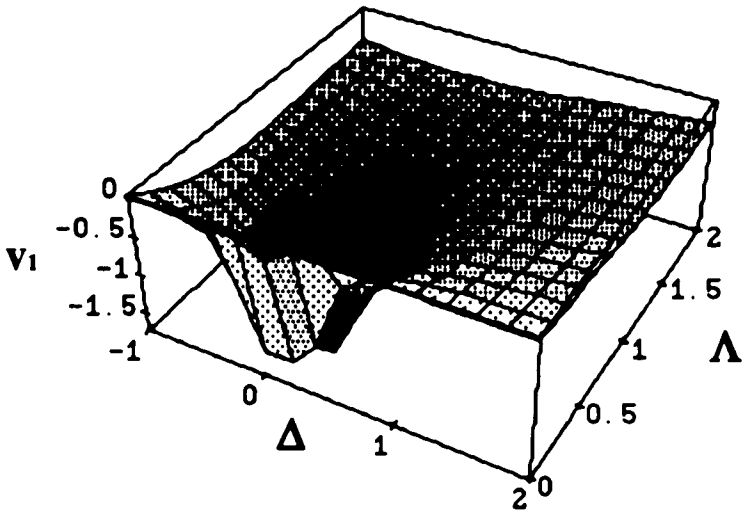

Figure 5.3.7 Coefficient v_1 for the absorptive part of the macroscopic polarization **P** as a function of Δ and Λ for s=0.

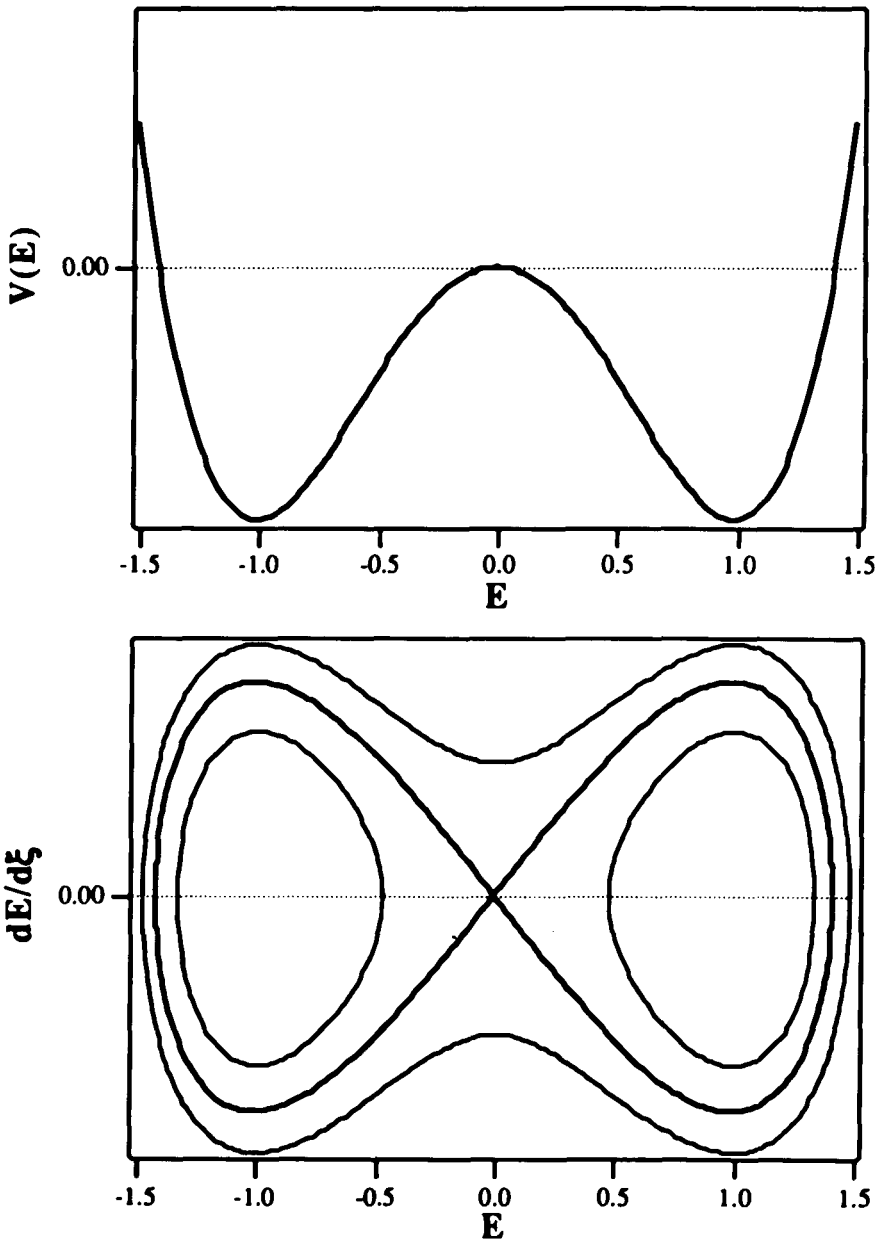

Figure 5.4.1 A ball rolling down a potential $V(E)=-E^2/2+E^4/4$.

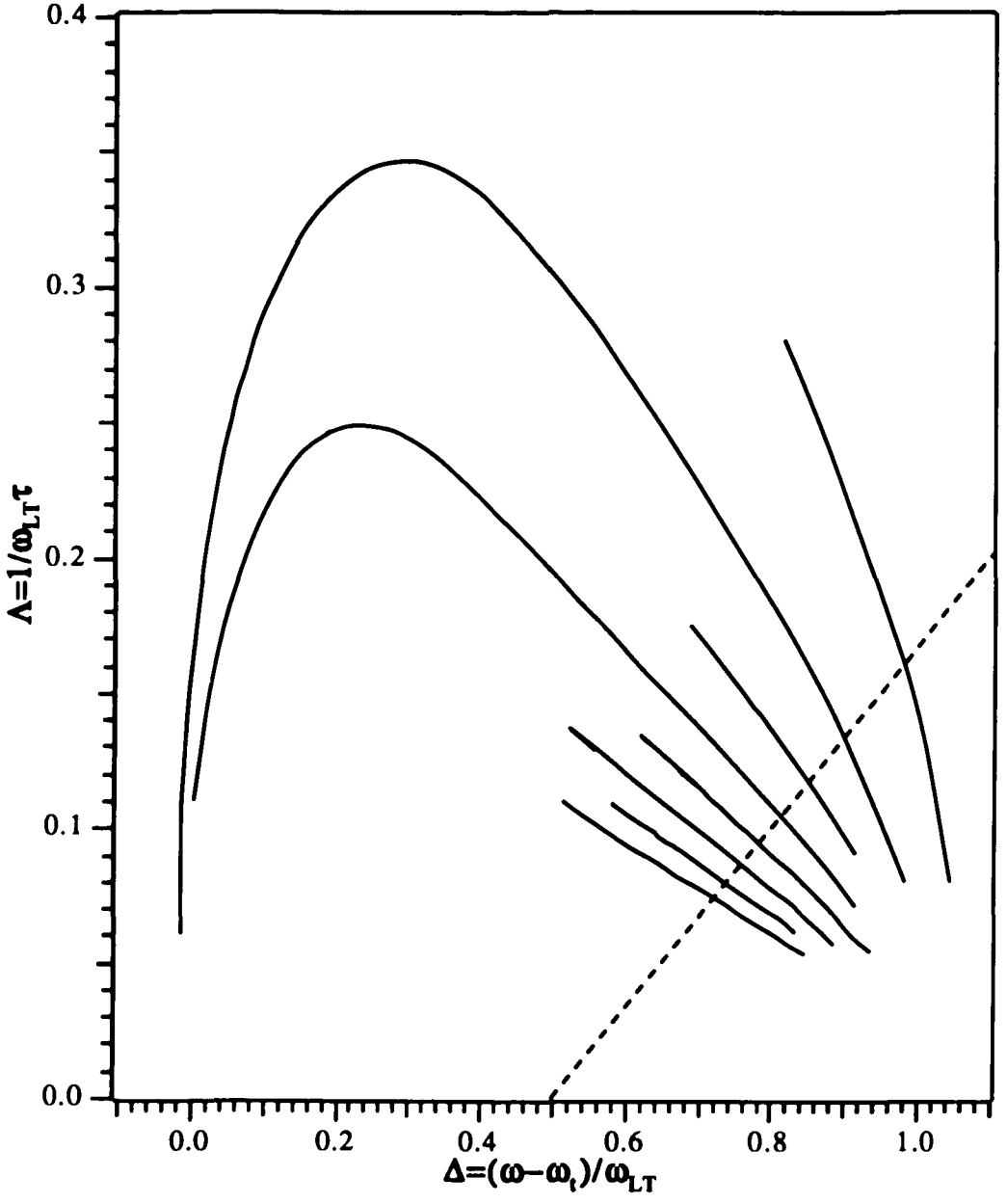

Figure 5.5.1 Numerical results for the locus of the solitary solutions in the (Λ, Δ) domain for $\omega_{LT}/\omega_t = 10^{-3}$.

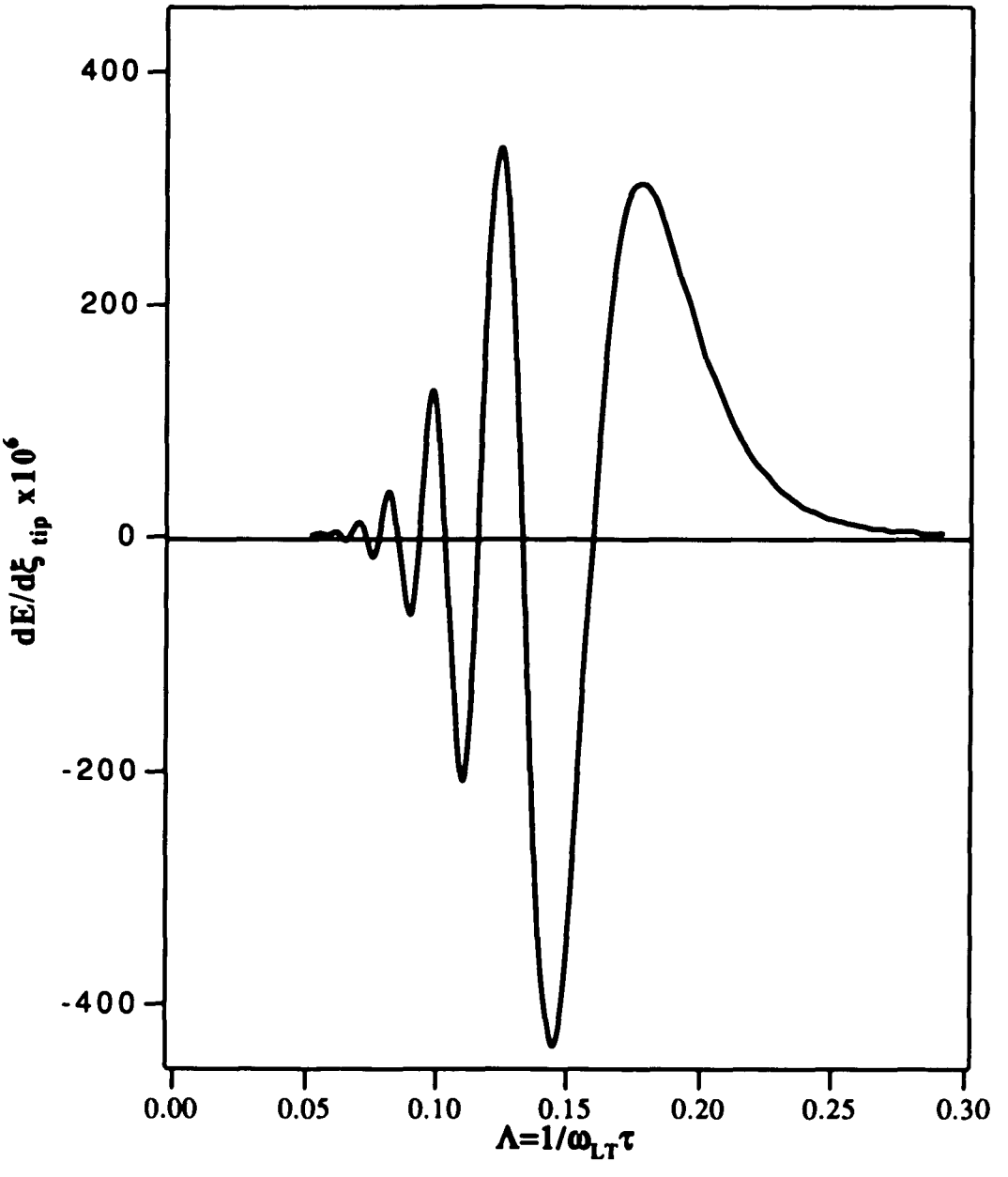

Figure 5.5.2 Mismatch function for Δ, Λ given by the dashed line of Fig. 5.5.1.

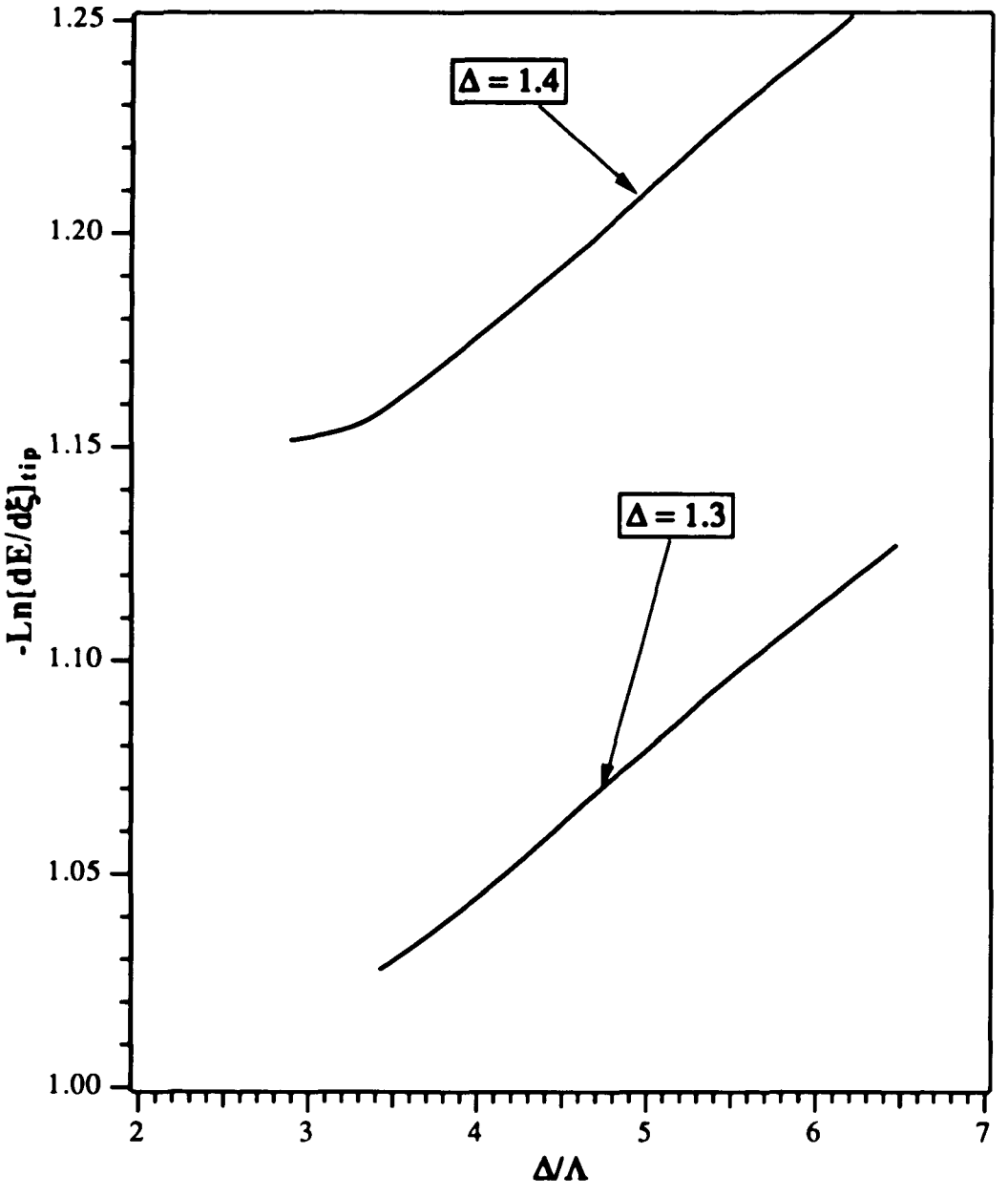

Figure 5.5.3 Exponential dependence of the mismatch function on Λ as $\Lambda \rightarrow 0$ outside the gap.

APPENDICES

Hunc igitur terrorem animi tenebrasque necessest non radii solis neque lucida tela diei discutiant, sed naturae species ratioque.
This terror, therefore, and darkness of the mind must be dispersed, not by the rays of the sun nor the bright shafts of daylight, but by the aspect and law of nature.

Lucretius, **De Rerum Natura**, 3, 91-93.

APPENDIX A

CONTOUR-INTEGRATION METHOD TO EVALUATE THE REFLECTED FIELD

In this appendix we outline the algebraic details to evaluate the integral in Eq. (3.2.6) in the complex ω-plane for t ≥ 2L/c. It is helpful to break the integral in two parts arising from each term in the curly brackets: {1-exp[i(ω-ω$_0$)T]}. The first part contributes for t > 2L/c while the second part contributes only for t > 2L/c+T. Eq. (3.2.6) can therefore be written in the form:

$$E_R(t) = \mathrm{Re}\Big[E(t-\frac{2L}{c})\,\Theta(t-\frac{2L}{c}) - \\ - \exp(-i\omega_0 T)\,E\,(t-\frac{2L}{c}-T)\,\Theta(t-\frac{2L}{c}-T)\Big] \qquad \text{(A1)}$$

where

$$E(\tau) = \lim_{\eta \to 0} \int_{-\infty}^{+\infty} f(n_1, n_2)\, d\omega \qquad \text{(A2a)}$$

for Pekar, Ting and Kiselev's ABC; and

$$E(\tau) = \lim_{\eta \to 0} \int_{-\infty}^{+\infty} f(n_1, n_2, n_+)\, d\omega \qquad \text{(A2b)}$$

for Birman's ABC; while

$$\left.\begin{matrix} f(n_1, n_2) \\ f(n_1, n_2, n_+) \end{matrix}\right\} = \frac{1}{2\pi}\,\frac{\rho(\omega)}{\omega_0 - \omega - i\eta}\exp[-i\omega\tau]\,,\ \tau > 0 \qquad \text{(A3)}$$

For notational convenient, we have explicitly shown the dependence of the integrands $f(n_1, n_2)$ and $f(n_1, n_2, n_+)$ on the refractive indices n_1, n_2 and n_+ (see Eq. (3.2.3)) and the ω-dependence is implicitly understood.

The choice of the appropriate contour depends on the singularities of $f(n_1, n_2)$ and $f(n_1, n_2, n_+)$. For this purpose we require an explicit form of n_1, n_2 and n_+. Using Eq. (3.2.2) in (3.2.5), we obtain:

$$n_{2,1} = +[a \pm (a^2 - \varepsilon_0 b)^{\frac{1}{2}}]^{\frac{1}{2}} \tag{A4}$$

$$n_+ = [2a - \varepsilon_0]^{\frac{1}{2}} \tag{A5}$$

$$a = (2\omega^2\delta^2)^{-1}[\varepsilon_0\omega^2\delta^2 + (\omega^2 - \omega_t^2 + i\omega\Gamma)] \tag{A6a}$$

$$b = (\omega^2\delta^2)^{-1}[(\omega^2 - \omega_t^2 + i\omega\Gamma) - \frac{\beta^2\omega_t^2}{\varepsilon_0}] \tag{A6b}$$

where $\beta^2 = (4\pi\alpha_0)$, $\delta^2 = (\frac{\hbar\omega_t}{m^* c^2})$

An examination of Eq. (A4) shows that the conditions $b=0$ and $a^2=\varepsilon_0 b$ correspond to the branch point singularities in $f(n_1, n_2)$. A further examination in Eq. (A5), reveals an additional condition $2a=\varepsilon_0$, which corresponds to the branch point singularities in $f(n_1, n_2, n_+)$, in addition to the two previous ones.

Using Eq. (A6) the first two complex conditions yield 6 branch points (in the complex ω plane) ω_j, j=1-6 whose location is given by Eqs. (3.3.1)-(3.3.3), while all three conditions

yield 8 branch points ω_j, j=1-6 whose location is given by Eqs. (3.3.1)-(3.3.4). So, the main difference between $f(n_1, n_2)$ and $f(n_1, n_2, n_+)$ is the number of branch points for each one. The expressions in Eqs. (3.3.1)-(3.3.4) have been obtained in the lower order in δ, $p=\beta^2/2\varepsilon_0$, and Γ/ω_t.In most cases of practical interest the three parameters δ, p, Γ/ω_t are much smaller than unity ($\leq 10^{-3}$). We are therefore justified in neglecting their products and higher powers. As a reminder, we have defined $p=\beta^2/2\varepsilon_0=(2\pi\alpha_0)/\varepsilon_0$ and physically $p=(\omega_\ell-\omega_t)/\omega_t$, where $\omega_\ell-\omega_t$ is the so-called LT splitting.

The branch points ω_1 and ω_2 arise from the condition b=0. Around these points the integrands $f(n_1, n_2)$ and $f(n_1, n_2, n_+)$ are made single-valued by going to the Riemann sheet on which $n_1 \rightarrow - n_1$ and n_2, n_+ remain unchanged.

The branch points ω_3, ω_4, ω_5, and ω_6 arise from the condition: $a^2=\varepsilon_0 b$; on the corresponding Riemann sheet n_1 and n_2 are interchanged ($n_1 \rightarrow n_2$) and n_+ remains unchanged.

The branch points ω_7, ω_8 arise from the condition $2a=\varepsilon_0$; in this case $f(n_1, n_2, n_+)$ is made single-valued by going to the Riemann sheet on which $n_+ \rightarrow - n_+$ and n_1, n_2 remain unchanged.

The appropriate contours to evaluate Eqs. (A2) and (A3) are shown in Figs. 3.3.1(a), and 3.3.1(b) (pages 48 and 49) and contain only a single pole at $\omega=\omega_0-i\eta$ for both cases.

A straightforward application of Cauchy's theorem shows that

$$\oint f(n_1,n_2)\,d\omega = \int_{-\infty}^{+\infty} f(n_1,n_2)\,d\omega + \int_{\omega_3}^{\omega_1} [f(n_1,n_2)-f(-n_1,n_2)]\,d\omega +$$

$$+ \int_{\omega_3}^{\mathrm{Re}\,\omega_3 - i\infty} [f(-n_2,n_1)-f(n_1,n_2)]\,d\omega + \int_{\omega_4}^{\omega_2} [f(-n_1,n_2)-f(n_1,n_2)]\,d\omega +$$

$$+\int_{\omega_4}^{\mathrm{Re}\,\omega_4 - i\infty}[f(n_1,n_2)-f(-n_2,n_1)]\,d\omega = 2\pi i\,\mathrm{Res}_1 \qquad \text{(A7)}$$

for Pekar, Ting and Kiselev's ABC; and

$$\oint f(n_1,n_2,n_+)\,d\omega = \int_{-\infty}^{+\infty} f(n_1,n_2,n_+)\,d\omega +$$

$$+\int_{\omega_3}^{\omega_1}[f(n_1,n_2,n_+)-f(-n_1,n_2,n_+)]\,d\omega +$$

$$+\int_{\omega_3}^{\mathrm{Re}\,\omega_3 - i\infty}[f(-n_2,n_1,-n_+)-f(n_1,n_2,n_+)]\,d\omega +$$

$$+\int_{\omega_7}^{\omega_1}[f(n_1,n_2,n_+)-f(-n_1,n_2,n_+)]\,d\omega +$$

$$+\int_{\omega_4}^{\omega_8}[f(-n_1,n_2,-n_+)-f(n_1,n_2,n_+)]\,d\omega +$$

$$+\int_{\omega_4}^{\mathrm{Re}\,\omega_4 - i\infty}[f(n_1,n_2,n_+)-f(-n_2,n_1,-n_+)]\,d\omega +$$

$$+\int_{\omega_8}^{\omega_2}[f(-n_1,n_2,n_+)-f(n_1,n_2,n_+)]\,d\omega = 2\pi i\,\mathrm{Res}_2 \qquad \text{(A8)}$$

for Birman's ABC; Res_1, Res_2 represent the residues of $f(n_1, n_2)$ and $f(n_1, n_2, n_+)$ at the pole: $\omega=\omega_0-i\eta$, respectively. Using Eqs. (A2) and (A7) or (A8), we formally decompose

E(τ) into a steady-state (pole contribution) and the transient (branch-point contribution) parts,

$$E(\tau)=E_S(\tau)+E_T(\tau) \tag{A9}$$

where

$$E_S(\tau)=-i\rho(\omega_0)\exp[-i\omega_0\tau] \tag{A10}$$

for all ABC's; and

$$E_T(\tau)=\int_{\omega_3}^{\omega_1} g(\omega)\,d\omega-\int_{\omega_4}^{\omega_2} g(\omega)\,d\omega-\int_{\omega_3}^{\mathrm{Re}\,\omega_3-i\infty} g'(\omega)\,d\omega+\int_{\omega_4}^{\mathrm{Re}\,\omega_4-i\infty} g'(\omega)\,d\omega \tag{A11}$$

for Pekar, Ting, Kiselev's ABC;

$$E_T(\tau)=\int_{\omega_3}^{\omega_7} g_1(\omega)\,d\omega-\int_{\omega_4}^{\omega_8} g_1(\omega)\,d\omega-\int_{\omega_3}^{\mathrm{Re}\,\omega_3-i\infty} g''(\omega)\,d\omega+\int_{\omega_4}^{\mathrm{Re}\,\omega_4-i\infty} g''(\omega)\,d\omega$$

$$+\int_{\omega_7}^{\omega_1} g_2(\omega)\,d\omega-\int_{\omega_8}^{\omega_2} g_2(\omega)\,d\omega \tag{A12}$$

for Birman's ABC; while

$$g(\omega)=[f(-n_1,n_2)-f(n_1,n_2)] \tag{A13a}$$

$$g'(\omega)=[f(-n_2,n_1)-f(n_1,n_2)] \tag{A13b}$$

$$g_1(\omega)=[f(-n_1,n_2,-n_+)-f(n_1,n_2,n_+)] \tag{A14a}$$

$$g_2(\omega)=[f(-n_1,n_2,n_+)-f(n_1,n_2,n_+)] \tag{A14b}$$

$$g''(\omega)=[f(-n_2,n_1,-n_+)-f(n_1,n_2,n_+)] \tag{A14c}$$

We have found useful to further decompose the transient part $E_T(\tau)$ into a "local" part and a "nonlocal" part. This facilitates comparison with a local medium for which the nonlocal part, by definition, vanishes identically. Such a decomposition can be carried out by noting for $f(n_1, n_2)$ that for a local medium the branch-cut line (joining ω_1 and ω_3) in Fig. 3.3.1(a) (page 48) is horizontal. For the case of $f(n_1, n_2, n_+)$ the branch-cut line (joining ω_1 and ω_7) in Fig. 3.3.1(b) (page 49) shrinks into the point ω_7. This can be easily verified using Eqs. (3.3.1), (3.3.2) and (3.3.4) with $\delta=0$. We then formally obtain:

$$E_T(\tau)=E_L(\tau)+E_{NL}(\tau) \tag{A15}$$

for all ABCs; while

$$E_L(\tau)=\int_{\mathrm{Re}\,\omega_3+i\,\mathrm{Im}\,\omega_1}^{\omega_1} g(\omega)\,d\omega - \int_{\mathrm{Re}\,\omega_4+i\,\mathrm{Im}\,\omega_1}^{\omega_2} g(\omega)\,d\omega \tag{A16}$$

$$E_{NL}(\tau)=\int_{\omega_3}^{\mathrm{Re}\,\omega_3+i\,\mathrm{Im}\,\omega_1} g(\omega)\,d\omega - \int_{\omega_4}^{\mathrm{Re}\,\omega_4+i\,\mathrm{Im}\,\omega_2} g(\omega)\,d\omega - \int_{\omega_3}^{\mathrm{Re}\,\omega_3-i\infty} g'(\omega)\,d\omega$$

$$+\int_{\omega_4}^{\mathrm{Re}\,\omega_4-i\infty} g'(\omega)\,d\omega \tag{A17}$$

for Pekar, Ting, Kiselev's ABC; and

$$E_L(\tau)=\int_{\omega_7}^{\omega_1} g_2(\omega)\,d\omega \;-\int_{\omega_8}^{\omega_2} g_2(\omega)\,d\omega \tag{A18}$$

$$E_{NL}(\tau)=\int_{\omega_3}^{\omega_7} g_1(\omega)\,d\omega-\int_{\omega_4}^{\omega_8} g_1(\omega)\,d\omega \;-\int_{\omega_3}^{\mathrm{Re}\,\omega_3-i\infty} g''(\omega)\,d\omega$$

$$+\int_{\omega_4}^{\mathrm{Re}\,\omega_4-i\infty} g''(\omega)\,d\omega \tag{A19}$$

for Birman's ABC.

We now, substitute $E=E_S+E_L+E_{NL}$ in Eq. (A1) and obtain:

$$E_R(0,t,\omega_0)=\mathrm{Re}[\tilde{E}_S(t)+\tilde{E}_L(t)+\tilde{E}_{NL}(t)] \tag{A20}$$

where

$$\tilde{E}_S(t)=i\rho(\omega_0)\,[\Theta(t-\frac{2L}{c})-\Theta(t-\frac{2L}{c}-T)]\exp[-i\omega_0(t-\frac{2L}{c})] \tag{A21}$$

$$\tilde{E}_T(t)=[E_j(t-\frac{2L}{c})\,\Theta(t-\frac{2L}{c})-$$

$$-\exp(-i\omega_0 T)E_j(t-\frac{2L}{c}-T)\Theta(t-\frac{2L}{c}-T)] \tag{A22}$$

with j=NL or L.

An appropriate change of variables permits us to rewrite the expressions in Eqs. (A16) through (A19) in the following simplified form:

$$E_L(\tau)=p\omega_t[\int_0^1 g(\omega_t+p\omega_t u-i\frac{\Gamma}{2})\,du+\int_0^1 g(-\omega_t+p\omega_t u-i\frac{\Gamma}{2})\,du] \tag{A23}$$

$$E_{NL}(\tau)=i\beta\delta\omega_t[\int_0^1 g(\omega_t-i\beta\delta\omega_t u-i\frac{\Gamma}{2})\,du$$
$$-\int_0^1 g(-\omega_t-i\beta\delta\omega_t u-i\frac{\Gamma}{2})\,du+\int_1^{\infty} g'(\omega_t-i\beta\delta\omega_t u-i\frac{\Gamma}{2})\,du$$
$$-\int_1^{\infty} g'(-\omega_t-i\beta\delta\omega_t u-i\frac{\Gamma}{2})\,du] \qquad \text{(A24)}$$

for Pekar, Ting, Kiselev's ABC; and

$$E_L(\tau)=p\omega_t[\int_0^1 g_2(\omega_t+p\omega_t u-i\frac{\Gamma}{2})\,du+\int_0^1 g_2(-\omega_t+p\omega_t u-i\frac{\Gamma}{2})\,du] \qquad \text{(A25)}$$

$$E_{NL}(\tau)=i\beta\delta\omega_t[\int_0^1 g_1(\omega_t-i\beta\delta\omega_t u-i\frac{\Gamma}{2})\,du$$
$$-\int_0^1 g_1(-\omega_t-i\beta\delta\omega_t u-i\frac{\Gamma}{2})\,du+\int_1^{\infty} g''(\omega_t-i\beta\delta\omega_t u-i\frac{\Gamma}{2})\,du$$
$$-\int_1^{\infty} g''(-\omega_t-i\beta\delta\omega_t u-i\frac{\Gamma}{2})\,du] \qquad \text{(A26)}$$

for Birman's ABC.

APPENDIX B

EVALUATION OF THE NONLOCAL TRANSIENT REFLECTIVITY $E_{NL}(\tau)$

In this appendix we simplify the nonlocal part of transient reflectivity, Eqs. (3.3.12) and (3.3.13). For this purpose we need to evaluate n_1, n_2 and n_+ at frequency: $\omega=\omega_t-i\beta\delta\omega_t u-i\Gamma/2$. Using Eqs. (A4) through (A6) to the leading order in δ we obtain:

$$n_{2,1} = +[a \pm (a^2 - \varepsilon_0 b)^{\frac{1}{2}}]^{\frac{1}{2}} \tag{B1}$$

$$n_+ = [2a - \varepsilon_0]^{\frac{1}{2}} \tag{B2}$$

where:

$$a \cong (\frac{\varepsilon_0}{2} - \frac{i\beta u}{\delta}) \quad , \quad b \cong -\frac{\beta^2}{(\varepsilon_0 \delta^2)} \tag{B3}$$

Substituting Eq. (B3) in (B1) and (B2) and assuming $\varepsilon_0\delta/2\beta<<1$, we obtain:

$$n_1 = -i\,(\frac{\beta}{\delta})^{\frac{1}{2}} \exp(\frac{i\theta}{2}) \tag{B4}$$

$$n_2 = (\frac{\beta}{\delta})^{\frac{1}{2}} \exp(-\frac{i\theta}{2}) \tag{B5}$$

for $0 \le u \le 1$, where $\theta=\sin^{-1}u$ and

$$n_1 = (\frac{\beta}{\delta})^{\frac{1}{2}} \exp(-\frac{i\pi}{4}) \exp(-\frac{z}{2}) \tag{B6}$$

$$n_2 = (\frac{\beta}{\delta})^{\frac{1}{2}} \exp(-\frac{i\pi}{4}) \exp(\frac{z}{2}) \tag{B7}$$

for u>1, where u=coshz, while:

$$n_+ = (\frac{2\beta}{\delta})^{\frac{1}{2}} \exp(-\frac{i\pi}{4}) \sqrt{u} \tag{B8}$$

for every $u \geq 0$.

Using Eqs. (3.2.4) and (B4) through (B8) the effective refractive index for each ABC is found to be given by:

$$\bar{n}(n_1, n_2) = \exp(-\frac{i\pi}{4})(\frac{\beta}{2\delta})^{\frac{1}{2}} (1+u)^{-\frac{1}{2}} \tag{B9a}$$

$$\bar{n}(-n_1, n_2) = \exp(\frac{i\pi}{4})(\frac{\beta}{2\delta})^{\frac{1}{2}} (1-u)^{-\frac{1}{2}} \tag{B9b}$$

$$\bar{n}(-n_2, n_1) = \exp(-\frac{i\pi}{4})(\frac{\beta}{2\delta})^{\frac{1}{2}} (u-1)^{-\frac{1}{2}} \tag{B9c}$$

for Pekar's ABC;

$$\bar{n}(n_1, n_2, n_+) = \left(\frac{2\beta}{\delta}\right)^{\frac{1}{2}} \exp\left(-\frac{i\pi}{4}\right) \left[\sqrt{1+u} - \sqrt{u}\right] \tag{B10a}$$

$$\bar{n}(-n_1, n_2, -n_+) = \left(\frac{2\beta}{\delta}\right)^{\frac{1}{2}} \exp\left(-\frac{i\pi}{4}\right) \left[i\sqrt{1-u} + \sqrt{u}\right] \tag{B10b}$$

$$\bar{n}(-n_2, n_1, -n_+) = \left(\frac{2\beta}{\delta}\right)^{\frac{1}{2}} \exp\left(-\frac{i\pi}{4}\right) \left[-\sqrt{u-1} + \sqrt{u}\right] \tag{B10c}$$

for Birman's ABC;

$$\bar{n}(n_1, n_2) = \left(\frac{2\beta}{\delta}\right)^{\frac{1}{2}} \exp\left(-\frac{i\pi}{4}\right) \frac{\sqrt{1+u}}{(2u+1)} \tag{B11a}$$

$$\bar{n}(-n_1, n_2) = \left(\frac{2\beta}{\delta}\right)^{\frac{1}{2}} \exp\left(\frac{i\pi}{4}\right) \frac{\sqrt{1-u}}{(1-2u)} \tag{B11b}$$

$$\bar{n}(-n_2, n_1) = \left(\frac{2\beta}{\delta}\right)^{\frac{1}{2}} \exp\left(-\frac{i\pi}{4}\right) \frac{\sqrt{u-1}}{(2u-1)} \tag{B11c}$$

for Ting's ABC; and

$$\bar{n}(n_1, n_2) = \left(\frac{\beta}{2\delta}\right)^{\frac{1}{2}} \left\{ \frac{\exp\left(-\frac{i\pi}{4}\right) + \gamma\left(\frac{2\beta}{\delta}\right)^{\frac{1}{2}} \sqrt{1+u}}{\sqrt{1+u} + i\gamma \exp\left(-\frac{i\pi}{4}\right) \left(\frac{\beta}{2\delta}\right)^{\frac{1}{2}} (1+2u)} \right\} \tag{B12a}$$

$$\bar{n}(-n_1, n_2) = \left(\frac{\beta}{2\delta}\right)^{\frac{1}{2}} \left\{ \frac{\exp\left(\frac{i\pi}{4}\right) - \gamma\left(\frac{2\beta}{\delta}\right)^{\frac{1}{2}} \sqrt{1-u}}{\sqrt{1-u} + i\gamma \exp\left(\frac{i\pi}{4}\right) \left(\frac{\beta}{2\delta}\right)^{\frac{1}{2}} (1-2u)} \right\} \tag{B12b}$$

$$\bar{n}(-n_2, n_1) = \left(\frac{\beta}{2\delta}\right)^{\frac{1}{2}} \left\{ \frac{\exp\left(-\frac{i\pi}{4}\right) - \gamma\left(\frac{2\beta}{\delta}\right)^{\frac{1}{2}} \sqrt{u-1}}{\sqrt{u-1} - i\gamma \exp\left(-\frac{i\pi}{4}\right) \left(\frac{\beta}{2\delta}\right)^{\frac{1}{2}} (2u-1)} \right\} \tag{B12c}$$

for Kiselev's ABC.

Eqs. (3.2.3) and (B9) through (B12) are used to evaluate the integrands in Eqs. (3.3.12) and (3.3.13) for $\beta/\delta >> 1$.

APPENDIX C

EVALUATION OF THE LOCAL TRANSIENT REFLECTIVITY $E_L(\tau)$

In this appendix we simplify the local part of transient reflectivity $E_L(\tau)$, Eqs. (3.3.10) and (3.3.11), following the procedure of Appendix B. For this purpose we need to evaluate n_1, n_2 and n_+ at frequency:$\omega=\omega_t+p\omega_t u-i\Gamma/2$. Using Eqs. (A4) through (A6) to the leading order in δ we obtain:

$$n_{2,1} = +[a \pm (a^2 - \varepsilon_0 b)^{\frac{1}{2}}]^{\frac{1}{2}} \tag{C1}$$

$$n_+ = [2a - \varepsilon_0]^{\frac{1}{2}} \tag{C2}$$

where

$$a \cong (\frac{\varepsilon_0}{2} - \frac{p u}{\delta^2}) \quad , \quad b \cong \frac{2pu}{\delta^2} - \frac{\beta^2}{(\delta^2 \varepsilon_0)} \tag{C3}$$

and $p=\beta^2/2\varepsilon_0$.

Substituting Eq. (C3) in (C1) and (C2) and assuming $\varepsilon_0\delta^2/2p<<1$, we obtain:

$$n_1 = [\varepsilon_0 (1 - \frac{1}{u})]^{\frac{1}{2}} \tag{C4}$$

$$n_2 = (\frac{\beta}{\delta})(\frac{u}{\varepsilon_0})^{\frac{1}{2}}[1+\frac{1}{2}(\frac{\delta\varepsilon_0}{\beta u})^2] \tag{C5}$$

$$n_+ = (\frac{\beta}{\delta})(\frac{u}{\varepsilon_0})^{\frac{1}{2}} \tag{C6}$$

Using Eqs. (3.2.4) and (C4)-(C6) the effective refractive index for each ABC is found to be given by:

$$\bar{n}(n_1, n_2) = [\varepsilon_0 (1-\frac{1}{u})]^{\frac{1}{2}}[1+(\frac{\delta\varepsilon_0}{\beta u})(u-1)^{-\frac{1}{2}}] \tag{C8a}$$

$$\bar{n}(-n_1, n_2) = -[\varepsilon_0 (1-\frac{1}{u})]^{\frac{1}{2}}[1-(\frac{\delta\varepsilon_0}{\beta u})(u-1)^{-\frac{1}{2}}] \tag{C8b}$$

for Pekar's ABC;

$$\bar{n}(n_1, n_2, n_+) = [\varepsilon_0 (1-\frac{1}{u})]^{\frac{1}{2}}[1+\frac{1}{2}(\frac{\delta\varepsilon_0}{\beta u})(u-1)^{-\frac{1}{2}}] \tag{C9a}$$

$$\bar{n}(-n_1, n_2, n_+) = -[\varepsilon_0 (1-\frac{1}{u})]^{\frac{1}{2}}[1-\frac{1}{2}(\frac{\delta\varepsilon_0}{\beta u})(u-1)^{-\frac{1}{2}}] \tag{C9b}$$

for Birman's ABC;

$$\bar{n}(n_1,n_2)=[\varepsilon_0(1-\frac{1}{u})]^{\frac{1}{2}}[1-(\frac{\delta\varepsilon_0}{\beta})^2\frac{1}{[u^2+(\frac{\delta\varepsilon_0}{\beta})^2]}] \tag{C10a}$$

$$\bar{n}(-n_1,n_2)=-[\varepsilon_0(1-\frac{1}{u})]^{\frac{1}{2}}[1-(\frac{\delta\varepsilon_0}{\beta})^2\frac{1}{[u^2+(\frac{\delta\varepsilon_0}{\beta})^2]}] \tag{C10b}$$

for Ting's ABC; and

$$\bar{n}(n_1,n_2)=[\varepsilon_0(1-\frac{1}{u})]^{\frac{1}{2}}[1+i\gamma-i\gamma(\frac{\delta\varepsilon_0}{\beta})^2\frac{1}{[u^2+(\frac{\delta\varepsilon_0}{\beta})^2]}] \tag{C11a}$$

$$\bar{n}(n_1,n_2)=-[\varepsilon_0(1-\frac{1}{u})]^{\frac{1}{2}}[1+i\gamma-i\gamma(\frac{\delta\varepsilon_0}{\beta})^2\frac{1}{[u^2+(\frac{\delta\varepsilon_0}{\beta})^2]}] \tag{C11b}$$

for Kiselev's ABC.

Eqs. (3.2.3) and (C8) through (C11) are used to evaluate the integrands in Eqs. (3.3.9) and (3.3.10).

APPENDIX D

GENERAL EXPRESSIONS FOR THE COEFFICIENTS (s≠0) IN THE ELECTRIC FIELD AMPLITUDE EXPANSION

In this Appendix, the general formulas for w_2, w_4 and the other lowest order coefficients C^2, ϕ_2, u_1, u_2, and v_1 for the case $s\neq 0$, are presented. All the algebraic calculations were done by using the symbolic calculation software program Mathematica™ on the Macintosh™. (We thank Prof. Joel Koplik of the Levitch Institute of CCNY for use of his hardware and software).

$$w_2 = \frac{1}{2(\Delta^2 + \Lambda^2)} \tag{D1}$$

$$w_4 = \frac{\left[\begin{array}{l} -3w_2^2(2\gamma^2 - 8\gamma\Lambda s w_2 + 8\Delta\gamma s^2 w_2 + 3\beta\Lambda s^2 w_2 \\ +3s^4 w_2 + 2(\Lambda s w_2)^2 - 4\Delta\Lambda s^3 w_2^2 + 2(\Delta s^2 w_2)^2 \end{array}\right]}{4\left[\begin{array}{l} -3\gamma^2 + 8(\Delta\gamma)^2 w_2 + 8\Delta\gamma(\Lambda w_2)^2 + 3\beta\Lambda^3 {w_2}^2 + 2\Lambda^4 {w_2}^3 \\ -16\gamma\Lambda s(\Delta w_2)^2 - 6\beta\Delta s(\Lambda w_2)^2 + 8\gamma\Delta^3(s w_2)^2 + 3\beta\Lambda(\Delta s w_2)^2 \\ +3(\Lambda s w_2)^2 - 6\Delta\Lambda s^3 w_2^2 + 3(\Delta s^2 w_2)^2 - 8\Delta s(\Lambda w_2)^3 \\ +12(\Delta\Lambda s)^2 w_2^3 - 8\Lambda(\Delta s w_2)^3 + 2w_2^3(\Delta s)^4 \end{array}\right]} \tag{D2}$$

$$v_1 = -\frac{\Lambda}{(\Delta^2 + \Lambda^2)} \tag{D3}$$

$$C^2 = \frac{8\Lambda^2\begin{bmatrix} -3\gamma^2+8(\Delta\gamma)^2 w_2+8\Delta\gamma(\Lambda w_2)^2+3\beta\Lambda^3 w_2{}^2+2\Lambda^4 w_2{}^3 \\ -16\gamma\Lambda s(\Delta w_2)^2-6\beta\Delta s(\Lambda w_2)^2+8\gamma\Delta^3(s w_2)^2+3\beta\Lambda(\Delta s w_2)^2 \\ +3(\Lambda s w_2)^2-6\Delta\Lambda s^3 w_2^2+3(\Delta s^2 w_2)^2-8\Delta s(\Lambda w_2)^3 \\ +12(\Delta\Lambda s)^2 w_2^3-8\Lambda(\Delta s w_2)^3+2w_2^3(\Delta s)^4 \end{bmatrix}}{w_2\begin{bmatrix} -24\gamma\Lambda s+12\Delta\gamma s^2+9\beta\Lambda s^2+9s^4+8\Delta\nu\gamma\Lambda^2 w_2+6\beta\Lambda^3 w_2 \\ +48\Delta^2\gamma\Lambda s w_2-12\beta\Delta\Lambda^2 s w_2-24\Delta^3\gamma s^2 w_2-18\beta\Delta^2\Lambda s^2 w_2 \\ +12(\Lambda s)^2 w_2-24\Delta\Lambda s^3 w_2-12\Delta^2 s^4 w_2+4\Lambda^4 w_2^2+16\Delta\Lambda^3 s w_2^2 \\ -56(\Delta\Lambda s w_2)^2+48\Lambda w_2^2(\Delta s)^3-12w_2^2(\Delta s)^4 \end{bmatrix}} \qquad \text{(D4)}$$

$$\phi_2 = \frac{3w_2\begin{bmatrix} -3\gamma s^2-2\gamma w_2\Lambda^2+4\Delta\gamma\Lambda s w_2+6\gamma w_2(\Delta s)^2 \\ +8s\Lambda^3 w_2^2-16\Delta(\Lambda s w_2)^2+8\Lambda(\Delta w_2)^2 s^3 \end{bmatrix}}{4\Lambda\begin{bmatrix} -3\gamma^2+8(\Delta\gamma)^2 w_2+8\Delta\gamma(\Lambda w_2)^2+3\beta\Lambda^3 w_2{}^2+2\Lambda^4 w_2{}^3 \\ -16\gamma\Lambda s(\Delta w_2)^2-6\beta\Delta s(\Lambda w_2)^2+8\gamma\Delta^3(s w_2)^2+3\beta\Lambda(\Delta s w_2)^2 \\ +3(\Lambda s w_2)^2-6\Delta\Lambda s^3 w_2^2+3(\Delta s^2 w_2)^2-8\Delta s(\Lambda w_2)^3 \\ +12(\Delta\Lambda s)^2 w_2^3-8\Lambda(\Delta s w_2)^3+2w_2^3(\Delta s)^4 \end{bmatrix}} \qquad \text{(D5)}$$

$$u_1 = -\frac{\Delta}{(\Delta^2+\Lambda^2)} \qquad \text{(D6)}$$

$$u_3 = \frac{w_2^2\begin{bmatrix} +4\Delta\gamma^2+3\gamma s^2+2\gamma w_2\Lambda^2-20\Delta\gamma\Lambda s w_2+10\gamma w_2(\Delta s)^2 \\ +6\beta\Delta\Lambda s^2 w_2+6\Delta s^4 w_2-8s\Lambda^3 w_2^2+20\Delta(\Lambda s w_2)^2 \\ -16\Lambda(\Delta w_2)^2 s^3+4\Delta^3 s^4 w_2^2 \end{bmatrix}}{2\begin{bmatrix} -3\gamma^2+8(\Delta\gamma)^2 w_2+8\Delta\gamma(\Lambda w_2)^2+3\beta\Lambda^3 w_2{}^2+2\Lambda^4 w_2{}^3 \\ -16\gamma\Lambda s(\Delta w_2)^2-6\beta\Delta s(\Lambda w_2)^2+8\gamma\Delta^3(s w_2)^2+3\beta\Lambda(\Delta s w_2)^2 \\ +3(\Lambda s w_2)^2-6\Delta\Lambda s^3 w_2^2+3(\Delta s^2 w_2)^2-8\Delta s(\Lambda w_2)^3 \\ +12(\Delta\Lambda s)^2 w_2^3-8\Lambda(\Delta s w_2)^3+2w_2^3(\Delta s)^4 \end{bmatrix}} \qquad \text{(D7)}$$

APPENDIX E

NUMERICAL INTEGRATION OF THE MAXWELL-BLOCH EQUATIONS

In this Appendix, details for the numerical integration of the Maxwell-Bloch equations are presented. The Maxwell-Bloch equations for the self-similar pulse [Eqs. (5.2.20a, b) and (5.2.13-15)] form a system of ODEs which can be written in a more convenient way for computational purposes as a system of first order equations. By making the following transformations: $\dot{E} = e$, and $\dot{\phi} = \Phi$ one has:

$$\dot{E} = e \tag{E1}$$

$$\dot{e} = \frac{\alpha}{\gamma} E + \frac{\beta}{\gamma} \Phi + \Phi^2 E + \left(\frac{s}{\gamma \Lambda}\right)\left(\frac{s\Delta}{\Lambda} - 2\right) w E - \left(\frac{s^2}{\gamma \Lambda}\right) \Phi w E - \frac{1}{\gamma}\left(\frac{s\Delta}{\Lambda} - 1\right)^2 u \tag{E2}$$

$$\dot{\Phi} = -\left(\frac{\beta}{\gamma}\right)\frac{e}{E} - 2\frac{\Phi e}{E} + \left(\frac{s^2}{\gamma \Lambda}\right)\frac{we}{E} - \frac{1}{\gamma}\left(\frac{s\Delta}{\Lambda} - 1\right)^2 \frac{v}{E} - \left(\frac{s^2}{\gamma \Lambda^2}\right) E v \tag{E3}$$

$$\dot{u} = \frac{\Delta}{\Lambda} v + \Phi v \tag{E4}$$

$$\dot{v} = -\frac{\Delta}{\Lambda} u - \Phi u + \frac{1}{\Lambda} E w \tag{E5}$$

$$\dot{w} = -\frac{1}{\Lambda} E v \tag{E6}$$

In order to integrate the system numerically, we use the expressions for E, $\dot{\phi}$, u, v, and w derived in Section 5.3 as asymptotic initial conditions:

$$\begin{aligned} E &= C\,\mathrm{sech}\,\xi & \dot{E} &= -C\,\mathrm{sech}\,\xi\tanh\xi \\ \Phi &= \phi_2 E^2 & u &= u_1 E + u_3 E^3 \\ v &= v_1 \dot{E} & w &= -1 + w_2 E^2 + w_4 E^4 \end{aligned} \tag{E7}$$

The general form of the coefficients C, ϕ_2, u_1, u_3, v_1, w_2, and w_4 ($s\neq 0$) is given in Appendix D (Eqs. D1-D7).

The transformed system of ODEs (Eqs. E1-6) is a stiff set of equations. Stiffness occurs in ODEs when there are two or more relevant scales of the independent variable ξ. In our case (Eqs. E1-6) the long scale corresponds to the pulse width τ, which has the overall structure of the solitary wave solutions. This short scale is of size ϵ, where ϵ is a small parameter associated with rapidly oscillating modes. These can be seen explicitly by linearizing the ODEs in the tail: two of the eigenvalues of linearized system are equal to $\pm i/\epsilon$, and thus rapidly oscillating. For stiff ODEs most integration methods (such as Runge-Kutta, Bulirsch-Stoer, and predictor-connectors [90]) fail, because the stability of these integration schemes is controlled by the most rapidly varying component. Therefore, to follow the long time behavior (the overall structure of the solitary wave solutions), one must choose time steps smaller than the shortest time scale. Then the large number of steps leads to laborious integrations plus potentially large accumulated errors. Fortunately, algorithms for stiff ODEs have been developed which do not have this problem. One of the most efficient ones due is to Kaps and Rentrop [91], and it is a generalization of the Runge-Kutta scheme that monitors the local truncation error to adjust stepsize. A introduction for this STIFF algorithm is given by Press and Teukolsky [92]. Thus we used the subroutine STIFF from Ref. [92]. It requires two subroutines JACOBI and DERIVS which we wrote

and these contain all the information regarding the system of six ODEs. STIFF uses the subroutines ODEINT, LUDCM, and LUBKSB from the *Numerical Recipes* book [90].

The overall program searches for solitary solutions by solving Eqs. (E1-6) with initial conditions given by Eq. (E7). The input parameters are the frequency detuning $\Delta = (\omega - \omega_t)/\omega_{LT}$, the inverse pulse width $\Lambda = 1/\omega_{LT}\tau$, and the material parameter ω_t/ω_{LT}. For different values of Δ and Λ, the program scans in the domain of (Δ, Λ) for solitary wave solutions. The solvability condition (c.f. Section 5.5) for the existence of solitary is that as $\xi \rightarrow \xi_{tip}$, both the derivative of the electric field amplitude $\dot{E}$, and the out of phase component of the polarization v, must both vanish simultaneously. The program integrates from some asymptotic value $\xi_{initial}$ near $\xi = -\infty$ and defines ξ_{tip} by the location of $v = 0$. Then one does a regular falsii method on Δ to find when $\dot{E}_{tip}=0$ at the tip. The program outputs the set of points in (Δ, Λ) space for which the solvability condition is satisfied.

Various tests on the program have been conducted. The initial value of ξ used in Eq. (E7) has been varied. The results of the integration show a fast convergence as the origin of integration process is taken to large negative values of $\xi_{initial}$. The results were seem to also converge as the accuracy at each step was increased. The integration was checked against Akimoto and Ikeda's solutions and Section's 5.3 perturbative solutions. Numerics agrees very well with analytic formulae for ξ away from zero in both cases. We also checked that the condition $u^2+v^2+w^2=1$ was preserved under integration to the expected accuracy.

Another check consists in using the conservation law for the Bloch components u, v, and w ($u^2+v^2+w^2=1$), to transform the system of six ODEs to a system of five ODEs (E, e, Φ, u, and v). We coded this 5 dimensional system and the agreement between these two programs for the selected values of (Δ, Λ) was as expected.

Finally, one can substract out from Y the analytically derived part: $\mathbf{Y}=\mathbf{Y}_{Ikeda}+\varepsilon\delta\mathbf{Y}$, where ε is a small expansion parameter related to the pulse width for Akimoto and Ikeda's

analysis. We linearized Eqs. (E1-6) in $\delta \mathbf{Y}$ and integrated numerically the corresponding system. As $\varepsilon \rightarrow 0$, the program for the linearized equations and for the original non-linear equations agreed to the expected order in ε.

The programs were run on the Celerity and VAX computer machines at the CCNY-Physics.

APPENDIX F

SPACE-TIME MAXWELL BOUNDARY CONDITIONS

In order to match the incident pulse with the pulse solutions inside the dielectric at z=0 for every time moment, it is necessary to derive the appropriate boundary conditions for this problem. In the case of intense pulses, the harmonic plane-wave approximation cannot be used for nonlinear media. A space-time representation of the Maxwell Boundary Conditions was derived for the first time by Karpman [93] and we will apply it to our case.

We assume that the dielectric fills the half-space z>0, and that at the boundary of the dielectric z=0, a pulse wave is incident with time-dependent amplitude $E_i(t)$

$$E_{INC} = E_i(t)\exp[-i\,\omega(t-\frac{z}{c})] \tag{F.1}$$

The expressions for the reflected and transmitted pulse waves from and in the dielectric may be written as follows:

$$E_{REFL} = E_r(t)\exp[-i\,\omega(t+\frac{z}{c})-\psi(t)] \tag{F2}$$

$$E_{TRANS} = E(z,t)\exp[-i(\omega t-\Phi(z,t))] \tag{F3}$$

where $\Phi(z,t)=Kz-\phi(z,t)$. The electric and magnetic fields for all three waves are parallel to the boundary plane z=0. The continuity conditions for the electric and magnetic fields lead to the following expressions

$$\left.\begin{aligned} &E_{INC}+E_{REFL}=E_{TRANS} \\ &\frac{\partial H_{INC}}{\partial t}+\frac{\partial H_{REFL}}{\partial t}=\frac{\partial H_{TRANS}}{\partial t} \end{aligned}\right\} \tag{F4}$$

and by taking into account Eqs. (F1)-(F3) we obtain

$$\left.\begin{aligned} &E_i+E_r\cos\psi=E_0\cos\phi_0 \\ &E_r\sin\psi=E_0\sin\phi_0 \\ &\frac{\omega}{c}\{E_i-E_r\cos\psi\}=-E_{0z}\sin\phi_0+(K-\phi_{0z})\cos\phi_0 \\ &-\frac{\omega}{c}E_r\sin\psi=E_{0z}\cos\phi_0+E_0(K-\phi_{0z})\sin\phi_0 \end{aligned}\right\} \tag{F5}$$

Here

$$\left.\begin{aligned} &\phi_0\equiv\phi(z=0,t) \\ &E_i\equiv E_i(t) \quad , \qquad E_r\equiv E_r(t), \\ &E_0\equiv E(0,t) \quad , \qquad \Phi_0\equiv-\phi(0,t)=-\phi_0, \\ &E_{0z}\equiv\left.\frac{\partial E(z,t)}{\partial z}\right|_{z=0} \quad , \qquad \Phi_{0z}\equiv\left.\frac{\partial\Phi(z,t)}{\partial z}\right|_{z=0}=K-\phi_{0z} \end{aligned}\right\} \tag{F6}$$

Introducing the reflection and transmission coefficients

$$R(t)=\frac{E_r^2(t)}{E_i^2(t)} \quad , \qquad T(t)=\frac{E_0^2(t)}{E_i^2(t)}\times\frac{c}{\omega}(K-\phi_{0z}) \tag{F7}$$

and using Eq. (F5), we obtain after some lengthy algebraic calculations

$$\left.\begin{aligned} R(t)&=1-\frac{c}{\omega}\left(K-\frac{\partial\phi(z=0,t)}{\partial z}\right)\frac{E_0^2(t)}{E_i^2(t)} \\ \frac{E_0^2(t)}{E_i^2(t)}&=4\left(1-\frac{c^2}{4\omega^2}\frac{E_{0z}^2}{E_i^2}\right)\left[1+\frac{c}{\omega}\left(K-\frac{\partial\phi(z=0,t)}{\partial z}\right)\right]^{-2} \\ \sin\phi_0&=-\frac{c}{2\omega}\frac{E_{0z}}{E_i} \quad , \quad \sin\psi=-\frac{c}{2\omega}\frac{E_0 E_{0z}}{E_i^2}R^{-1/2} \end{aligned}\right\} \qquad \text{(F8)}$$

These relations, together with the conditions for the electric field inside the nonlinear dielectric

$$E(z,t)\to 0\,(z\to\infty) \quad , \quad \int_0^\infty E^2(z,t)dz<\infty \qquad \text{(F9)}$$

form a complete system of boundary conditions for Maxwell-Bloch Eqs. (5.2.4) and (5.2.7-9) which define the EM-field inside the dielectric.

BIBLIOGRAPHY

Κακοι μαρτυρες ανθρωποισιν οφθαλμοι
και ωτα βαρβαρους ψυχας εχοντων.

ΗΡΑΚΛΕΙΤΟΣ

1. S.I. Pekar, Zh. Eksp. Teor. Fiz. **33**, 1022 (1957) [Sov. Phys. JETP **6**, 785 (1958)]; Zh. Eksp. Teor. Fiz. **34**, 1176 [Sov. Phys. JETP **7**, 813 (1958)]; Zh. Eksp. Teor. Fiz. **38**, 1786 (1958) [Sov. Phys. JETP **11**, 1286 (1960)].

2. H.A Lorentz, Verh. d.k. Akad.Wet. Amsterdam **18**, (1879).

3. V.M. Agranovich, and A.A. Rukhadze, Zh. Eksp. Teor. Fiz. **35**, 982 (1958) [Sov. Phys. JETP **7**, 685 (1959)].

4. V.M. Agranovich, and V.L. Ginzburg, Usp. Fiz. Nauk **76**, 643; **77**, 663 [Sov. Phys. Uspekhi **5**, 323, 675 (1962)].

5. S.I. Pekar, *Crystal Optics and Additional Light Waves*, (Benjamin/Cummings Publ. Co., NY, 1983).

6. V.M. Agranovich, and V.L. Ginzburg, *Spatial dispersion in Crystal Optics and the Theory of Excitons*, 2nd ed. (Nauka, Moscow); Engl. Transl. (Springer, Berlin, 1981).

7. J.J. Hopfield, Phys. Rev. **112**, 1555 (1958).

8. J.J. Hopfield, and D.G. Thomas, Phys. Rev. **132**, 563 (1963).

9. S.I. Pekar, Fiz. Tverd. Tela (Leningrad) **4**, 1301 [Sov. Phys.- Solid State **4**, 953 (1962)].

10. J.J. Hopfield, J. Phys. Soc. Jpn. **21** (Supplement), 77 (1966).

11. J.S. Jackson, *Classical Electrodynamics*, (Wiley, New York, 1975).

12. L.D. Landau, and E.M. Lifschitz, *Electrodynamics of Continuous Media*, (Pergamon Press, London/New York, 1960).

13. J.A. Stratton, *Electromagnetic Theory*, (McGraw Hill, New York, 1941).

14. M. Born, and E. Wolf, *Principles of Optics*, 5th ed. (Pergamon Press, Oxford, 1958).

15. J.L. Birman, in *Excitons*, Chapter 2, ed. by E.I. Rashba and M.D. Sturge (North-Holland Publishing Company, NY, 1982).

16. V.L. Ginzburg, Zh. Eksp. Teor. Fiz. **34**, 1593 [Sov. Phys. JETP **7**, 813 (1958)].

17. V.M. Agranovich, and V.L. Ginzburg, *Spatial dispersion in Crystal Optics and the Theory of Excitons*, (Wiley, New York, 1966).

18. V.A. Kiselev, Fiz. Tverd. Tela (Leningrad) [Sov. Phys.- Sol. State **15**, 2338 (1974).

19. J.J. Sein, and J.L. Birman, Phys. Rev. **B6**, 2482 (1972); J.J. Sein, Ph.D. thesis, NYU (1969) (unpublished).

20. A.A. Maradudin, and D.L. Mills, Phys. Rev. **B7**, 2787 (1973).

21. G.P. Agrawal, D.N. Pattanayak, and E. Wolf, Phys. Rev. Lett. **27**, 1022 (1971); Phys. Rev. **B10**, 1477 (1974).

22. R. Zeyher, J.L. Birman, and W. Brenig, Phys. Rev. **B6**, 4613 (1972).

23. M. Bishop, and A.A. Maradudin, Phys. Rev. **B14**, 3384 (1976).

24. C.S. Ting, M. Frankel, and J.L. Birman, Sol. State Comm. **17**, 1285 (1975).

25. J.J. Sein, Phys. Lett. **32A**, 141 (1970); Optics Commun. **2**, 170 (1970).

26. E.S. Koteles, in *Excitons*, Chapter 3, ed. by E.I. Rashba and M.D. Sturge (North-Holland Publishing Company, NY, 1982).

27. E.L. Ivchenko, in *Excitons*, Chapter 4, ed. by E.I. Rashba and M.D. Sturge (North-Holland Publishing Company, NY, 1982).

28. V.A. Kiselev, B.S. Razbirin, and I.N. Uraltsev, Zh. Eksp. Teor. Fiz. Pisma Red. **18**, 504 [JETP Lett. **18**, 296 (1973)]; Proc. XII Int. Conf. Phys. Semicond. p. 996 (Stuttgard, 1974).

29. V.A. Kiselev, B.S. Razbirin, I.N. Uraltsev, and V.P. Kochereshko, Fiz. Tverd. Tela (Leningrad) [Sov. Phys.- Sol. State **17**, 418 (1975)].

30. R.G. Ulbrich, and C. Weisbuch, Phys. Rev. Lett. **38**, 865 (1977).

31. G. Winterling, and E. Koteles, Sol. State Comm. **23**, 95 (1977).

32. V.A. Kiselev, B.S. Razbirin, and I.N. Uraltsev, Phys. Stat. Sol. **B72**, 161 (1975).

33. Y. Segawa, Y. Aoyagi, K. Azuma, and S. Namba, Sol. State Commun. **28**, 853, (1978); *ibid.* **32**, 299 (1979).

34. R.G. Ulbrich, and G.W. Fehrenbach, Phys. Rev. Lett. **43**, 963 (1979).

35. Y. Aoyagi, Y. Segawa, T. Baba, and S. Namba in *Picosecond Phenomena II*, ed. by R.M. Hochstrasser, W. Keiser, and C.V. Shank, Springer Ser. Chem. Phys. **14**, p. 298 (Springer, Berlin, 1980).

36. T. Itoh, P. Lavallard, J. Raydellet, C. Benoit a la Guillaume, Sol. State Comm. **37**, 925 (1981).

37. D. Elert, Ann. Phys. (Leipzig) Ser. 5, **7**, 65 (1930).

38. J.C. Eilbeck, J. Phys. **A5**, 1355 (1972).

39. D.N. Pattanayak, G.P. Agrawal, and J.L. Birman Phys, Rev. Lett. **46**, 174 (1981); G.P. Agrawal, J.L. Birman, D.N. Pattanayak, and A. Puri, Phys. Rev. **B25**, 2715 (1982).

40. A. Puri, and J.L. Birman, in *Semiconductors Probed by Ultrafast Laser Spectroscopy*, Chapter 22, **Vol. II**, ed. by R.R. Alfano (Acad. Press, NY, 1984).

41. J. Aaviksoo, J. Lipmaa, and J. Kuhl, JOSA **B5**, 1631 (1988).

42. S.V. Branis, K. Arya, and J.L. Birman, Bull. Am. Phys. Soc. **33**, 351 (1988).

43. I.H. Campell, and P.N. Fauchet, Opt. Lett. **13**, 634 (1988).

44. J. Aaviksoo, and J. Kuhl, IEEE J. Quantum Electron. **QE-25**, 2523 (1989); J. Aaviksoo, J. Kuhl, and I. Reimand, Sol. State Comm. **72**, 49 (1989); J. Aaviksoo, J. Kuhl, and I. Reimand, in *The Physics of Optical Phenomena and Their Use as Probes of Matter*, ed. by A.A. Maradudin (Plenum Press, NY 1990).

45. T. Shigenari, X.Z. Lu, and H.Z. Cummins, Phys. Rev. **B30**, 1962 (1984).

46. M. Dagenais, and W.F. Sharfin, Phys. Rev. Lett. **58**, 1776 (1987).

47. M. Kuwata, J. Phys. Soc. Jpn. **53**, 4456 (1984).

48. P. Lavallard, and C. Gourdon, Phys. Rev. **B31**, 6654 (1985).

49. C. Gourdon, thèse de troisième cycle, Université Paris VI, (1984).

50. J.E. Rothenberg, D. Grischkowsky, and A.C. Balant, Phys. Rev. Lett. **53**, 552 (1984).

51. J.E. Rothenberg, IEEE J. Quantum Electron. **QE-22**, 174 (1986).

52. B. Segard, and B. Macke, Phys. Lett. **109A**, 213 (1985).

53. I.V. Makarenko, I.N. Uraltsev, and V.A. Kisilev, Phys. Stat. Sol. **B98**, 773 (1980).

54. A. D'Andrea, and R. Del Sole, Phys. Rev. **B25**, 3714, (1982); *ibid.* **B38**, 1197 (1988).

55. S.L. McCall and E. L. Hahn, Bull. Am. Phys. Soc. **10**, 1189 (1965); Phys. Rev. Lett. **18**, 908 (1967); Phys. Rev. **183**, 457 (1969).

56. A. Sommerfeld, Ann. Phys. (Leipzig) **44**, 177 (1914); L. Brillouin, *Wave Propagation and Group Velocity* (Acad. Press, NY 1960).

57. L. Allen and J.H. Eberly, *Optical Resonance and Two-Level Atoms* (Dover, NY 1987).

58. G. L. Lamb Jr., Rev. Mod. Phys. **43**, 99 (1971).

59. R.E. Slusher, in *Progress in Optics XII*, p. 55, ed. by E. Wolf (North-Holland Publishing Company, NY, 1974).

60. C.K.N. Patel, and R.E. Slusher, Phys. Rev. Lett. **19**, 1019 (1967).

61. R.E. Slusher and H.M. Gibbs, Phys. Rev. **A5**, 1634 (1972).

62. H.M. Gibbs, and R.E. Slusher, Phys. Rev. **A6**, 2326 (1972).

63. F. Bloch, Phys. Rev. **70**, 460 (1946).

64. H.M. Gibbs, in *Optical Bistability: Controlling Light with Light*, Appendix C, p. 343 (Academic Press, NY, 1985).

65. I.A. Poluektov and Yu. M. Popov, Zh. Eksp. Teor. Fiz. Pisma Red. **9**, 542 [JETP Letters **9**, 330 (1969)].

66. N. Tzoar, and J.I. Gersten, Phys. Rev. Lett. **28**, 1203 (1972).

67. T.L. Gvardzhaladze, A.Z. Grasyuk, P.G. Kryukov, and O.B. Shatberashvili, Zh. Eksp. Teor. Fiz. Pisma Red. **13**, 159 [JETP Lett. **13**, 111 (1971)].

68. V.V. Samartsev, A.I. Siraziev, and Yu E. Sheibut, Izv. Akad. Nauk SSSR Ser. Fiz. **37**, 2175 [Bull. Acad. Sc. SSR **37**, 140 (1973)].

69. F. Brukner, V.S. Dneprovskii, D.G. Koshchug, and V.U. Khattarov, Zh. Eksp. Teor. Fiz. Pisma Red. **18**, 27 [JETP Lett. **18**, 14 (1973)].

70. V.S. Dneprovskii, Izv. Akad. Nauk SSSR Ser. Fiz. **46**, 586 [Bull. Acad. Sc. SSR **46**, 155 (1982)].

71. H. Haken, and A. Schenzle, Z. Phys. **258**, 231 (1973).

72. E. Hanamura, J. Phys. Soc. Jpn. **37**, 1553 (1974).

73. M. Inoue, J. Phys. Soc. Jpn. **37**, 1561 (1974).

74. O. Akimoto, and K. Ikeda, J. Phys. **A10**, 425 (1977).

75. J. Goll, and H. Haken, Optics Comm. **24**, 1 (1978); Phys. Rev. **A18**, 2241 (1978).

76. V.M. Agranovich, and V.I. Rupasov, Fiz. Tverd. Tela (Leningrad) **18**, 801 [Sov. Phys. Solid State, **18**, 459 (1976)].

77. S.N. Belkin, P.I. Khadzhi, S.A. Moskalenko, and A.H. Rotary, J. Phys. **C14**, 4109 (1981).

78. S.N. Belkin, S.A. Moskalenko, A.H. Rotary, and P.I. Khadzhi, Izv. Akad. Nauk SSSR Ser. Fiz. **43**, 355 [Bull. Acad. Sc. SSR **43**, 113 (1979)].

79. L. Matulic and J.H. Eberly, Phys. Rev. **A6**, 822 (1972).

80. M.D. Crisp, Appl. Opt. **11**, 1124 (1972).

81. R.A. Marth, D.A. Holmes, and J.H. Eberly, Phys. Rev. **A9**, 2733 (1974).

82. Z. Bialynicka-Birula, Phys. Rev. **A10**, 999 (1974).

83. K. Ikeda, and O. Akimoto, J. Phys. **A12**, 1105 (1979).

84. J.S. Russel, in *Report on Waves*, Rept. 14th Meet. Brit. Assoc. Adv. Sci. York, p. 311 (1844); D.J. Korteweg-deVries, Phil. Mag. (5) **39**, 422 (1895).

85. A.C. Scott, F.Y.F. Chu, and D. W. McLaughlin, IEEE Proc. **61**, 1443 (1973).

86. G.L. Lamb Jr., Phys. Rev. Lett. **31**, 196 (1973); Phys. Rev. **A9**, 422 (1974).

87. V.E. Zakharov and A.B. Shabat, Zh. Eksp. Teor. Fiz. **61**, 118 (1971) [Sov. Phys. JETP **34**, 62 (1972)].

88. H.A. Hauss, Rev. Mod. Phys. **51**, 331 (1979).

89. H.T. Davis, *Introduction to Nonlinear Differential and Integral Equations*, p. 207 (Dover, NY, 1962).

90. W.H. Press, B.P. Flammery, S.A. Teukolsky, and W.T. Vetterling, in *Numerical Recipes: The Art of Scientific Computing*, (Cambridge Un. Press, NY, 1986).

91. P. Kaps, and P. Rentrop, Numer. Math. **33**, 55 (1979).

92. W.H. Press, and S.A. Teukolsky, Computer in Physics **3**(3), 88 (1989).

93. V.I. Karpman, Plasma Physics **13**, 477 (1971); in *Non-Linear Waves in Dispersive Media*, (Pergamon Press, NY, 1974).

LIST OF PUBLICATIONS

[1]. "Transient Optical Reflectivity from Bounded Non-Local Media", S.V. Branis, K. Arya, and J.L. Birman in *Ultrafast Lasers Probe Phenomena in Bulk and Microstructure Semiconductors*, SPIE Proceedings **793**, ed. by R.R. Alfano (1987).

[2]. "Theory of Transient Optical Response and Pulse Propagation in Bounded Spatially Dispersive Media", S.V. Branis, K. Arya, and J.L. Birman in *Laser Optics of Condensed Matter*, ed. by J.L. Birman, H.Z. Cummins and A.A. Kaplyanskii (Plenum Press, NY, 1988).

[3]. "Novel Effects in Transient Optical Reflectivity from Bounded Non-Local Media via Exciton Polaritons", S.V. Branis, K. Arya, and J.L. Birman, Optics Comm. **70**, 355 (1989).

[4]. "Transient Optical Reflectivity from Bounded Non-Local Media: Normal Incidence", S.V. Branis, K. Arya, and J.L. Birman, Phys. Rev. **B39**, 8371 (1989).

[5]. "Quantum Optic and Transient effects of Excitonic Polaritons, and Properties of Phonoritons", J.L. Birman, M. Artoni, S.V. Branis, O. Martin, and B.S. Wang in *The Physics of Optical Phenomena and Their Use as Probes of Matter*, ed. by A.A. Maradudin (Plenum Press, NY 1990).

[6]. "Solitary-Wave Velocity Selection in Self-Induced Transparency", S.V.Branis, O. Martin, and J.L. Birman (submitted to Phys. Rev. Letters, July 1990).

[7]. "Self-Induced Transparency Selects Discrete Velocities for Solitary-Wave Solutions", S.V.Branis, O. Martin, and J.L. Birman (submitted to Phys. Rev. **A**, August 1990).

AUTOBIOGRAPHICAL STATEMENT

Spiros V. Branis was born in Melbourne, Australia on February 12, 1959. He graduated from the 3rd Elementary School of Nea Philadelphia, Athens, Greece in 1970, and from the High School of Nea Philadelphia, Athens, Greece in 1976. He attended courses as an undergraduate student of Biology, in Athens University, Greece for the academic year 1976-77. In 1977, he registered at the Physics Department of the same University. He graduated in Physics (B.Sc.) in 1982, and was accepted as a Ph.D. student in Physics, at Rutgers University, NJ, USA. In 1983, he transferred to City College of NY-Physics Dept. first as a Masters student, and after passing the 1st exam (qualifying exams) in September 1984, as a Ph.D. student at the City University of NY-Graduate Center. Mr. Branis passed his second exam in July 1987, and defended his thesis on May 8th, 1990.